2018

The Role of Ceramide in Neutrophil Elastase Induced Inflammation in the Lungs

Sophia Karandashova
Virginia Commonwealth University

The Role of Ceramide in Neutrophil Elastase Induced Inflammation in the Lungs

A dissertation submitted in partial fulfillment of the requirements for the degree of Doctor of Philosophy at Virginia Commonwealth University

by

Sophia Karandashova
Honors Bachelor of Science, Microbiology, Oregon State University, 2008
Master of Science, Biotechnology, Stephen F Austin State University, 2010

Advisor: Judith A. Voynow, M.D.
Professor, Edwin L. Kendig Jr. Professor of Pulmonology
Department of Pediatrics, Division of Pediatric Pulmonology

Virginia Commonwealth University
Richmond, Virginia
March 2018

Acknowledgement

If I had to list the people that have been integral to this dissertation project Dr. Judy Voynow, my mentor and advisor, would always come to mind first. The mentorship she has provided me over the past four years, the opportunities that I would not have had without her undying support, would place her firmly at the top of said list every time. Her passion for medicine and research, as well as her dedication to her students—in clinic or in lab— are inspiring. Next, without the other members of Voynow Lab, Drs. Apparao Kummarapurugu, and Shuo Zheng, this project would not have been possible; they have been instrumental, involved in every facet of this venture, from planning and carrying out experiments to editing manuscripts. I would also like to thank the members of my thesis committee: Drs. Daniel Conrad, Bruce K. Rubin, Charles Chalfant, Devanand Sarkar, and Rahman Natarajan, every time we met, they provided a wealth of ideas and advice, helping shape my dissertation project. Also, thank you to the Children's Hospital Foundation Research Fund of the Children's Hospital of Richmond at VCU, who helped fund the earliest stage of this project, allowing us to gather preliminary data.

Next, I would like to thank the many individuals that offered their expertise to this project. Thank you to Rubin Lab, who maintain the VCU Biospecimen Repository, as well as the many patients from the Adult and Pediatric Cystic Fibrosis Centers at VCU Medical Center that contributed to this unique collection. To Dr. Jeremy Allegood and the other members of the VCU Lipidomics and Metabolomics Core (supported by the NIH-NCI Cancer Center Support Grant (P30 CA016059) to the VCU Massey Cancer Center, and shared resource grant (S10RR031535) from the NIH), who analyzed our many samples for sphingolipid content. Thank you to Drs Shumei Sun and Le Kang, who helped design our retrospective clinical trial and analyze the results; their statistical expertise has been integral to this project. A special thank you to Dr. Michael S. Schechter, and all the staff at the VCU Adult and Pediatrics Cystic Fibrosis Centers, who helped me remember why we do clinical research— for the patients, both current and future.

Additionally, I would like to thank all that have attended Rubin Lab and ACHOO meetings; their feedback helped fine-tune my presentation skills, and open new avenues to explore in my research. A large and sincere thank you to the students and staff of the Center for Clinical and Translational Research and VCU's MD/PhD program, who provided emotional, social, and scientific support. Last, but certainly not least, thank you to my family, who laughed, cried, and struggled alongside me every step of the way.

Thank you all for your unwavering support.

Table of Contents

List of Tables

List of Figures

List of Abbreviations

ANOVA .....analysis of variance
ARDS /ALI .....acute respiratory distress syndrome /acute lung injury
BAL .....bronchoalveolar lavage
CerS.....ceramide synthase
CF.....cystic fibrosis
CFTR.....cystic fibrosis transmembrane conductance regulator
COPD.....chronic obstructive pulmonary disease
C1P.....ceramide-1-phosphate
DTT.....dithiothreitol
DEPC .....diethyl pyrocarbonate
EDTA.....ethylenediaminetetraacetic acid
ELISA .....enzyme-linked immunosorbent assay
ENaC.....epithelial sodium channel
FEV .....forced expiratory volume
FVC.....forced vital capacity
HEPES .....4-(2-hydroxyethyl)-1-piperazineethanesulfonic acid
HMGB1.....High Mobility Group Box 1
HPLC-ESI-MS/MS ....reverse phase high-performance liquid chromatography/electrospray ionization tandem mass spectrometry
KC.....keratinocyte chemokine
LTB4 .....leukotriene B4
MRSA .....methicillin resistant *Staphylococcus aureus*
NE .....neutrophil elastase
ORMDL3 .....ORM (yeast)-like protein isoform 3
PMSF .....phenylmethanesulfonyl fluoride
Q/RT PCR.....quantitative, real-time reverse-transcription polymerase chain reaction
RAGE.....Receptor for Advanced Glycation Endproducts
ROS.....reactive oxygen species
RTN4.....reticulon-4
SEM .....standard error of the mean
SMase.....sphingomyelin synthase
SPT.....serine palmitoyltrasnferase
SPTLC.....serine palmitoyltrasnferase long chain
Sa1P sphinganine-1-phosphate
S1P sphingosine-1-phosphate
VCU .....Virginia Commonwealth University

Abstract

THE ROLE OF CERAMIDE IN NEUTROPHIL ELASTASE INDUCED INFLAMMATION IN THE LUNGS

Sophia Karandashova, M.S., Honors B.S.

A dissertation submitted in partial fulfillment of the requirements for the degree of Doctor of Philosophy at Virginia Commonwealth University

Virginia Commonwealth University, 2018

Advisor: Judith A. Voynow, M.D.
Professor, Edwin L. Kendig Jr. Professor of Pulmonology
Department of Pediatrics, Division of Pediatric Pulmonology

Alterations to sphingolipid metabolism are associated with increased pulmonary inflammation, but the impact of inflammatory mediators, such as neutrophil elastase (NE), on airway sphingolipid homeostasis remains unknown. NE is a protease associated CF lung disease progression, and can be found in up to micromolar concentrations in patient airways. While sphingolipids have been investigated in the context of CF, the focus has been on loss of cystic fibrosis transmembrane conductance regulator (CFTR) function. Here, we present a novel observation: oropharyngeal aspiration of NE increases airway ceramides in mice. Using a previously characterized mouse model of NE-induced inflammation, we demonstrate that NE increases *de novo* ceramide production, which is likely mediated via increased SPTLC2 levels.

Inhibition of *de novo* sphingolipid synthesis using myriocin, an SPT inhibitor, decreases airway ceramide as well as the release of pro-inflammatory signaling molecules induced by NE. Furthermore, in a retrospective study of the sphingolipid content of CF sputum—the largest of its type in this patient cohort to date, we investigated the association between NE and sphingolipids. There were linear correlations between the concentration of active NE and ceramide, sphingomyelin, and monohexosylceramide moieties as well as sphingosine-1-phosphate. The presence of Methicillin-resistant *Staphylococcus aureus* (MRSA) positive culture and female gender both strengthened the association of NE and sphingolipids, but higher FEV_1 % predicted weakened the association, and *Pseudomonas aeruginosa* had no effect on the association between NE and sphingolipids. These data suggest that NE may increase sphingolipids in CF airways as it did in our *in vivo* model, and that this association is stronger in patients that have worse lung function, are female, and whose lungs are colonized with MRSA. Modulating sphingolipid homeostasis could provide novel pharmacological approaches for alleviating pulmonary inflammation.

Chapter 1: Introduction

I. An Overview of Cystic Fibrosis.

Cystic fibrosis (CF) is an autosomal recessive disease that is caused by loss of functioning cystic fibrosis transmembrane conductance regulator (CFTR) protein. CFTR is an ion channel, responsible for chloride and bicarbonate transport across the plasma membrane. It also regulates other ion channels such as the epithelial sodium channel (ENaC) (33, 126, 144). When a genetic mutation causes the absence or malfunction of CFTR, a variety of organ systems can be affected, depending on the severity of the disease, including the lungs, pancreas, gastrointestinal system, sweat glands, and reproductive organs. The most common mutation in Caucasians of Northern European descent, the population in which the CF incidence is highest, is c.1521_1523delCTT (p.Phe508del or F508del, known colloquially as CFTRΔF508 or ΔF508), a class II mutation (9, 18).

Genetic Basis of Cystic Fibrosis. In total there are currently over two thousand known *CFTR* mutations, which can affect CFTR protein biosynthesis, localization, and functionality (18). Disease-causing mutations have been organized into six classes (Class I-VI) (7, 33). In class I mutations, functional CFTR protein is not synthesized due to nonsense, frameshift or splicing mutations; truncated CFTR are degraded in the endoplasmic reticulum. Thus, no CFTR protein is present on cell plasma membranes. Class II mutations likewise yield a loss of CFTR protein on plasma membranes; this class of mutation, caused by missense and deletion mutations, produces a

misfolded CFTR protein that is subsequently targeted for degradation. Patients with class III mutations have gating defects; their cells produce non-functional CFTR that is localized to the plasma membrane, but does not conduct ions or regulate other channels. Class IV mutations include missense mutations that produce CFTR with decreased chloride conductance— there is some residual function, but the channel is inefficient. Patients with class V mutations have fully functioning CFTR, but the protein is expressed at a low level due to splicing or missense mutations that reduce CFTR biosynthesis. Finally, class VI mutations include missense mutations that produce CFTR that is unstable when incorporated into the plasma membrane; thus, there is rapid turnover of the protein. Patients with class I, II, and III, mutations on average have a more severe CF phenotype, whereas patients with class IV, V, and VI mutations usually have milder disease, as they maintain some residual CFTR function (33, 144).

Cystic Fibrosis Lung Disease. Although many organ systems can be affected depending on the severity of the mutations, lung disease is the predominant cause of morbidity and mortality in CF (144). Loss of CFTR function has multiple consequences on the airways, including: reduced hydration of airway surface liquid, increased airway surface liquid acidity, poor mucociliary clearance, and abnormal mucus tethering and function (33). These conditions cause retention of abnormal mucus in the airways leading to infections with opportunistic organisms (33). CF lung disease is typified by recurring cycles of infection and neutrophilic inflammation (144), leading to bronchiectasis— transmural injury to the bronchi with airway inflammation, loss of mucociliary clearance, and patulent bronchial regions that retain infected sputum. This progressive airway injury leads to gradual loss of lung function, and ultimately respiratory failure that necessitates lung transplantation.

The dominant pathology in CF is considered to be a failure to clear microbial infections, resulting in a toxic pro-inflammatory local microenvironment in the airway (24). Children with CF have repeated viral and bacterial respiratory infections, with microbes such as *Haemophilus influenzae* and *Staphylococcus aureus*, and lung damage is caused both directly and indirectly by their bodies' inflammatory responses (44). As patients age and airway injury progresses, they become more susceptible to infection by Gram-negative bacteria. These include environmental microorganisms such as *Pseudomonas aeruginosa*, a prevalent bacterial pathogen in CF, which usually only causes disease in immunocompromised patients (24, 91). With repeated infection and colonization of the airways by viruses, bacteria— including atypical mycobacteria, and fungi— including *Aspergillus* sp., the patient's immune system responds with chronic inflammation, which contributes to lung damage, leading to more recurrent infections, and subsequently more inflammation.

This vicious cycle of pulmonary infection and inflammation in CF begins early. Neutrophils and the serine protease neutrophil elastase (NE) are detectable in patient bronchoalveolar lavage (BAL) within three months after birth, although less than half of the infants assayed had indications of an active pulmonary infection or a patient history consistent with previous infections (103, 109, 121). This implies that several factors contribute to the development of the maladaptive inflammation present in CF airways, and indeed there are many studies demonstrating that *CFTR*-deficiency alters immune system function, including aberrant responses in inflammatory cells and airway epithelium (17, 23, 43, 126). Likewise, lung damage begins early; computed tomography scans have shown that patients with CF can have bronchiectasis within the first year of life (120). The development of bronchiectasis in patients with CF is strongly associated with inflammatory proteases; neutrophil-derived proteases such as NE, cathepsin G, and proteinase

3, as well as macrophage-derived proteases like cathepsin S, and matrix metalloproteinase 9 (75, 112, 113). In particular, NE is strongly associated with the development of CF (113, 121) and non-CF bronchiectasis (19). This protease can degrade a variety of proteins (58, 142), including opsonins and proteins involved in the innate immune response such as lactoferrin and lysozyme (142), which help control infection in the lungs. Furthermore, NE digests components of the extracellular matrix (8, 61) and the peptides generated from extracellular matrix degradation also function as pro-inflammatory mediators (150). Not surprisingly, NE is also associated with the development of emphysema in chronic obstructive pulmonary disease (COPD) (8).

Neutrophil Elastase and Cystic Fibrosis Lung Disease. CF airways have up to micromolar concentrations of NE, which further stimulates an inflammatory response (142) as well as the production of MUC5AC, a prominent airway mucin (37, 62, 143, 146) that increases the risk for airway mucus obstruction (35). Release of proteolytically active NE injures the airway epithelium, triggering the release of pro-inflammatory signaling molecules. *In vitro* studies have shown that NE upregulates IL8 in human airway epithelial cell culture (84). Administering NE to mouse airways initiates an inflammatory response, increasing the concentration of pro-inflammatory cytokines, including keratinocyte chemokine (KC; murine homologue of CXCL8/IL8) (143) and High Mobility Group Box 1 (HMGB1) (47) in murine BAL. HMGB1 is an alarmin that further stimulates neutrophilic inflammation, and is another biomarker that correlates with CF lung disease severity (20, 73). HMGB1 activation of the Receptor for Advanced Glycation Endproducts (RAGE) is a feature of airway inflammation observed in COPD (29). The concentration of inflammatory biomarkers like NE and HMGB1 in sputum and BAL predict lung disease progression in CF (43, 76, 121). Given that chronic infection and rampant inflammation are characteristic of CF lung disease, eliminating pulmonary infections and decreasing inflammation

are two of the primary therapeutic approaches to CF (33, 43). While antibiotic therapy is a staple of CF therapy, there remains a need for effective anti-inflammatory therapy (33, 43).

Current and Upcoming Treatments of Cystic Fibrosis Lung Disease. First and foremost in the therapeutic repertoire of CF patients is daily airway clearance, to facilitate the removal of the abnormal, tenacious mucus from the airways (33, 81). The biological purpose of airway mucus is to trap bacterial pathogens and help clear them from the airways (145). In CF, this mechanism is hindered; mucus lingers in patient airways, and can even form a mucus plug, clogging the airway (11). Patients are given nebulized mucolytics like dornase alfa or therapy with hypertonic saline, to facilitate removal of mucus via airway clearance techniques such as chest physiotherapy or the high frequency chest wall compression therapy vest (152). Antibiotics become a mainstay of treatment early in life, with administration of oral antibiotics for *H. influenzae* and *S. aureus* bronchitis in children (33, 70). After the first culture of *P. aeruginosa*, patients are given antibiotics aimed at eradicating this pathogen: a three month regimen of oral ciprofloxacin and inhaled colistin or one month of inhaled tobramycin (30, 98, 104, 130). Both treatments have comparable efficacy, between 70 and 80%, for eliminating *P. aeruginosa*. Eradication of *P. aeruginosa* is important, as persistent infection with this species is associated with poorer outcomes, including a more rapid decline of lung function.

Patients with CF present with repeated flare-ups or exacerbations of bronchitis, labeled pulmonary exacerbations. These are diagnosed using clinical signs and symptoms— including increased cough and sputum production— and are usually accompanied by a significant drop in lung function (123). Depending on the bacteria present in the airways and the severity of symptoms, patients may be treated with oral or intravenous antibiotics and increased airway clearance (30, 81). Some patients become severely ill during pulmonary exacerbations, requiring

further support with supplemental nutrition and oxygen (33). Effective treatment of exacerbations is critical, as an increasing rate of exacerbations is associated with a more rapid decline in patient lung function and increased morbidity and mortality (28, 123, 149). Several therapies are used to maintain health and reduce the incidence of pulmonary exacerbations: inhaled dornase alfa and hypertonic saline, mentioned already as therapeutic staples for CF, as well as a variety of inhaled antibiotics, and oral azithromycin (33).

Since the successful identification of the *CFTR* gene in 1989, the holy grail of CF therapeutics has been correction or replacement of the mutant gene using molecular therapies. There has been a recent breakthrough in non-viral CFTR gene therapy in patients with CF, patients showed a modest improvement in lung function after a year of therapy— including a statistically significant increase of approximately 3.7% in forced expiratory volume in 1 second (FEV_1)— but the treatment requires further vetting before it can be approved for clinical use (3). There has also been an advent of innovative molecular therapies that target specific CFTR defects over the past decade. These include "corrector" drugs that increase the localization of CFTR to the plasma membrane and "potentiator" drugs that increase CFTR function when on the plasma membrane. Ivacaftor, a "potentiator" drug that increases CFTR-mediated chloride transport in most class III and IV mutations, thereby restoring mucociliary function *in vitro* using primary airway epithelial cells, is the first of these small molecule therapies to be approved for clinical use (25, 27, 77, 102, 111, 138, 139, 154). Clinical trials proved that ivacaftor is highly efficacious in patients with class III mutations, resulting in an average increase in FEV_1 of 10% and reducing the incidence of pulmonary exacerbations by 40% (26). A second small molecule therapeutic has been designed for patients homozygous for the c.1521_1523delCTT (p.Phe508del) mutation. This therapy is a combination of two drugs, a "corrector" and a "potentiator"— lumacaftor and ivacaftor,

respectively (138). This combination therapy increased FEV_1 by 3% and reduced the frequency of pulmonary exacerbations by 30% in patients homozygous for c.1521_1523delCTT (p.Phe508del) (12). The modest increase in lung function with this combination therapy appears be due to ivacaftor destabilizing "corrector" drugs, resulting in a lower dosage (21, 140). Thus, effective molecular therapies for c.1521_1523delCTT (p.Phe508del), the most common *CFTR* mutation, are still needed, as are drugs for Class I mutations to facilitate promoter read-through for premature stop codons and to prolong mRNA half-life.

In CF, acute and chronic neutrophilic inflammation in the lungs contributes to irreversible lung damage. Although there are many innovative treatments in development, including gene therapy and new CFTR-targeting molecular drugs, investigators have been less successful in developing effective anti-inflammatory agents. The steroid prednisone has been shown to increase forced vital capacity (FVC) in CF patients, but the many drawbacks of long-term systemic steroid use, including increased risk of opportunistic infection, CF related diabetes, and growth failure, limit its usefulness in CF (32, 43). Although research has spanned decades, only high-dose ibuprofen and chronic oral azithromycin have been identified as effective agents (33). High-dose ibuprofen has been shown to slow the rate of lung function decline in teenagers, and reduced neutrophil migration into the lungs (63-65). However, this approach is seldom used; the danger of gastrointestinal bleeds and renal toxicity necessitate regular tests to determine the levels of ibuprofen in patient blood in order to minimize the risk of either complication occurring (43). Chronic use of azithromycin may increase risk for resistant atypical mycobacteria and therefore, if mycobacteria are cultured from sputum, this therapy is discontinued (122). Current avenues of research into inflammation in CF include investigations of compounds that promote rapid resolution of infection, and those that would protect against damage mediated by proteases (33).

In order to develop more efficacious anti-inflammatory therapy, a more in-depth understanding of the factors that contribute to inflammation in CF is necessary, as a potential therapeutic must potently reduce inflammation but not interfere with the patient's ability to resolve infection (43). Until a cure for CF is developed, there is a need for efficacious anti-inflammatory therapies, as profound airway inflammation is a key driver of progressive lung disease in CF (14, 43, 112).

II. Animal Models of Cystic Fibrosis.

Translational research uses animal models in order to better understand disease pathogenesis, and for the development of novel therapeutics. An ideal animal model would both recapitulate the development of human disease and have anatomical and molecular similarities that would make it a viable candidate for testing new therapeutics. There are many animal models that approximate CF lung disease, including several in mice, and in at least three other species— rats, ferrets, and pigs (66). Each animal model has benefits and drawbacks. CF, at its core, is the consequence of a genetic mutation that causes the absence or dysfunction of CFTR at the plasma membrane; thus, the majority of CF animal models were created by deleting the *CFTR* gene.

Genetically Modified Mouse Models. Mouse models are the most prolific and best characterized of the animal models of CF currently in existence; they were the first animal models of CF to be developed (38). As a whole, mice are relatively easy to work with, and there exist well-defined methods for genetic manipulation. Consequently, there is an abundance of mouse models with CFTR knockout and knock-in mutations, on various genetic backgrounds (66). Recently, the popularity of mice with CFTR dysfunction as a model of CF has begun to wane, due to several key drawbacks. First, the relatively short lifespan of mice makes them a poor model for studying

the progression of chronic diseases, including lung disease in CF (66). Furthermore, unlike humans, mice with CFTR dysfunction do not develop spontaneous lung disease, nor do they spontaneously develop mucus obstruction or chronic airway bacterial infection (38, 157). In part, this is likely due to the fact that mice have an alternative chloride channel that compensates for loss of CFTR (66), and lack a proton (H+) cotransporter that is present in pigs and humans that increases airway acidity (118). Mice with CFTR dysfunction may be better used to study CFTR dysfunction in other organ systems, such as the gastrointestinal tract (24, 144).

The βENaC mouse model, which overexpresses said epithelial sodium channel, has also been touted as a possible model for CF (157). This model is relevant to CF because in epithelial cells with mutant CFTR, the ENaC channel is uninhibited and increases influx of sodium causing apical surface dehydration (157). These mice more closely approximate spontaneous CF pulmonary disease than mice with CFTR dysfunction, presenting with depleted airway surface liquid, reduced mucociliary clearance and airway mucus obstruction, as well as chronic airway inflammation (157). However, unlike human patients, these mice do not develop spontaneous lung infections (157).

Non-murine Animal Models of Cystic Fibrosis. CFTR-deficient ferrets are a well-characterized animal model rapidly gaining popularity in CF research (66). These ferrets have comparable CFTR expression in their lungs to that observed in humans, and neonatal ferrets with CFTR dysfunction develop spontaneous lung infections, which they have difficulty clearing (60, 128). Like humans with CF, CFTR-deficient ferrets also present with defects in mucociliary clearance in the lungs (127). On the other hand, CFTR-knockout ferrets are more difficult and costly to maintain than mice. These animals have a high incidence of meconium ileus, with up to 75% of animals dying within the first two days of life without surgical intervention (128).

CF rats are a relatively new model, initially described by Tuggle et al. in 2014 (136). In terms of pulmonary phenotype, CFTR knockout rats have decreased chloride conductance, decreased airway surface liquid, and increased intracellular mucus in the airways. Like many other animal models of CF (66), CFTR knockout rats do not have baseline differences in inflammation at birth, when compared to wild-type littermates (136). Much remains unknown regarding CFTR-deficient rats, including whether they recapitulate CF pulmonary disease as they age and their susceptibility to bacterial infection. The major drawback of the CF rat model is that its characteristics have yet to be fully explored.

Within the past decade, we have seen the advent of larger animal CF models. CFTR knockout and p.Phe508del homozygous pigs were described in 2008 (108). Pigs have a long life span, allowing for more in-depth studies of disease pathogenesis, and longitudinal trials for describing the effects of long-term use of different therapies (66). Like human patients, CF pigs develop lung disease spontaneously, although they demonstrate comparable levels of neutrophils and inflammatory markers as their wild-type littermates. Additionally, newborn pigs with CFTR dysfunction cannot successfully clear *S. aureus* infection (108, 125). On the other hand, pigs are a far more difficult model to work with. They are significantly more expensive for husbandry and care. Newborn pigs with *CFTR*-deficiency also require significant veterinary care early in life; 100% of CFTR-knockout pigs develop meconium ileus, necessitating surgery for the animals to survive (79).

A Mouse Model of Neutrophil Elastase-induced Inflammation. In summary, none of the mouse models discussed recapitulate the clinical course of lung disease seen in human patients. They do not demonstrate the spontaneous infections and inflammation that are the clinical characteristics of CF lung disease in humans. On the other hand, non-murine animal models of

CF, while more representative than mice, are also more burdensome both economically and in terms of manpower needed to maintain them.

To investigate the role of NE in regulating inflammation in CF airways, we chose to use a previously characterized mouse model of NE-induced inflammation and goblet (mucous) cell metaplasia (47, 143). This model is intended for investigating the effects of NE, and the downstream inflammatory signals triggered by NE, on the airway. Three doses of proteolytically active NE derived from human sputa, at a concentration comparable to that seen in the airways of patients with CF and chronic bronchitis (84, 124), are delivered by oropharyngeal aspiration on days 1, 4, and 7 (143). NE stimulates a robust inflammatory response in mouse lungs; within 24 h after the installation of the last NE dose (day 8), there is an influx of macrophages, neutrophils, and eosinophils and increasing airway concentrations of pro-inflammatory cytokines, including KC (143) and HMGB1 (47), readily detectible in mouse BAL. Goblet cell metaplasia, which begins on day 8, peaks on day 11 (143). This model has been useful for investigating NE-induced pulmonary oxidative stress (78), inflammatory mediators regulated by NE (47, 143), and has been used to test anti-protease and anti-inflammatory therapies (47). However, this model is not *CFTR*-deficient, and therefore not useful for evaluating the impact of loss of CFTR on innate immune function or overexuberant inflammation in the lungs. While our chosen model has many of the same benefits and drawbacks as other mouse models, it focuses on the effects of NE and neutrophilic inflammation— a crucial factor in CF lung disease. Because sphingolipids are reported to regulate inflammation (42, 74, 119) and the host response to infection (96, 131), we sought to determine whether alteration in airway sphingolipids were involved in NE-induced airway inflammation *in vivo*.

III. Sphingolipids and Inflammatory Lung Disease

Sphingolipid Structure and Biosynthesis. Sphingolipids are complex, bioactive lipids; they are canonically known as components of plasma membranes and extracellular fluids, but have more recently been recognized to be signaling molecules that can act both intra- and extracellularly (42). The sphingolipid ceramide forms the backbone of all other sphingolipids (**Figure 1**). Ceramide is composed of a sphingoid base, a long-chain amino alcohol, and an amide-linked fatty acid of various chain lengths (137). In mammalian cells, sphingosine (18-20 carbon chain lengths) and non-hydroxy fatty acids (typically, 16-24 carbon chain lengths) are the predominant constituents of ceramide (137). Sphingoid bases like sphinganine (dihydrosphingosine) and phytosphingosine (1,3,4-trihydroxydihydrosphingosine) and other fatty acids (e.g. 2-hydroxy fatty acids) can also be components of ceramide in mammals, but these are significantly rarer (137).

Ceramide can be produced through three major pathways: 1) *de novo* sphingolipid biosynthesis, 2) sphingomyelin hydrolysis by sphingomyelinases (SMases), and 3) degradation of complex sphingolipids (**Figure 2**) (74, 137). The first, rate-limiting step of *de novo* sphingolipid synthesis is catalyzed by serine palmitoyltransferase (SPT), a multimeric protein, predicted to be an octamer, consisting of three major subunit types— SPT long chain 1, 2, and 3 (SPTLC1-3, LCB1-3) (57). Regulation of SPT expression and modulators of SPT activity are under investigation but currently poorly understood (15, 16, 41, 89). It has been postulated that SPT activity could be affected by the ratio of SPTLC2 to SPTLC3, with SPTLC2 responsible for the production of $d_{18:1/18:0}$ and long chain ceramides, including $d_{18:1/22:0}$, $d_{18:1/24:0}$, and $d_{18:1/24:1}$ (68), and SPTLC3 responsible for the production of shorter chain ceramides like $d_{18:1/14:0}$ and $d_{18:1/16:0}$ (56). Orosomucoid-like protein isoform 3 (ORM (yeast)-like protein isoform 3, ORMDL3) (15, 89) and Reticulon-4 (RTN4; also referred to as Neurite OutGrowth inhibitor, NOGOB) (16, 115) are

known negative regulators of SPT activity. Additionally, downregulation of microRNA miR-137, 181c, -9 or 29a/b, increases SPT expression and thus activity (41). Ceramide synthases (CerS), of which there are six different isoforms (CerS1-6, *LASS1-6*), are responsible for forming the different chain lengths of amide-linked fatty acids on ceramide (**Table 1**). CerS show both substrate and tissue specificity, with the predominant species in the lungs reported to be CerS2 (93). Interestingly, different chain lengths of fatty acids on ceramide are not only generated by different CerS, but also have different biological activities (137). Regulation of CerS activity is currently under investigation; recent data indicate that CerS activity can be modulated post-translationally by the formation of hetero-and homodimers between different CerS (e.g. CerS2 and CerS5) (67). In cells, both SPT and CerS can be localized to the endoplasmic reticulum, where *de novo* sphingolipid occurs. In the SMase pathway, sphingomyelin is hydrolyzed into ceramide via the action of SMases. Six isoforms of SMase have been identified in mammalian cells— acid SMase, four varieties of neutral SMase, and alkaline SMase. SMases that produce ceramide associated with signaling are associated with the plasma membrane and with the endoplasmic reticulum (137). Finally, the third pathway to ceramide production is the scavenger pathway, wherein complex glycosphingolipids are broken down into sphingosine via lysosomal enzymes; ceramide is again synthesized from sphingosine via CerS (92).

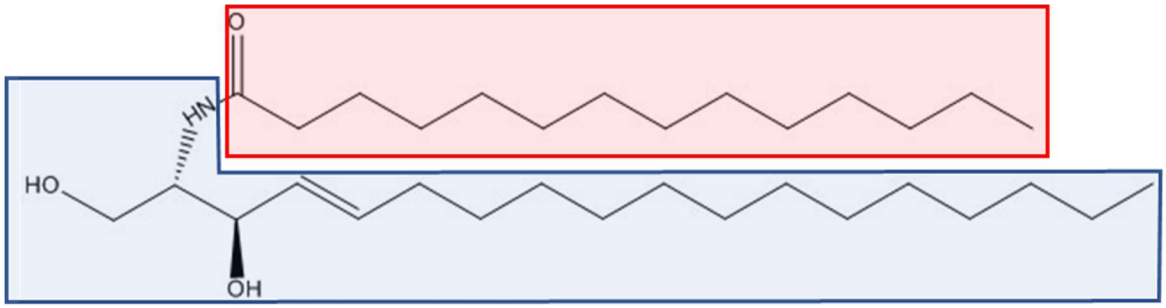
O
HN
HO
OH

Figure 1. Composition of $d_{18:1/14:0}$ ceramide. A ceramide consists of a sphingoid base such as sphingosine ranging from 18 to 20 carbon chain lengths (an 18:1 sphingosine, above, framed in blue), and an amide-linked fatty acid, usually between 14 and 36 carbon chain lengths (14:0, above, framed in red).

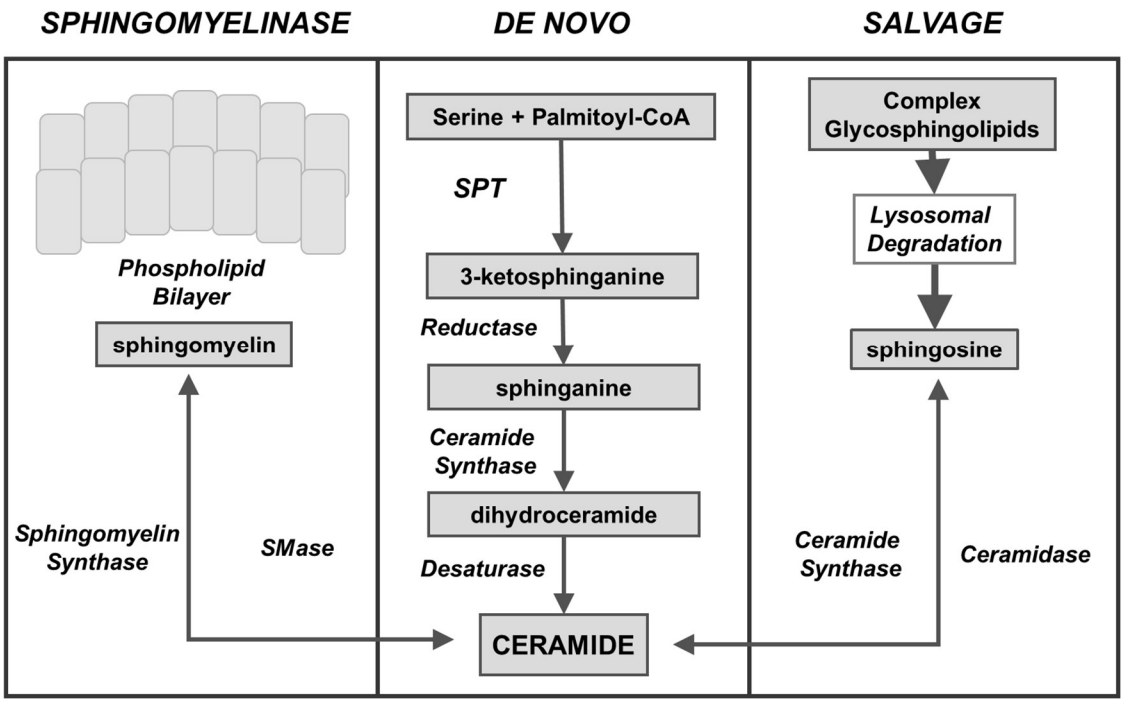
SPHINGOMYELINASE
DE NOVO
SALVAGE
Phospholipid Bilayer
sphingomyelin
Sphingomyelin Synthase
SMase
Serine + Palmitoyl-CoA
SPT
3-ketosphinganine
Reductase
sphinganine
Ceramide Synthase
dihydroceramide
Desaturase
CERAMIDE
Complex Glycosphingolipids
Lysosomal Degradation
sphingosine
Ceramide Synthase
Ceramidase

Figure 2. Pathways to ceramide synthesis. *De novo* biosynthesis of ceramide is a multi-step process. The first step is catalyzed by SPT, which combines serine and palmitoyl-CoA into 3-ketosphinganine. Next, 3-ketosphinganine is reduced to sphinganine (dihydrosphingosine) via a reductase. Sphinganine is converted to dihydroceramide by a CerS. Finally, dihydroceramide is converted by a desaturase to ceramide. In the sphingomyelinase pathway, sphingomyelin, a major plasma membrane component, is degraded by SMases to produce ceramide. The salvage pathway involves the breakdown of complex sphingolipids into sphingosine in lysosomes, followed by conversion of sphingosine to ceramide via CerS (74, 137).

Table 1. Ceramide synthases produce ceramides using acyl-CoA of different chain lengths, resulting in ceramides with different fatty acid chain lengths.

Ceramide Synthase	Acyl Chain Length Specificity
CerS1	18-carbon
CerS2	20-, 22-, 24-, 26-carbon
CerS3	22-, 24-, 26-carbon
CerS4	18-, 20-carbon
CerS5	16-carbon
CerS6	14-, 16-carbon

Sphingolipids and Inflammation. Regardless of the pathway producing the sphingolipid, these bioactive lipids are important contributors to the inflammatory response— ceramide, ceramide-1-phosphate (C1P), and sphingosine-1-phosphate (S1P) regulate inflammation when released by cells (74, 119). Ceramide, in particular, is considered to be pro-inflammatory, and recent findings indicate that ceramide can initiate a signaling cascade via the inflammasome, eventually resulting in the activation of caspase 1, and the release of pro-inflammatory cytokines including IL1β and KC (132). Ceramides of various chain lengths are induced by different stressors, and consequently facilitate cell and tissue-specific responses (48). For example, in the airway epithelium, neutral SMase is upregulated by oxidative stress, e.g. cigarette smoke, and this change is associated with increased ceramide levels in COPD (22). On the other hand, inhibition of vascular endothelial growth factor receptors stimulated *de novo* sphingolipid synthesis and facilitates the overproduction of acid SMase in rodent models of emphysema (95). Finally, direct intratracheal administration of an analogue of $d_{18:1/12:0}$ ceramide into murine airways triggers the synthesis of long-chain ceramides, septal apoptosis and emphysema (95). In the lungs, sphingolipid metabolism is closely related to inflammation, and increases in ceramide favor the development of pathological inflammation (42). Importantly, several sphingolipid species affect neutrophil biology (34). In ulcerative colitis, CerS2 and CerS6 have opposing regulatory effects on neutrophil chemotaxis into tissue (34). In the intestine, several sphingolipids affect various neutrophil functions including phagocytosis, generation of oxidants, and production of neutrophil extracellular traps (34).

Sphingolipids and Inflammatory Respiratory Diseases. Among the earliest connections discovered between pulmonary inflammation and increased levels of sphingolipids was the association between acute respiratory distress syndrome (ARDS)/acute lung injury (ALI) and

ceramide overexpression. Ceramide and glycosphingolipids are known to be increased in the BAL of patients with ARDS (106). Likewise, in pulmonary edema, increased acid SMase activity leads to higher levels of ceramide in fluids and tissue (45), and pharmacological inhibition of SMase activity or genetic ablation of acid SMase in animal models decreased pulmonary inflammation and edema (141).

Sphingolipids in Asthma. Sphingolipids have been shown to contribute to the development of lung diseases typified by chronic inflammation. Asthma, a lung disease that varies in severity, is characterized by chronic airway inflammation, increased mucus production, and airflow obstruction (87). Patients with asthma have been found to have elevated levels of S1P in their airways; this sphingolipid metabolite has been shown to stimulate airway hyperresponsiveness and inflammation in asthma models (86, 135). Likewise, animal models of allergic asthma demonstrate increased airway S1P and ceramide (85, 97). *De novo* ceramide synthesis has also been linked with asthma; a single nucleotide polymorphism that results in altered expression of ORMDL3, a negative regulator of SPT activity, has been linked to childhood asthma by a Genome-Wide Association Study (80). Interestingly, inhibiting sphingosine kinase activity, and therefore S1P production, mitigates airway inflammation in rodent models of asthma (85, 97). FTY720, an analogue of sphingosine, inhibits the activity of sphingosine kinase and interacts with S1P receptors after it is phosphorylated (74). FTY720 has been shown to decrease ceramide levels in the lungs and concurrently alleviate airway hyperresponsiveness, inflammation, and mucus production in an allergic mouse models of asthma (89).

Sphingolipids in Chronic Obstructive Pulmonary Disease. In COPD, a disease characterized by chronic inflammation in the airways, sphingolipid moieties facilitate the onset and progression of lung disease (42). In emphysema, ceramide accumulates in alveolar epithelia

and induces alveolar epithelial cell apoptosis and inflammation (42, 94). Analysis of sputum samples from patients with COPD reveals an increase in various sphingolipids, including ceramides, in patients who smoked compared with nonsmoking COPD patients (133). Environmental stresses, such as cigarette smoke, hypoxia, and chronic inflammation, downregulate CFTR expression; therefore, it is possible that loss of CFTR may be a shared mechanistic link driving the progression of lung disease in COPD and CF (101). However, there is a paucity of data published on airway sphingolipids in patients with CF, therefore, it is not yet known whether there are similarities between the airway sphingolipid profiles in COPD and CF.

Sphingolipids in Cystic Fibrosis. The maladaptive, hyperinflammatory response to airway infection characteristic of CF lung disease is associated with altered lipid homeostasis, including sphingolipids. Studies of sphingolipid imbalance in CF have focused on changes that result from CFTR dysfunction (10, 132). In human airway and nasal cells that have dysfunctional CFTR (51, 96, 132), alterations in ceramide expression are attributed to loss of CFTR activity. However, examining sphingolipid biosynthesis in experiments with human airway epithelial cell lines has yielded contradictory results, and different pathways have been implicated as responsible for changes in sphingolipid expression. Hamai et al. demonstrated that decreasing CFTR expression through genetic manipulation or expressing mutant p.Phe508del in airway epithelial cell lines results in increased intracellular sphingosine, sphinganine, and sphingomyelin, as well as $d_{18:0/16:0}$, $d_{18:1/22:0}$, $d_{18:1/24:0}$, and $d_{18:1/26:0}$ ceramide, with concurrent decreases in $d_{18:1/18:1}$ and $d_{18:0/18:0}$ ceramide (51). As decreased expression of CFTR was also associated with increased protein SPTLC1, the authors link CFTR dysfunction and *de novo* sphingolipid biosynthesis (51). In contrast, Yu et al. observed that decreased or mutant CFTR affects the function of acid SMase in human airway epithelial cell lines, with *CFTR*-deficient cells expressing less acid SMase and

producing less ceramide in response to *P. aeruginosa* infection (156). A similar defect in acid SMase activity in response to *P. aeruginosa* was observed in CFTR knockout mice (156).

There are several mouse models with different *Cftr* mutations which display varying levels of deficiency in Cftr function (158), and, much like experiments with human airway epithelial cell lines, disparate results regarding changes in ceramide levels. One variable is whether in *Cftr*-null mice, the deficiency in gut *Cftr* is corrected by replacement with intestinal fatty acid binding protein-driven human *CFTR*. The impact of gut correction is that these mice do not require a special cholesterol rich diet and the change in diet affects sphingolipid homeostasis (132). Teichgräber et al. tested two different strains of *Cftr*-deficient, gut-corrected mice (*CFTR*^{tm1Unc}-*Tg*$^{(FABPCFTR)}$ and B6.129P2(CF/3)-C*FTR*$^{TgH(neoim)Hgu}$); in both mouse models, loss of Cftr appears to result in increased acid SMase and decreased ceramidase activity, which increases ceramide production and decreases breakdown, respectively (132). Ceramide accumulation and inflammation in gut-corrected *Cftr*-deficient mice can be abrogated by decreasing the activity of acid SMase, whether by knocking down expression of the protein though genetic manipulation or through the use of SMase inhibitors (132). Guilbault et al., in contrast, observed decreased ceramides in the lung tissue of *Cftr*-knockout mice; treatment with fenretinide induced ceramide synthesis and corrected this defect, also improving the ability of these mice to clear *P. aeruginosa* pulmonary infections (49). Fenretinide has multifactorial effects on *de novo* ceramide synthesis, inducing SPT activity but also inhibiting conversion of dihydroceramide to ceramide and downregulating CerS5 expression (40, 155). Although studies in *CFTR*-deficient mouse models report both increased (46) and decreased (49) ceramide in mouse airways, normalizing pulmonary ceramide levels in these animals decreases pro-inflammatory signals (46, 49).

The impact of sphingolipids on CF lung disease in humans remains largely unexplored. To the extent of our knowledge, limited data are available regarding the sphingolipid content in the sputum and lung tissue of patients with CF. What data are available indicate that, like in COPD (92, 93), increased levels of several ceramide moieties are associated with poorer lung function and increased inflammation (133). Brodlie et al. analyzed the ceramide content of late-stage diseased CF lungs from lung transplant recipients, describing an increase in ceramide in the lower airways (13). They observed correlations between $d_{18:1/16:0}$, $d_{18:1/18:0}$, and $d_{18:1/20:0}$ ceramide moieties and markers of neutrophilic inflammation— NE and myeloperoxidase (13). In CF versus non-CF sputum, Quinn et al. observed that sphingomyelin $d_{18:1/14:0}$, $d_{18:1/15:0}$, $d_{18:1/16:1}$, and $d_{18:1/16:0}$ as well as two $d_{18:1/16:0}$ glycosphingolipids, tetraglycosylceramide and lactosylceramide were elevated (100). In a single subject with CF followed for 4.2 years, ceramide was consistently increased during treatment of pulmonary exacerbation (99). There are also limited data that indicate acid SMase may play a role in increased ceramide in patients with CF. Two early Phase II clinical trials reveal that treating patients with CF with amitriptyline (1, 83, 107), an acid SMase inhibitor, marginally increases lung function (FEV_1 % predicted). However, these trials had very limited numbers of subjects, and await confirmation in larger prospective trials.

IV. Hypothesis and Specific Aims.

Ceramide is a bioactive sphingolipid, a driver of pulmonary inflammation (74) that also negatively affects host antimicrobial responses (117, 132). In the current paradigm, ceramide accumulation in CF is attributed to dysregulation of sphingolipid homeostasis due to the loss of functional CFTR (132). However, elevated levels of ceramide have been correlated with

neutrophilic inflammation in lung tissue from patients with CF and in sputum from patients with COPD (13, 133), and is likewise increased in airway diseases typified by acute inflammation (106, 141). Additionally, administration of the protease porcine pancreatic elastase induces *de novo* synthesis of ceramide in a mouse model of emphysema (134). NE, a serine protease and major inflammatory mediator in the CF airway, is a biomarker for lung disease progression in patients (113, 121). We hypothesize that NE and ceramide create an inflammatory feedback loop, wherein NE increases ceramide biosynthesis, which subsequently potentiates neutrophilic inflammation, thereby increasing local NE levels, resulting in a correlation between NE activity and ceramide in the lungs. In order to test this hypothesis, we proposed the following aims. In Aim 1, we tested whether NE increases airway ceramide levels in Balb/C mice, using a mouse model of intratracheal NE administration that causes airway inflammation (47). In Aim 2, we determined if inhibiting ceramide biosynthesis mitigates NE-induced inflammation in Balb/C mice. Finally, in Aim 3, we analyzed sputum samples collected from subjects with CF to determine whether levels of active NE in sputum correlate with airway ceramide levels, and whether these levels vary with clinical status. This dissertation alters the current CFTR-centric paradigm of the regulation of sphingolipid homeostasis in the lungs of patients with CF, and tests whether altered sphingolipid homeostasis is required for NE-induced airway inflammation.

Chapter 2: Methods

I. A Mouse Model of Neutrophil Elastase-induced Inflammation.

A mouse model of NE-induced inflammation and mucous (goblet) cell metaplasia has been developed and characterized in both male C57BL/6J and Balb/C mice. Male Balb/C mice, 6 to 8 weeks of age, (Jackson Laboratories, Bar Harbor, ME) were maintained and treated as per an approved IACUC protocol at Virginia Commonwealth University (VCU) (AD10000870). On days 1, 4 and 7, following isoflurane anesthesia, mice were administered NE (50μg, 42μM; SE563, Elastin Products, Owensville, MO) or vehicle control by oropharyngeal aspiration (**Figure 3**). To test the effect of the inhibition of *de novo* sphingolipid synthesis, mice were administered myriocin (SPT inhibitor, 0.3mg/kg; 35891-70-4; Cayman Chemicals, Ann Arbor, MI (89, 134)) or a vehicle control by intraperitoneal (IP) injection 2h prior to aspiration of NE or vehicle control on days 1, 4 and 7. In all experiments, mice were euthanized with Euthasol (200-071; Virbac, Carros, France) at 4h, 8h, or 24h (day 8) following the final aspiration dose on day 7. After euthanasia, mice were carefully dissected. First, the thoracic cavity was opened, the sternum and ribs resected to expose the heart and lungs, and the diaphragm carefully cut. Using a 1mL syringe, blood was collected from the right and left ventricles, and diluted 1:5 in 0.5M ethylenediaminetetraacetic acid (EDTA). To isolate plasma from blood, samples were centrifuged for 10 min at 1500 ×g at 4°C, and the supernatant aliquoted and stored at -80°C. The cut to the chest was then extended to the neck, carefully exposing the trachea, and a thread looped underneath it. An intravenous catheter

(24G×3/4" Exel Safelet Catheter) was inserted into the trachea, the needle slowly removed, and looped thread tied securely to hold the catheter in place inside the trachea. A 1mL syringe, containing sterile normal saline (1mL), was attached to the catheter. The lungs were perfused with saline, and BAL extracted from the lungs. Lungs were extracted from the thoracic cavity and separated, with one lung snap-frozen in liquid nitrogen and the second stored in formalin.

Bronchoalveolar Lavage, Cell Counts, Cytospins. Collected BAL samples were centrifuged (500×g, 10 min), and the supernatant, to be used for cytokine and sphingolipid analyses, was aliquoted and stored at -80°C. The cell pellet was re-suspended in 0.5mL of ACK (Ammonium-Chloride-Potassium) Lysing Buffer to lyse any red blood cells present, mixed thoroughly, and centrifuged (500×g, 10 min). The lysing buffer was removed, and the cell pellet re-suspended in 0.1mL saline. A sample of 10µL of BAL cell pellet was aliquoted and mixed with trypan blue for cell count with a haemocytometer. A sample of 1×10^5 cells per slide were used for each cytospin and centrifuged (800rpm, 3min), with two slides prepared per mouse. Slides were air-dried overnight prior to staining with PROTOCOL HEMA3 Fixative and Solutions, as per manufacturer's instructions (122-911; Fisher Scientific, Hampton, NH). In summation, slides were dipped in Fixative solution (5×), followed by Stain 1 (5×), and Stain 2 (5×), with excess solution allowed to drain after every immersion. Slides were rinsed in distilled water and air-dried prior to mounting with VectaMount Permanent Mounting Medium (H-5000; Vector Laboratories, Burlingame, CA), and applying a glass coverslip.

Cytokine Quantitation by Sandwich ELISA. The concentration of KC in BAL fluid was measured by sandwich ELISA (MKC00B; R&D Systems, Minneapolis, MN), per the manufacturer's instructions. In summation, a mouse KC standard stock solution was reconstituted with calibrator diluent (1000 pg/mL stock) and serially (1:2) diluted in Calibrator Diluent with the

final solutions being as follows: 1000 pg/mL, 500 pg/mL, 250 pg/mL, 125 pg/mL, 62.6 pg/mL, 31.3 pg/mL, 15.6 pg/mL, and 0 pg/mL (diluent alone). A volume of 50µL Assay Diluent and 50µL of standard, control, or sample was added to each well and mixed thoroughly. Microtiter strips that were in use were covered with provided adhesive and incubated at room temperature for 2h under gentle agitation. After incubation, samples were aspirated, and the wells thoroughly washed five times with Wash Buffer (400µL per well, per wash). Mouse KC Conjugate (100µL) was added to each well, the well covered with a new adhesive strip, and the plate incubated at room temperature for 2h under gentle agitation. After incubation, samples were again aspirated, and the wells thoroughly washed five times with Wash Buffer (400µL per well, per wash). Next, 100µL of Substrate Solution were added to each well, mixed gently, and incubated for 30 min, in the dark, at room temperature. Finally, 100µL Stop Solution were added to end the reaction, mixed thoroughly, and the optical density at λ=570 nm for each well determined using a spectrophotometer. Concentrations of KC in each sample were determined using the standard curve.

Lung Homogenization. Frozen lungs were manually homogenized with a mortar and pestle and suspended in 300-500µL of either QIAzol (15596026; ThermoFisher Scientific, Waltham, MA), for later processing for RNA analysis or in a total cell lysis buffer (50mM Tris, pH 7.5, 150mM NaCl, 1mM EDTA, 1mM dithiothreitol (DTT), 1mM phenylmethanesulfonyl fluoride (PMSF), 1× protease inhibitor (P8340) , and 1× phosphatase inhibitor (P5726), Sigma-Aldrich, St. Louis, MO) for protein analysis.

Sample Processing for Q/RT-PCR. Total RNA was isolated from tissue homogenate by using QIAzol (15596026; ThermoFisher Scientific, Waltham, MA) and then processed as per manufacturer's instructions. In summation, after the sample was homogenized and QIAzol added,

for every mL of QIAzol, 0.2 mL of chloroform was added to the sample. After capping the tube securely, samples were vigorously shaken of 15-20 sec, then allowed to sit for 3 min at room temperature. Samples were centrifuged at 12000×g at 4°C, for 15 min. The aqueous phase, present at the top of the tube, was transferred to a new microfuge tube, and 0.5mL (per initial mL of QIAzol used) of isopropanol and 5µL of glycogen was added to each sample and mixed thoroughly by vortexing. Samples were incubated at -20°C overnight, and then centrifuged at 12000×g at 4°C, for 10 min. The supernatant was aspirated and discarded, with care taken not to disturb the pellet. A volume of 75% ethanol (1mL for every mL of QIAzol Lysis Buffer used) was added, and the sample centrifuged at 7500×g for 5 min, at 4°C. The supernatant was removed, and the sample spun again at 7500×g for 5 min, at 4°C so that any remaining ethanol could be aspirated. The RNA pellet was briefly air-dried at room temperature, for no more than 5-10 min, and then dissolved in 25µL of diethyl pyrocarbonate (DEPC)-treated water, warmed to 55-60°C for 10 min. RNA was quantified by determining sample absorbance at λ=260/280, and diluted for DNAse treatment.

A sample of 5µg RNA was treated with DNase (18068-015, ThermoFisher Scientific, Waltham, MA), according to the manufacturers protocol. In summary, 5µg RNA was combined with 5µL DNase I Reaction Buffer and 5µL DNase I (Amplification Grade) and brought to a volume of 50µL with DEPC-treated water. Each sample was mixed thoroughly and then incubated for 15 min at room temperature. Next, 5µL of 25mM EDTA was added to each sample to stop the reaction, and samples were incubated at 65°C for 10 min. DNase-treated RNA was quantified by determining sample absorbance at λ=260/280 and diluted in DEPC-treated water for Q/RT-PCR. Q/RT-PCR was performed on a SDS 7300 machine (Applied Biosystems). In summary, 5µL of diluted RNA was combined with 15µL of master mix, consisting of: 10µL qScript XLT One-Step RT-qPCR ToughMix, ROX (2X) (95133-500, Quanta Biosciences), 1µL 20X TaqMan Assay

Reagent (primer and probe mix), and 4μL DEPC-treated water in each sample well. Universal amplification conditions were used: 50°C for 30 min, then 95°C for 2 min, and finally 40 cycles of 95°C for 15 sec followed by 60°C, 1 min.

Q/RT-PCR was performed to determine if administering NE modulated the expression of genes relevant to sphingolipid synthesis (**Table 2**) in mouse lungs. Mouse β-actin (4352341E; ThermoFisher Scientific, Waltham, MA) was used as an endogenous control. The relative level of gene expression was calculated using the ΔΔCT method, which represents the fold difference in gene expression, corrected for expression of an endogenous control gene, and then normalized to control treated samples.

Table 2. List of target genes assayed by Q/RT-PCR.

Target Gene	Primer ID[a]
SPTLC1	Mm00447343_m1
SPTLC2	Mm00448871_m1
β-actin	Mm00607939_s1

[a] Primers acquired from ThermoFisher Scientific (Waltham, MA).

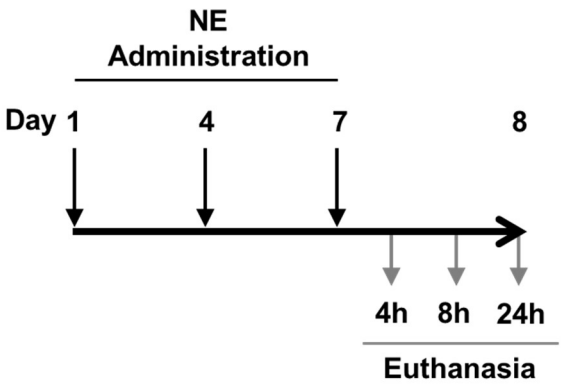
NE
Administration
Day 1
4
7
8
4h
8h
24h
Euthanasia

Figure 3. Overview of the treatment protocol for NE aspiration. Mice received 3 doses of NE, with a dose delivered via oropharyngeal aspiration on days 1, 4, and 7. After euthanasia, at 4, 8, or 24 h (day 8) after final NE dose, lungs and BAL were harvested.

Sample Processing for Western Blot. After homogenization, samples were sonicated three times for 15sec and incubated with agitation for 1h, at 4°C. Homogenates were clarified by centrifugation (16,000×g, 4°C, 30 min). The resulting supernatant was the lung lysate protein, ready for quantitation and storage at -80°C in single use aliquots for western blot. A DC Protein Assay (5000116; BioRad, Hercules, CA) was used to determine sample protein concentrations, as per the manufacturer's instructions.

Western Blot. Mouse whole lung lysate (50µg) or BAL (40µL) were separated by electrophoresis on a 4-20% SDS-PAGE gel (17000436; BioRad Hercules, CA), transferred to a nitrocellulose membrane, and blocked with 5% nonfat milk in 15mM Tris, 150mM NaCl, 0.1% Tween-20 (TBST). Membranes were incubated in mouse monoclonal anti-HMGB1 (sc-56698; 1:5000 in 5% Milk/TBST; SantaCruz Biotechnology, Dallas, TX), rabbit polyclonal anti-SPTLC1 (15376-1-AP; 1:5000 in 5% Milk/TBST; Proteintech, Chicago, IL), rabbit polyclonal anti-SPTLC2 (ab23696; 0.5µg/mL in 5% Milk/TBST; AbCam, Cambridge, United Kingdom), mouse monoclonal anti-NOGO (sc-271878; 1:1000 in 5% Milk/TBST; SantaCruz Biotechnology, Dallas, TX) or anti-ORMDL3 (ABN417; 1:1000 in 2%BSA/TBST; Millipore, Billerica, MA) primary antibody overnight at 4°C, followed by either HRP-conjugated goat anti-mouse antibody (SC-2005, SCBT, Dallas, TX) or HRP-conjugated goat anti-rabbit antibody (7074,Cell Signaling Technology, Danvers, MA). Antigen-antibody complexes were visualized by chemiluminescence (ECL Plus; RPN2132; GE Healthcare Life Sciences, Piscataway, NJ), as per the manufacturer's instructions. Membranes with whole lung lysate were washed three times, 10min each, in TBST and re-probed with a monoclonal antibody against β-actin (A5441; 1:5000 in 5% Milk/TBST; Sigma, St. Louis, MO) to confirm equivalent protein loading. Densitometry of target bands was

determined by ImageJ Software (116), normalized to actin, and then compared to average control values in each experiment.

II. Analyses of Sputum from Subjects with CF.

Subject Demographics and Sputum Collection. Subjects were recruited from the VCU CF Center. The study was approved by the Institutional Review Board at VCU (HM12402); subjects or parents/guardians provided written informed consent before enrollment into the VCU Biospecimen Repository and for participation in the CF Foundation Registry. Fifteen subjects were selected for this retrospective study. Two sputum samples per subject, one collected during a hospitalization for a pulmonary exacerbation and a second sample collected during an outpatient visit within six months of that hospitalization, were analyzed. All subjects spontaneously expectorated sputum and had mild-to-moderate (FEV_1 50-98% predicted) or severe (FEV_1<50% predicted) obstructive lung disease. Inclusion criteria consisted of: age greater than or equal to 6 years old, and positive sweat chloride test. Exclusion criteria included: inability to perform spirometry, inability to spontaneously expectorate sputum, current treatment with tricyclic antidepressants, which have been demonstrated to inhibit acid SMase activity (e.g. amitriptyline)(6), or lung transplantation. There were no further exclusion criteria concerning medication use or participation in other research studies. Subject demographics are detailed in **Table 3**.

An aliquot of sputum was sent for bacteriology cultures, performed according to CF Foundation standard protocols at the beginning of therapy (114). Any remaining aliquots of sputum were visually separated from saliva and oral detritus, and stored for later analysis at -80°C.

Table 3. Subject demographics.

Subject	Gender	Age	CF Genotype	Clinical Status	FEV_1 % predicted	MRSA	*P. aeruginosa*
1	M	21	c.1022_1023insTC, c.1521_1523delCTT	H O	65 80	+ +	- -
2	M	25	c.1521_1523delCTT, c.2825delT	H O	44 59	+ +	- -
3	F	19	Unknown	H O	21 27	- -	+ +
4	M	16	c.1521_1523delCTT, c.1021T>C	H O	58 73	+ +	- -
5	M	17	c.1521_1523delCTT, c.1680-1G>A	H O	28 33	- -	- +
6	M	39	c.1521_1523delCTT, c.1521_1523delCTT	H O	60 57	+ +	- -
7	F	15	c.1521_1523delCTT, c.1521_1523delCTT	H O	42 39	- -	+ +
8	F	19	c.1521_1523delCTT, c.54-5940_273+10250del21kb	H O	33 28	- -	+ +
9	M	37	c.1521_1523delCTT, c.1521_1523delCTT	H O	41 48	- -	+ +
10	M	20	c.1521_1523delCTT, c.1521_1523delCTT	H O	42 49	- +	+ +
11	F	13	c.1521_1523delCTT, c.3909C>G	H O	50 59	+ +	- +
12	F	16	c.1521_1523delCTT, c.1397C>A	H O	26 27	- -	+ +
13	F	18	c.1521_1523delCTT, c.1521_1523delCTT	H O	39 45	+ +	- -
14	F	17	c.1521_1523delCTT, c.1400T>C	H O	26 28	- +	+ +
15	M	12	c.1521_1523delCTT, c.1521_1523delCTT	H O	84 82	- -	- -

H, hospitalization; O, outpatient clinic visit; M, male; F, Female; +, positive culture; -, negative culture.

Sputum Processing. Frozen sputum samples were thawed on ice. Afterwards, samples were weighed, and mixed with an equal volume (1:1, weight (mg):volume (mL)) of normal saline with 10% Sputolysin (0.1% DTT; Calbiochem/EMD Millipore, Billerica, MA). Diluted sputum samples were mixed by vortexing at room temperature for 15-30 sec. Next, samples were incubated at 37°C for 15 min. After mixing samples gently by inversion, they were centrifuged at 25000×g for 30 min at 4°C to collect the sputum supernatant which was immediately aliquoted and either used for measuring NE activity or sent for sphingolipid analysis.

Neutrophil Elastase Activity Assay. NE activity in sputum supernatants was measured using a chromogenic microtiter plate assay with Succinyl-Ala-Ala-Pro-Val-p-nitroanalide (3mM, in 50% DMSO; Sigma-Aldrich, St. Louis, MO) as the substrate, as detailed previously (39, 146). In summation, NE standards, using human sputum-derived active NE (SE563, Elastin Products, Owensville, MI), were made at concentrations of: 30, 15, 7.5, 3.75, 1.875, 0.94, 0.47, 0.23 and 0 µg/mL in 4-(2-hydroxyethyl)-1-piperazineethanesulfonic acid (HEPES) Buffer (0.125M HEPES, pH 7.5, 0.125% Triton-X 100). A volume of 100µL of standard or sample was mixed with 100µL of saline in the wells of a 96-well plate, and 50µL of substrate were added to each well. Absorbance at λ=405nm was read with a spectrophotometer for 3 min. NE activity (µg/mL) was plotted against the slope of the increase of absorbance (OD/min). The concentration of active NE was expressed in nM, extrapolated from the standard curve (30, 15, 7.5, 3.75, 1.875, 0.94, 0.47, 0.23 and 0 µg/mL).

III. Sphingolipid Analysis.

Both BAL fluid (350µL) and sputum supernatants were assessed for sphingolipid content by the Lipidomics/Metabolomics Core at VCU, using reverse phase high-performance liquid chromatography/electrospray ionization tandem mass spectrometry (HPLC-ESI-MS/MS) (119, 151). In summary, samples were processed to extract lipids as follows. After transferring samples into borosilicate tubes with a Teflon-lined cap (#60827-453, VWR, West Chester, PA), 2mL of CH3OH, 1mL of CHCl3 and the internal standard cocktail (250pmol of each sphingolipid species, dissolved in a final total volume of 10µl of 7:2:1 ethanol:methanol:water) were added. Contents were dispersed by applying an ultra sonicator (30sec, at room temperature), and the resulting single-phase mixture incubated at 48°C overnight. Samples were cooled, and 150µl of 1M KOH in CH3OH added. After sonication, samples were incubated in a shaking water bath (37°C, 2h). Glacial acetic acid (12µl) was added to bring the extract to neutral pH. Samples were centrifuged, the supernatant transferred to a new tube, and dried using a Speed Vac. Dried sample residue was reconstituted in 0.5 mL of the starting mobile phase solvent for LC-MS/MS analysis and sonicated briefly for 15sec. After centrifugation for 5min in a tabletop centrifuge, supernatant was transferred to autoinjector vials for analysis. Sphingolipids were separated by reverse phase liquid chromatography using a Supelco 2.1 (i.d.) × 50 mm Ascentis Express C18 column (Sigma, St. Louis, MO) and binary solvent system (flow rate, 0.5 mL/min) with the column oven set to a temperature of 35°C.

Samples separated by reverse phase chromatography were nebulized, charged using an electrospray ionization source, and resolved in an AB Sciex 5500 quadrupole/linear ion trap (QTrap) (SCIEX Framingham, MA) operating in a triple quadrupole mode. Q1 and Q3 were set to pass molecularly distinctive precursor and product ions (or a scan across multiple *m/z* in Q1 or

Q3), using N_2 to collisionally induce dissociations in Q2 (which was offset from Q1 by 30-120 eV); the ion source temperature was set to 500°C.

Samples were assayed for the following sphingolipids: sphingosine, sphinganine, S1P, sphinganine-1-phosphate (Sa1P), as well as sphingomyelin, ceramide, monohexosylceramide moieties with the following fatty acid chain lengths— $d_{18:1/14:0}$, $d_{18:1/16:0}$, $d_{18:1/18:1}$, $d_{18:1/18:0}$, $d_{18:1/22:0}$, $d_{18:1/24:1}$, $d_{18:1/24:0}$, $d_{18:1/26:1}$, and $d_{18:1/26:0}$. For sphingolipid nomenclature (for example, $d_{18:1/14:0}$), the first number describes the sphingoid base (18:1 represents sphingosine) and the second the fatty acid chain (14:0 for a 14-carbon chain).

IV. Statistical Analyses.

Mouse Data. Quantitation of sphingolipids— ceramide, monohexosylceramides, sphingosine, sphinganine, S1P, Sa1P, and sphingomyelin in BAL, BAL total cell numbers differentials, BAL cytokine levels, as well as relative mRNA and protein expression were compared among the treatment groups using either Mann-Whitney U Tests (Wilcoxon Rank Sum Test), or, if there were more than two conditions, using one-way nonparametric ANOVA analyses (Kruskal-Wallis Test) with *post hoc* multiple comparison adjustments using Mann-Whitney U Tests (Wilcoxon Rank Sum Test) (GraphPad Prism, La Jolla, CA). Data are presented as mean ± SEM, with differences of $p<0.05$ considered statistically significant.

Human Data. For human samples, we used a two-tailed, nonparametric paired statistical test: the Wilcoxon Signed Rank Test, to determine whether there were significant differences between stable and exacerbated sputum measures for sphingolipid levels, and for the concentration

of active NE, and FEV_1 % predicted using GraphPad Prism 5 (GraphPad Software, Inc., La Jolla, CA)(153). Differences between groups were considered significant at $p<0.05$. We used linear correlation to determine the association between concentrations of active NE and sphingolipid levels using GraphPad Prism 5 (GraphPad Software, Inc., La Jolla, CA). Again, p-value of less than 0.05 was considered statistically significant.

Data were also analyzed using a linear mixed model (148), to determine the likelihood of an association between the concentration of NE and various sphingolipids, as well as whether (i) bacterial culture positive for methicillin resistant *Staphylococcus aureus* (MRSA) or *Pseudomonas aeruginosa*, (ii) patient lung function, or (iii) patient sex, modified the association. A p-value less than 0.05 was considered statistically significant.

Chapter 3: Results

I. Neutrophil Elastase Induced Changes in Sphingolipid Levels in Mouse Airways.

Oropharyngeal Aspiration of Neutrophil Elastase Increased the Levels of Ceramide in Murine Airways. Previously, it has been shown that oropharyngeal aspiration of NE causes airway inflammation in mice (47, 143); we used this model to determine whether NE-induced inflammation correlated with increased airway sphingolipids. As detailed previously (47, 143) and in the Methods section, mice were administered three doses of NE or vehicle control on days 1, 4, and 7 (**Figure 3**). At 4h (n=4 animals per group), 8h (n=4 animals per group), or 24h (n=14 control,

n=16 NE) after the final dose of NE was administered, mice were euthanized, and BAL and tissue samples collected for analysis. In order to characterize the sphingolipid profile associated with airway inflammation in this model, sphingolipid concentrations in BAL were determined by HPLC-ESI-MS/MS (**Tables 4-7**).

First, we assessed BAL for the presence of sphingomyelin, ceramide, and monohexosylceramide moieties ($d_{18:1/14:0}$, $d_{18:1/16:0}$, $d_{18:1/18:1}$, $d_{18:1/18:0}$, $d_{18:1/22:0}$, $d_{18:1/24:1}$, $d_{18:1/24:0}$, $d_{18:1/26:1}$, and $d_{18:1/26:0}$) as well as sphingosine, sphinganine, S1P and Sa1P. Levels of these sphingolipids after aspiration of NE were compared with controls at the same time point— 4, 8, or 24h after the third and final NE dose was administered. To track overarching trends in sphingolipid levels, we calculated the sum of sphingomyelin, ceramide, and monohexosylceramide moieties, reported as total sphingomyelin (**Table 4**), total ceramide (**Table 5**), and total monohexosylceramide (**Table 6**), respectively, and depicted in **Figure 4**. At 24h, we observed that mice administered NE demonstrated a 2.5-fold increase in total ceramide, a statistically significant difference ($p<0.001$) from the levels observed in control treated animals (**Table 5**, **Figure 4**). However, the levels of total sphingomyelin (**Table 4**) and monohexosylceramide (**Table 6**), and likewise levels of sphingosine, sphinganine, S1P and Sa1P (**Table 7**) did not differ significantly between control and NE groups at 24h. Analyzing the different ceramide moieties present in BAL revealed that total ceramide was increased due to statistically significant increases in long chain ceramides. Specifically, levels of $d_{18:1/22:0}$, $d_{18:1/24:0}$ and $d_{18:1/24:1}$ ceramide moieties increased by approximately 145% ($p= 0.003$), 211% ($p=0.001$), and 256%, ($p=0.001$), respectively (**Table 5**, **Figure 5**). There was also a statistically significant increase in $d_{18:1/26:0}$ ceramide (**Table 5**), but the levels of the moiety present in murine BAL— below 10 pmol/mL— led us to conclude the effects of this ceramide were likely negligible.

Analyzing individual sphingomyelin and monohexosylceramide moieties revealed no further statistically significant differences in sphingolipid levels between control and NE groups at 24h (**Table 4, 6**). However, there were trends towards increased $d_{18:1/22:0}$, $d_{18:1/24:1}$, $d_{18:1/24:0}$ sphingomyelin moieties at 4 and 8h after NE was administered compared to controls. Similarly, there were no significant variations in sphingolipid levels between animals that were administered vehicle control versus NE at either 4 or 8h when the total sphingolipids or individual moieties were analyzed (**Tables 4-7**).

Table 4. Levels of sphingomyelin moieties in BAL in mice administered vehicle control or NE.

	4h[a]		8h[b]		24h[c]	
Sphingomyelin (pmol/ml)	**Control**	**NE**	**Control**	**NE**	**Control**	**NE**
$d_{18:1/14:0}$	18.48±0.89	23.25±2.42	26.03±6.25	23.9±3.21	17.70±0.68	27.68±3.48
$d_{18:1/16:0}$	584.53±13.68	676.33±32.12	641.73±31.68	735.20±20.40	1196.73±103.19	1371.26±154.38
$d_{18:1/18:1}$	48.20±0.94	51.68±4.40	52.23±4.74	56.20±1.66	1630.47±252.92	2232.50±475.68
$d_{18:1/18:0}$	527.83±12.34	609.70±26.59	520.20±63.91	625.70±9.29	2073.24±274.02	2075.27±284.77
$d_{18:1/20:0}$	1243.18±11.63	1260.18±46.95	1280.58±80.29	1322.23±70.25	2867.21±265.25	2936.53±300.19
$d_{18:1/22:0}$	378.65±12.60	536.75±27.06	374.58±44.72	555.47±79.14	258.48±20.90	414.88±40.11
$d_{18:1/24:1}$	260.63±4.17	383.43±24.19	296.33±25.99	424.03±56.12	232.93±13.63	514.47±58.21
$d_{18:1/24:0}$	182.23±6.14	247.95±16.21	206.85±28.06	293.30±47.27	138.83±11.04	282.31±29.03
$d_{18:1/26:1}$	14.63±0.43	16.68±1.77	17.35±3.26	19.37±2.72	6.86±1.19	11.31±1.66
$d_{18:1/26:0}$	18.63±0.92	19.03±1.76	21.35±3.89	22.57±2.59	7.99±1.57	12.74±2.20
Total[d]	3276.97±39.07	3824.96±168.32	3437.27±195.57	4077.94±189.75	10470.43±1154.85	11669.64±1437.65

[a] BAL collected at 4h (n=4 per group). [b] BAL collected at 8h (n=4 control, 3 NE, respectively). [c] BAL collected at 24 h (n=16 control, n=14 NE). [d] Total sphingomyelin represents the mean of a summation of individual sphingomyelin moieties at each time point; total sphingomyelin at 24 h is also shown in **Figure 2**. Samples were collected and processed using LC-MS/MS. Data are expressed as mean ± SEM pmol/mL BAL fluid, with comparisons between control and NE treated groups at each time point. There are no statistically significant differences in sphingolipid profile at each time point.

Table 5. Levels of ceramide moieties in BAL in mice administered vehicle control or NE.

	4h[a]		8h[b]		24h[c]	
Ceramide (pmol/ml)	**Control**	**NE**	**Control**	**NE**	**Control**	**NE**
$d_{18:1/14:0}$	0.20± 0.02	0.13±0.02	0.24±0.07	0.14±0.01	5.83±1.35	3.43±0.88
$d_{18:1/16:0}$	245.02±28.27	120.47±13.9	236.23±31.64	124.73±4.25	89.31±16.33	110.17±15.30
$d_{18:1/18:1}$	5.14±0.33	3.15±0.15	5.31±0.37	5.00±1.00	17.01±2.79	21.33±4.87
$d_{18:1/18:0}$	3.14±0.64	1.92±0.08	2.14±0.23	3.40±1.65	8.96±1.36	10.18±1.96
$d_{18:1/20:0}$	4.99±0.30	3.25±0.54	4.97±0.70	6.34±3.28	8.41±1.03	13.34±2.23
$d_{18:1/22:0}$	22.72±2.70	19.01±1.84	22.96±3.15	25.38±5.56	29.23±4.85	63.81±10.89*
$d_{18:1/24:1}$	85.41±3.39	46.86±3.51	69.74±7.90	79.41±21.95	76.91±9.26	227.03±38.19*
$d_{18:1/24:0}$	91.54±19.27	67.93±10.44	104.52±5.79	101.96±19.20	98.85±10.66	268.46±41.43*
$d_{18:1/26:1}$	6.32±0.15	4.03±0.25	7.12±0.60	5.91±0.79	8.70±1.04	8.79±1.73
$d_{18:1/26:0}$	5.03±0.10	3.25±0.23	5.79±0.55	4.72±0.67	3.79±0.72	7.05±0.62*
Total[d]	469.52±40.10	270.01±16.92	459.04±39.52	357.00±55.31	349.34±32.57	738.52±96.90*

[a] BAL collected at 4h (n=4 per group). [b] BAL collected at 8h (n=4 control, 3 NE, respectively). [c] BAL collected at 24 h (n=16 control, n=14 NE). [d] Total ceramide represents the mean of a summation of individual ceramide moieties at each time point; total ceramide at 24 h is also shown in **Figure 2**. Samples were collected and processed using LC-MS/MS. Data are expressed as mean ± SEM pmol/mL BAL fluid, with comparisons between control and NE treated groups at each time point. *, $p<0.05$, when compared to control animals at the same time point. Ceramide moieties $d_{18:1/22:0}$, $d_{18:1/24:1}$, and $d_{18:1/24:0}$ at 24 h are also displayed in **Figure 3**.

Table 6. Levels of monohexosylceramide moieties in BAL in mice administered vehicle control or NE.

	4h[a]		8h[b]		24h[c]	
Monohexosylceramide (pmol/ml)	**Control**	**NE**	**Control**	**NE**	**Control**	**NE**
$d_{18:1/14:0}$	1.24±0.17	1.61±0.20	1.17±0.19	1.60±0.21	1.92±0.44	2.35±0.46
$d_{18:1/16:0}$	20.35±1.95	14.02±0.80	20.20±1.33	20.25±2.85	39.83±7.22	28.40±4.08
$d_{18:1/18:1}$	0.00±0.00	0.00±0.00	0.00±0.00	0.00±0.00	0.10±0.02	0.18±0.06
$d_{18:1/18:0}$	0.14±0.04	0.33±0.08	0.03±0.02	0.12±0.09	0.41±0.11	0.43±0.09
$d_{18:1/20:0}$	0.98±0.15	1.21±0.25	0.74±0.14	0.95±0.03	0.63±0.12	0.71±0.17
$d_{18:1/22:0}$	12.40±1.23	12.70±2.03	13.51±3.45	13.24±2.61	12.23±2.70	7.97±2.28
$d_{18:1/24:1}$	22.28±4.38	22.49±2.09	30.93±5.01	31.41±3.23	12.30±3.61	12.17±7.31
$d_{18:1/24:0}$	55.70±2.70	69.15±7.77	64.75±5.45	80.42±11.69	22.99±6.19	22.31±11.11
$d_{18:1/26:1}$	4.89±0.21	5.22±0.75	5.11±0.21	7.45±1.77	2.18±0.58	0.74±0.39
$d_{18:1/26:0}$	1.23±0.25	1.14±0.09	1.01±0.10	1.51±0.32	0.44±0.20	1.00±0.31
Total[d]	119.20±8.51	127.88±12.69	137.46±13.58	156.94±17.84	144.71±20.21	193.79±26.34

[a] BAL collected at 4h (n=4 per group). [b] BAL collected at 8h (n=4 control, 3 NE, respectively). [c] BAL collected at 24 h (n=16 control, n=14 NE). [d] Total monohexosylceramide represents the mean of a summation of individual monohexosylceramide moieties at each time point; total monohexosylceramide at 24 h is also shown in **Figure 2**. Samples were collected and processed using LC-MS/MS. Data are expressed as mean ± SEM pmol/mL BAL fluid, with comparisons between control and NE treated groups at each time point. There are no statistically significant differences in sphingolipid profile at each time point

Table 7. Levels of sphingosine, S1P, sphinganine, and Sa1P in BAL in mice administered vehicle control or NE.

	4h[a]		8h[b]		24h[c]	
Sphingolipid (pmol/ml)	**Control**	**NE**	**Control**	**NE**	**Control**	**NE**
sphingosine	15.00±1.21	26.04±0.96	20.12±1.33	23.12±3.33	70.83±24.31	64.18±28.68
S1P	5.34±0.19	6.50±0.42	7.85±1.03	8.20±1.03	4.58±0.90	9.90±3.83
sphinganine	1.97±0.30	1.86±0.25	1.88±0.37	3.17±1.03	2.64±0.53	7.90±3.38
Sa1P	0.50±0.02	0.56±0.03	0.44±0.07	0.43±0.03	1.59±0.40	3.11±1.25

[a] BAL collected at 4h (n=4 per group). [b] BAL collected at 8h (n=4 control, 3 NE, respectively). [c] BAL collected at 24 h (n=16 control, n=14 NE). Samples were collected and processed using LC-MS/MS. Data are expressed as mean ± SEM pmol/mL BAL fluid, with comparisons between control and NE treated groups at each time point. Sphingosine levels in BAL as 24 h — as sphingosine is the sphingoid base component within the sphingolipid moieties assessed— are also shown in **Figure 2** as total sphingosine. There are no statistically significant differences in sphingolipid profile at each time point.

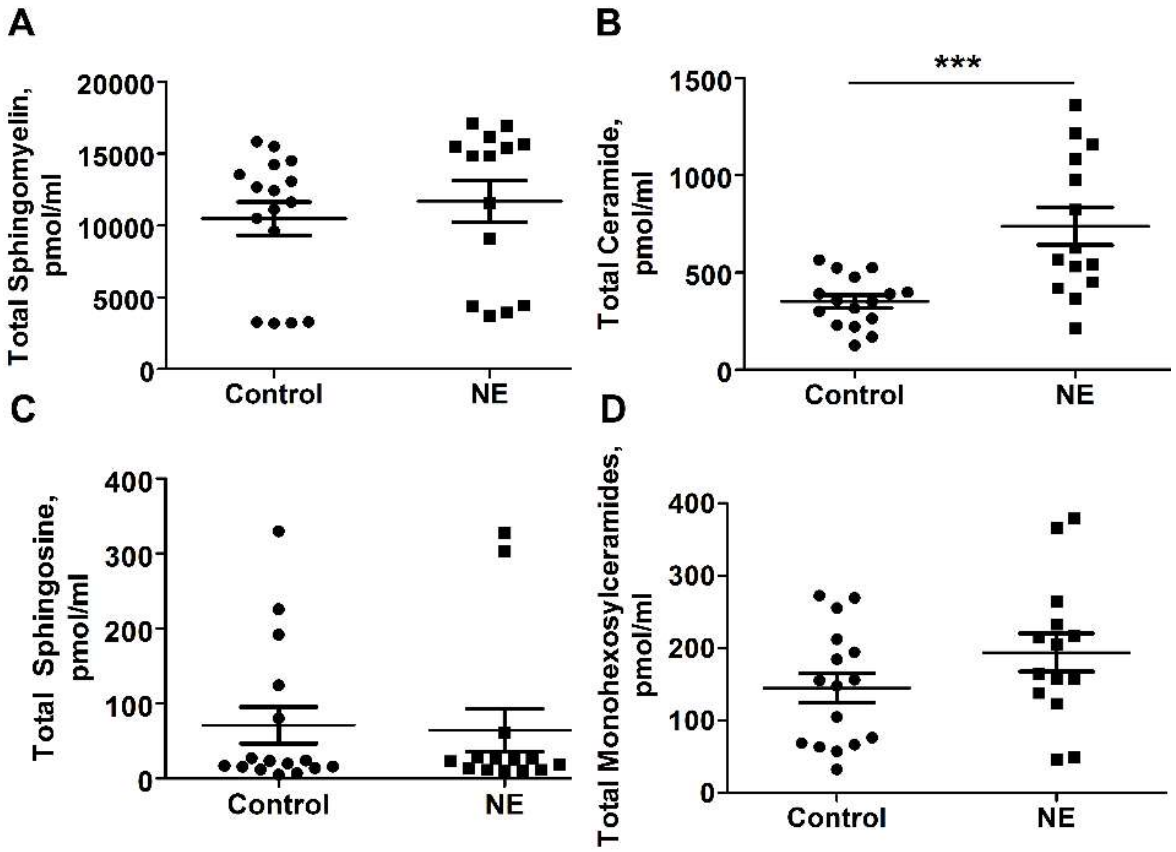
A
Total Sphingomyelin, pmol/ml
20000
15000
10000
5000
0
Control
NE
B
***
Total Ceramide, pmol/ml
1500
1000
500
0
Control
NE
C
Total Sphingosine, pmol/ml
400
300
200
100
0
Control
NE
D
Total Monohexosylceramides, pmol/ml
400
300
200
100
0
Control
NE

Figure 4. Total sphingolipid analysis of BAL from mice treated with control vehicle or NE. Mice were treated with NE (50μg; 42μM) or control vehicle by oropharyngeal aspiration on days 1, 4, and 7. BAL (1mL) was harvested on day 8. The levels of total sphingomyelin (**A**), ceramide (**B**), sphingosine (**C**) and monohexosylceramide (**D**) in 350μL of murine BAL, measured by HPLC-ESI-MS/MS, were increased at 24h (day 8) after final NE administration compared to vehicle control. The data show sphingolipid content of BAL in pmol/mL, summarizing 2 experiments, n=16 control, n=14 NE. Data (mean ± SEM) were compared by Mann-Whitney U (Wilcoxon Rank Sum) Test; ***, $p<0.001$. These data have been published (59).

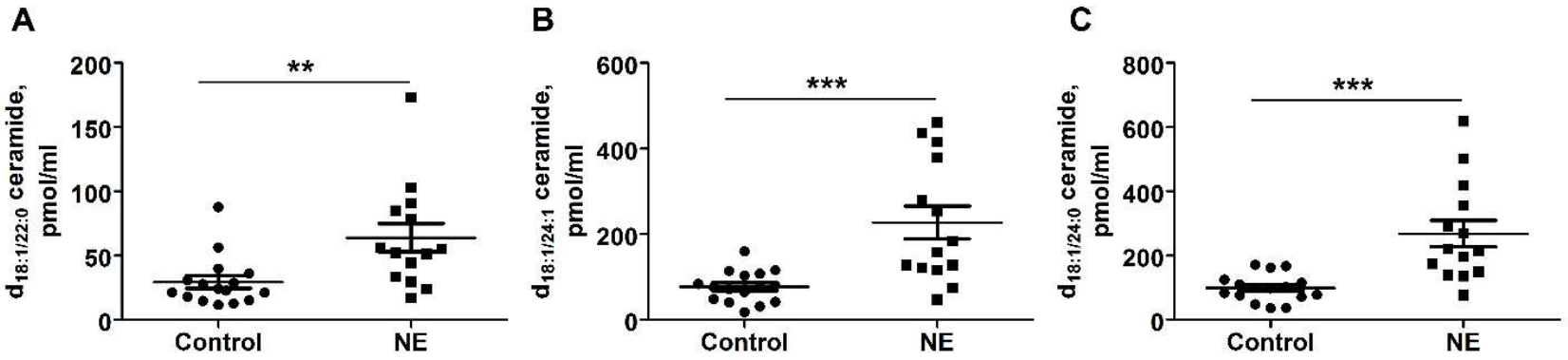
A
B
C
$d_{18:1/22:0}$ ceramide, pmol/ml
$d_{18:1/24:1}$ ceramide, pmol/ml
$d_{18:1/24:0}$ ceramide, pmol/ml
**
***
***
200
150
100
50
0
600
400
200
0
800
600
400
200
0
Control
NE
Control
NE
Control
NE

Figure 5. Analysis of ceramide chain length in BAL of mice treated with control vehicle or NE. Mice were treated with NE (50µg, 42µM) or control vehicle on days 1, 4, and 7. BAL (1mL) was harvested on day 8. The ceramide levels in murine BAL (350µL) were measured by HPLC-ESI-MS/MS at 24h after final NE administration compared to vehicle control. Ceramide $d_{18:1/22:0}$ (**A**), $d_{18:1/24:1}$ (**B**), $d_{18:1/24:0}$ (**C**) moieties were increased. The data show sphingolipid content of BAL in pmol/mL, summarizing 2 experiments, n=16 control, n=14 NE. Data are summarized as mean ± SEM and compared by Mann-Whitney U (Wilcoxon Rank Sum) Test; **, $p<0.01$, ***, $p<0.001$. These data have been published (59).

Administering Neutrophil Elastase Increased the Concentration of SPTLC2 Protein in Murine Lungs. To determine how NE modulated ceramide levels, we investigated whether NE stimulated *de novo* ceramide synthesis by modulating SPT expression. We analyzed the protein expression levels of the two best-characterized subunits of SPT, the enzyme responsible for the rate-limiting step of *de novo* sphingolipid synthesis. At 4 and 8h, SPTLC2 protein expression did not differ between mice administered NE and those given vehicle control (**Figure 6**). In contrast, at 24h, the level of SPTLC2 protein in whole lung lysates was increased in NE-treated animals by approximately 2.5-fold ($p<0.001$) (**Figure 7**). The levels of SPTLC1 protein were decreased, dropping by approximately 30% ($p=0.019$) compared to control treated mice at the same time point (**Figure 7**).

To determine whether the observed changes in SPT subunits' protein concentration reflected a change in transcription, we assessed the levels of *SPTLC1* and *SPTLC2* mRNA in mouse lungs using Q/RT-PCR. Interestingly, there were no significant changes in *SPTLC1* or *SPTLC2* mRNA levels detectable in mouse lungs at 4, 8, or 24h following the final NE exposure, compared to vehicle controls (**Figure 8**).

There are two known modulators of SPT activity— ORMDL3 and RTN4 (15, 16), but their effect on the expression of SPT are unknown. Since an increase in SPT expression could be accompanied by a change in the levels of ORMDL3 or RTN4, we investigated the expression of these proteins in mouse whole lung lysates. Protein expression of ORMDL3 and RTN4 was unchanged in NE-treated mice compared to controls at 24h ($p=0.068$ and $p=0.579$, respectively) (**Figure 9**), although there was a trend towards increased levels of ORMDL3 in NE-treated animals. Thus, currently, we have no evidence to support a role for ORMDL3 or RTN4 to regulate SPT activity or expression in this mouse model. Therefore, the increase in $d_{18:1/22:0}$, $d_{18:1/24:0}$ and

$d_{18:1/24:1}$ ceramide (**Table 5**, **Figure 5**) was likely due to increased SPT enzymatic activity due to increased expression of SPTLC2.

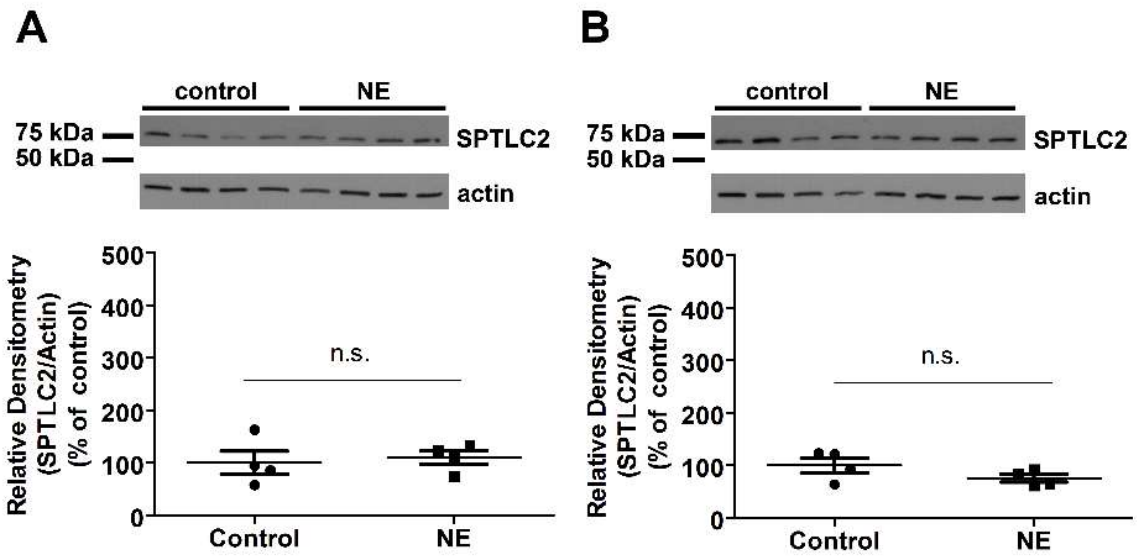
A
control
NE
75 kDa
50 kDa
SPTLC2
actin
Relative Densitometry (SPTLC2/Actin) (% of control)
500
400
300
200
100
0
n.s.
Control
NE
B
control
NE
75 kDa
50 kDa
SPTLC2
actin
Relative Densitometry (SPTLC2/Actin) (% of control)
500
400
300
200
100
0
n.s.
Control
NE

Figure 6. Oropharyngeal aspiration of NE did not alter the level of SPTLC2 in murine lungs at 4 or 8h. Representative western blots of SPT long chain subunit 2 in mouse lung lysates at 4h (**A**) and 8h (**B**) after the final oropharyngeal aspiration of vehicle control or NE. In the top panel, representative westerns for SPTLC2 and actin are shown. In the bottom panel, the relative densitometries of bands are presented following normalization to actin and average control, expressed as percent of control. Data are presented as mean ± SEM, summarized from 1 experiment (4h, 8h, n=4 mice per group) and compared by Mann-Whitney U (Wilcoxon Rank Sum) Test; ***, $p<0.001$.

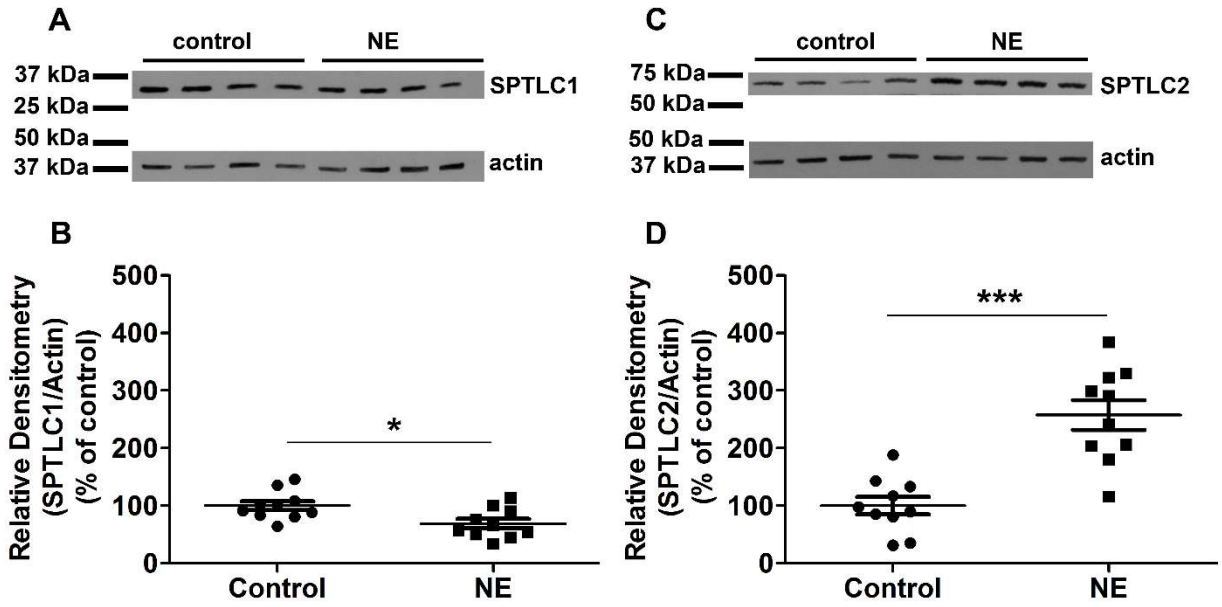
A
control
NE
37 kDa
25 kDa
50 kDa
37 kDa
SPTLC1
actin
C
control
NE
75 kDa
50 kDa
50 kDa
37 kDa
SPTLC2
actin
B
Relative Densitometry (SPTLC1/Actin) (% of control)
500
400
300
200
100
0
*
Control
NE
D
Relative Densitometry (SPTLC2/Actin) (% of control)
500
400
300
200
100
0
***
Control
NE

Figure 7. Oropharyngeal aspiration of NE altered expression of SPTLC1 and SPTLC2 in mouse lungs. Representative western blots of SPT long chain subunits 1 and 2 in mouse lung lysates at 24h after administration of NE or control vehicle, probed for SPTLC1 (**A, B**), or SPTLC2 (**C, D**) after the final oropharyngeal aspiration of vehicle control or NE. In the top panel (**A**, **C**), representative westerns for SPTLC1 or SPTLC2 and actin are shown. In the bottom panel (**B**, **D**), the relative densitometries of bands are presented following normalization to actin, shown as percentage of average control. Data are expressed as mean ± SEM; summarized from 2 experiments, n=10 mice per group, and compared by Mann-Whitney U (Wilcoxon Rank Sum) Test; ***, $p<0.001$; *, $p<0.05$. These data have been published (59).

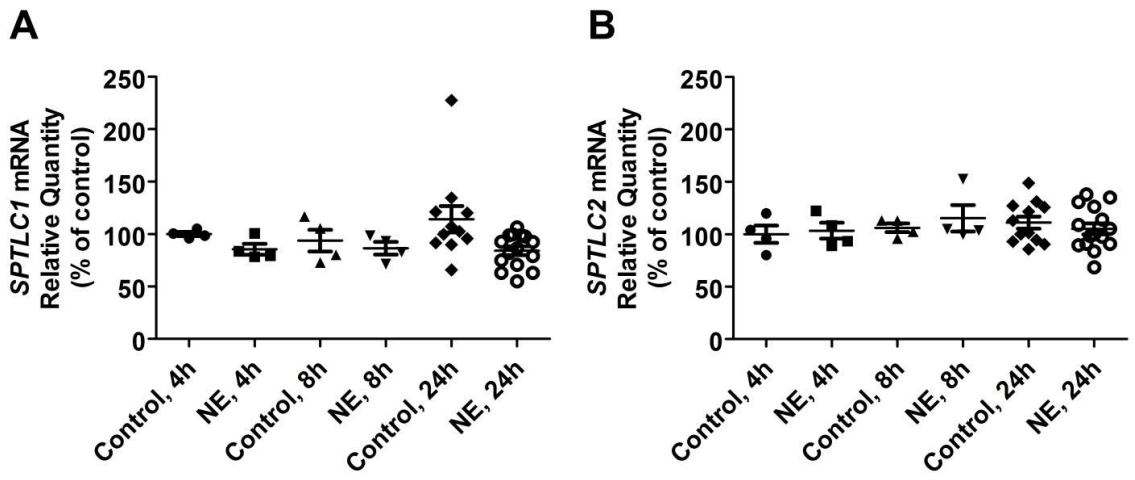
A
SPTLC1 mRNA Relative Quantity (% of control)
250
200
150
100
50
0
Control, 4h
NE, 4h
Control, 8h
NE, 8h
Control, 24h
NE, 24h
B
SPTLC2 mRNA Relative Quantity (% of control)
250
200
150
100
50
0
Control, 4h
NE, 4h
Control, 8h
NE, 8h
Control, 24h
NE, 24h

Figure 8. Q/RT-PCR analysis of *SPTLC1* and *SPTLC2* expression in the lungs of mice at 4, 8, and 24 h after exposure to control vehicle or NE. Relative expression of *SPTLC1* (**A**) and *SPTLC2* (**B**) mRNA in mouse lung lysates at 4, 8, or 24h after the final oropharyngeal aspiration of vehicle control or NE. RNA was isolated from frozen murine lungs using QIAzol, a Trizol reagent, and the levels of target mRNA expression determined using Q/RT-PCR. *SPTLC1* and *SPTLC2* were normalized to *β-actin*, the endogenous control, and expressed relative to controls at the same time point using the ΔΔCt method. Data are summarized from 1 (4h, 8h) or 3 (24h) experiments, n=4 per group (4h, 8h) or n=11 or 12 (24h, control, SPTLC1 and SPTLC2, respectively), n=15 (24h NE). Data are expressed as mean ± SEM and compared by Mann-Whitney U (Wilcoxon Rank Sum) Test; $p>0.05$.

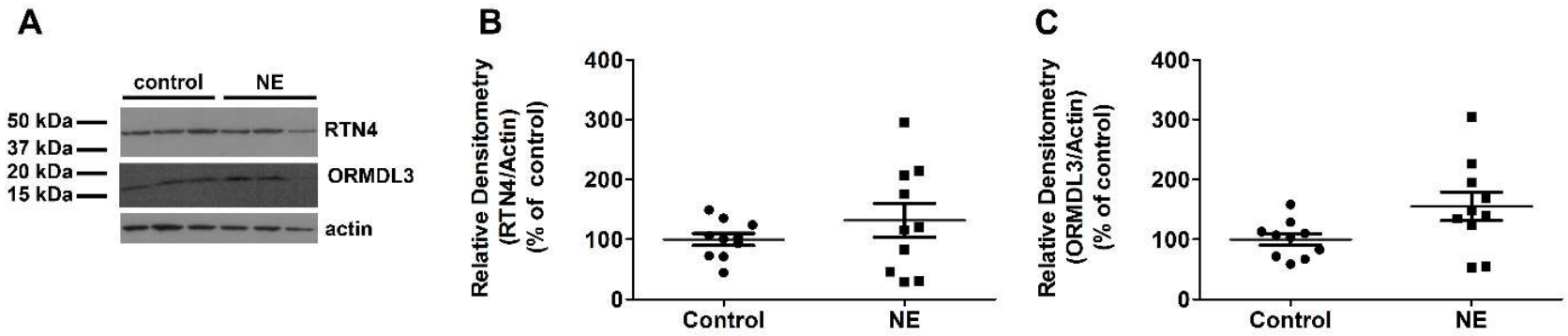
A
control
NE
50 kDa
37 kDa
20 kDa
15 kDa
RTN4
ORMDL3
actin
B
Relative Densitometry
(RTN4/Actin)
(% of control)
400
300
200
100
0
Control
NE
C
Relative Densitometry
(ORMDL3/Actin)
(% of control)
400
300
200
100
0
Control
NE

Figure 9. Oropharyngeal aspiration of NE did not alter the concentration of RTN4 or ORMDL3 in murine lungs at 24h. Representative western blots of RTN4 and ORMDL3 in mouse lung lysates at 24h after the final oropharyngeal aspiration of vehicle control or NE (**A**). The relative densitometries of bands are presented following normalization to actin and shown as percent of average control, with relative densitometry for RTN4 depicted in panel in (**B**) and ORMDL3 in (**C**). Data are expressed as mean ± SEM; summarized from 2 experiments (n=10 mice per group) and compared by Mann-Whitney U (Wilcoxon Rank Sum) Test.

II. Inhibiting SPT Activity Decreased Ceramide Expression and Airway Inflammation.

Inhibiting SPT Activity Decreased Neutrophil Elastase-induced Ceramide Expression.

To verify that increased ceramide in the BAL from mice administered NE was due to an increase in *de novo* biosynthesis of ceramide, we pre-treated mice with intraperitoneal injections of myriocin or vehicle control on days 1, 4, and 7 and euthanized mice at day 8, 24h after final administration of NE. Myriocin is a fungus-derived inhibitor that forms covalent bonds at the active site of SPT and irreversibly inhibits enzyme activity (147). In order to characterize the sphingolipid profile associated with pre-treatment with myriocin prior to induction of airway inflammation in this model, sphingolipid concentrations in BAL were determined via HPLC-ESI-MS/MS (**Tables 8-11**). The variability among the three experiments in murine response to NE, warranted analysis of the data as percent of control (% of control), with sphingolipid profile in control animals as 100% for each of the three experiments.

Administering myriocin to mice abrogated NE-induced changes in the expression of $d_{18:1/22:0}$ ($p=0.005$) and $d_{18:1/24:1}$ ($p=0.011$) ceramide; both ceramide moieties decreased by approximately 34% compared to levels in BAL in mice pre-treated with a vehicle control before NE was administered (**Table 9, Figure 10**). Similarly, there was a downward trend in the levels of $d_{18:1/24:0}$ ceramide, which decreased by about 27% ($p= 0.077$). Thus, we observed a downward trend in the levels of total ceramide, which dropped by approximately 18% in mice pre-treated with myriocin in comparison to vehicle control prior to oropharyngeal aspiration of NE, but not a statistically significant difference ($p= 0.111$) (**Table 9, Figure 10**). Pre-treatment with myriocin also decreased levels of $d_{18:1/26:1}$ and $d_{18:1/26:0}$ ceramide (**Table 9**). However, as in prior experiments, the levels of the moiety present in murine BAL— below 15pmol/mL— led us to conclude the effects of these two ceramide moieties were likely negligible.

Pre-treatment with myriocin also decreased levels of $d_{18:1/14:0}$ sphingomyelin by about 24% compared to animals pre-treated with vehicle control (**Table 8**); however, as the levels of this sphingomyelin moiety was not increased by NE compared to controls, we did not pursue this further. Similarly, we observed an increase in $d_{18:1/22:0}$, $d_{18:1/24:1}$, $d_{18:1/24:0}$, and $d_{18:1/26:1}$ sphingomyelin (**Table 8**) and $d_{18:1/24:1}$ and $d_{18:1/26:1}$ monohexosylceramide (**Table 10**) in mice administered NE compared to vehicle control. There were no statistically different alterations in these sphingolipids in mice pre-treated with myriocin prior to NE, compared to those pre-treated with vehicle control before NE, so we did not pursue these trends further.

Interestingly, pre-treatment with myriocin did not significantly affect the levels of monohexosylceramide (**Table 10)**, sphingosine, sphinganine, S1P, or Sa1P (**Table 11**). Likewise, myriocin did not alter the expression of SPTLC2 protein in mouse lung lysates (**Figure 11**). Thus, ceramides generated via the *de novo* pathway significantly contributed to the increased ceramide levels observed in BAL after NE exposure.

Table 8. Levels of sphingomyelin moieties in BAL in mice administered myriocin prior to aspiration of vehicle control or NE.

Sphingomyelin[a] (% of control)	Control	NE	Myriocin	NE + Myriocin
$d_{18:1/14:0}$	100.01±3.17	100.53±6.99	77.72±6.34	76.71±5.29^{+}
$d_{18:1/16:0}$	93.58±3.61	106.62±7.19	84.74±3.07	101.51±5.10
$d_{18:1/18:1}$	100.00±4.08	148.30±16.41	87.49±4.79	147.22±21.84
$d_{18:1/18:0}$	100.00±3.43	106.76±6.09	82.80±3.86	98.10±5.69
$d_{18:1/20:0}$	100.00±5.06	93.36±5.57	90.58±3.95	96.10±7.70
$d_{18:1/22:0}$	100.00±2.56	184.78±16.03*	98.10±6.43	143.28±20.49
$d_{18:1/24:1}$	100.00±3.03	144.51±8.83*	90.14±5.28	137.51±14.46
$d_{18:1/24:0}$	100.00±3.42	159.94±10.89*	93.07±7.35	140.01±16.38
$d_{18:1/26:1}$	100.02±4.56	149.89±9.24*	93.70±3.85	1400.76±14.56
$d_{18:1/26:0}$	99.99±5.01	129.02±10.39	92.68±5.59	135.58±16.98
Total	100.00±2.88	128.68±7.65	90.86±4.21	122.89±11.87

[a] BAL collected from n= 15 per group, except NE+myriocin where n=14. Samples were collected and processed using LC-MS/MS. Data are expressed as mean ± SEM, after normalizing to average control within each experiment. *, $p<0.05$, when compared to control animals at the same time point; $^{+}$, $p<0.05$, when compared to NE-treated animals at the same time point.

Table 9. Levels of ceramide moieties in BAL in mice administered myriocin prior to aspiration of vehicle control or NE.

Ceramide[a] (% of control)	Control	NE	Myriocin	NE + Myriocin
$d_{18:1/14:0}$	100.16±5.43	95.67±14.33	102.09±10.73	82.08±4.55
$d_{18:1/16:0}$	99.99±5.89	99.82±10.15	78.83±6.62	89.57±7.77
$d_{18:1/18:1}$	103.44±15.30	147.83±12.86	119.63±13.19	128.52±22.35
$d_{18:1/18:0}$	100.01±7.58	115.39±16.09	107.43±16.58	109.32±14.63
$d_{18:1/20:0}$	100.00±7.78	116.87±11.56	95.46±11.36	94.33±6.27
$d_{18:1/22:0}$	100.00±5.17	175.75±13.24*	100.89±12.21	123.67±7.21^{+}
$d_{18:1/24:1}$	100.00±5.56	204.20±16.47*	92.53±7.83	151.21±9.92^{+}
$d_{18:1/24:0}$	100.00±5.89	178.95±15.07*	85.65±5.85	139.27±9.02
$d_{18:1/26:1}$	100.03±4.03	212.57±20.81*	82.25±6.54	162.20±15.59
$d_{18:1/26:0}$	100.00±4.95	198.52±19.91*	84.57±5.15	159.05±15.08
Total	100.00±5.03	150.65±11.00 *	85.98±6.48	123.33±8.52

[a] BAL collected from n= 15 per group, except NE+myriocin where n=14. Samples were collected and processed using LC-MS/MS. Data are expressed as mean ± SEM, after normalizing to average control within each experiment. *, $p<0.05$, when compared to control animals at the same time point; $^{+}$, $p<0.05$, when compared to NE-treated animals at the same time point.

Table 10. Levels of monohexosylceramide moieties in BAL in mice administered myriocin prior to aspiration of vehicle control or NE.

Monohexosylceramide[a] (% of control)	Control	NE	Myriocin	NE + Myriocin
$d_{18:1/14:0}$	100.27±7.87	91.55±5.55	91.12±8.53	99.97±12.29
$d_{18:1/16:0}$	100.01±8.53	98.89±8.00	91.85±10.25	83.63±9.04
$d_{18:1/18:1}$	58.49±12.65	89.63±24.80	110.18±42.43	118.10±31.99
$d_{18:1/18:0}$	100.21±6.31	309.59±105.34	161.88±31.17	178.23±81.15
$d_{18:1/20:0}$	99.95±6.82	128.19±19.20	105.53±10.84	100.56±8.11
$d_{18:1/22:0}$	100.04±7.42	133.77±10.96	107.57±12.50	115.10±7.11
$d_{18:1/24:1}$	100.00±7.77	148.05±13.13*	112.96±15.25	144.02±13.85
$d_{18:1/24:0}$	100.00±5.69	127.44±10.42	96.44±10.00	113.80±11.24
$d_{18:1/26:1}$	100.07±5.29	152.11±15.73*	114.57±15.06	148.86±9.58
$d_{18:1/26:0}$	99.98±5.67	211.06±32.05	106.78±13.27	148.57±18.22
Total	100.00±5.93	128.20±9.74	100.96±10.66	115.86±10.20

[a] BAL collected from n= 15 per group, except NE+myriocin where n=14. Samples were collected and processed using LC-MS/MS. Data are expressed as mean ± SEM, after normalizing to average control within each experiment. *, $p<0.05$, when compared to control animals at the same time point.

Table 11. Levels of sphingosine, S1P, sphinganine, and Sa1P in BAL in mice administered myriocin prior to aspirating vehicle control or NE.

Sphingolipid[a] (% of control)	Control	NE	Myriocin	NE + Myriocin
sphingosine	100.09±6.86	123.91±9.89	94.64±7.55	137.98±14.29
S1P	99.39±7.97	132.09±10.89	94.09±9.48	143.70±12.58
sphinganine	100.74±5.94	113.81±9.34	109.71±7.97	108.58±7.97
Sa1P	106.69±14.93	136.94±24.33	94.61±13.54	151.32±24.31

[a] BAL collected from n= 15 per group, except NE+myriocin where n=14. Samples were collected and processed using LC-MS/MS. Data are expressed as mean ± SEM, after normalizing to average control within each experiment. There are no statistically significant differences in sphingolipid profile among these four groups.

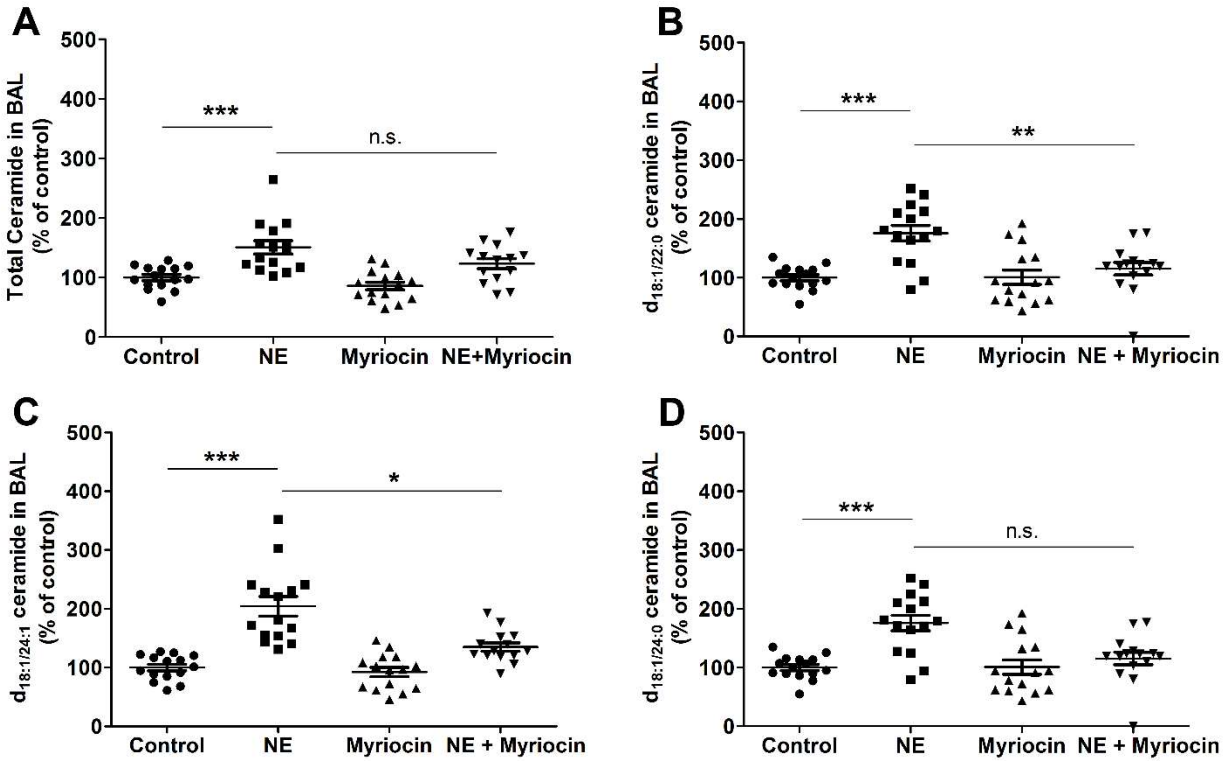
A
Total Ceramide in BAL (% of control)
500
400
300
200
100
0
***
n.s.
Control
NE
Myriocin
NE+Myriocin
B
d18:1/22:0 ceramide in BAL (% of control)
***
**
Control
NE
Myriocin
NE + Myriocin
C
d18:1/24:1 ceramide in BAL (% of control)
***
*
Control
NE
Myriocin
NE + Myriocin
D
d18:1/24:0 ceramide in BAL (% of control)
***
n.s.
Control
NE
Myriocin
NE + Myriocin

Figure 10. BAL sphingolipid analysis following myriocin pretreatment followed by NE or control vehicle. Mice were exposed to control vehicle or myriocin (0.3 mg/kg IP) 2h prior to NE or control vehicle on days 1, 4, and 7; BAL and mouse lungs were harvested on day 8. Sphingolipid concentration in BAL (350μL) was determined by HPLC-ESI-MS/MS. Expression of total ceramides (**A**) and ceramide $d_{18:1/22:0}$ (**B**), $d_{18:1/24:1}$ (**C**), $d_{18:1/24:0}$ (**D**) in BAL were increased following NE exposure. With the addition of myriocin, a significant decrease in $d_{18:1/22:0}$ and $d_{18:1/24:1}$ ceramide was observed, with non-significant decreases for the $d_{18:1/24:0}$ chain length and total ceramide. Data were normalized to the average control and compared using nonparametric one-way ANOVA (Kruskal-Wallis Test), with *post hoc* analyses among treatment groups using Mann-Whitney U (Wilcoxon Rank Sum Test). Data represent the sum of 3 experiments expressed as mean ± SEM, with n=15 animals per group except NE+myriocin (n=14). ***, $p<0.001$; **, $p<0.01$; *, $p<0.05$; n.s., not significant, $p>0.05$. These data have been published (59).

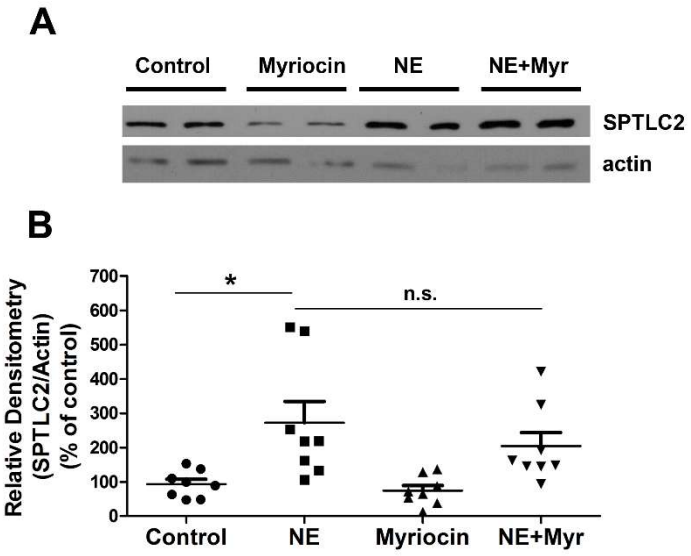
A
Control
Myriocin
NE
NE+Myr
SPTLC2
actin
B
Relative Densitometry
(SPTLC2/Actin)
(% of control)
700
600
500
400
300
200
100
0
*
n.s.
Control
NE
Myriocin
NE+Myr

Figure 11. Oropharyngeal aspiration of NE increased the concentration of SPTLC2 in murine lungs at 24h; pre-treatment with myriocin did not abrogate this effect. Mice were administered myriocin (0.3 mg/kg IP) or vehicle control on days 1, 4, and 4 prior to oropharyngeal aspiration of NE or vehicle control; BAL and mouse lungs were harvested on day 8. Representative western blots of SPT long chain subunit 2 in mouse lung lysates at 24h (**A**) after the final oropharyngeal aspiration of vehicle control or NE. In the top panel, representative westerns for SPTLC2 and actin are shown. In the bottom panel, the relative densitometries of bands are presented following normalization to actin and average control, expressed as percent of control. Data are presented as mean ± SEM, summarized from 2 experiments (n=8 mice per group) and compared by Mann-Whitney U (Wilcoxon Rank Sum) Test; *, $p<0.05$; n.s., not significant, $p>0.05$.

Myriocin Alleviated Aspects of Neutrophil Elastase-induced Inflammation. We measured the levels of inflammatory markers and quantity of inflammatory cells present in murine BAL in order to determine the effects of myriocin mediated inhibition of SPT activity on NE-induced inflammation. Administering myriocin to mice prior to aspiration of NE induced a 36% decrease in the levels of KC ($p=0.021$) and 44% drop in the levels of HMGB1 ($p=0.015$) present in murine BAL (**Figure 12**). Pre-treatment with myriocin decreased the total leukocytes (total white blood cell count, total cell count) in mouse BAL by about 11% (**Figure 13**); a change that was not statistically significant. Likewise, while proportion of neutrophils present decreased by roughly 4% in the BAL of mice pre-treated with myriocin prior to oropharyngeal aspiration of NE (**Figure 13**), this drop was also not statistically significant.

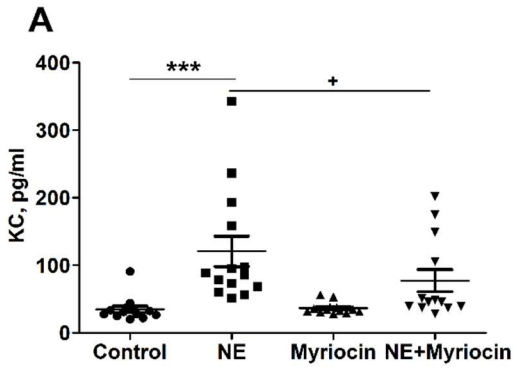
A
400
300
200
100
0
KC, pg/ml
***
+
Control
NE
Myriocin
NE+Myriocin

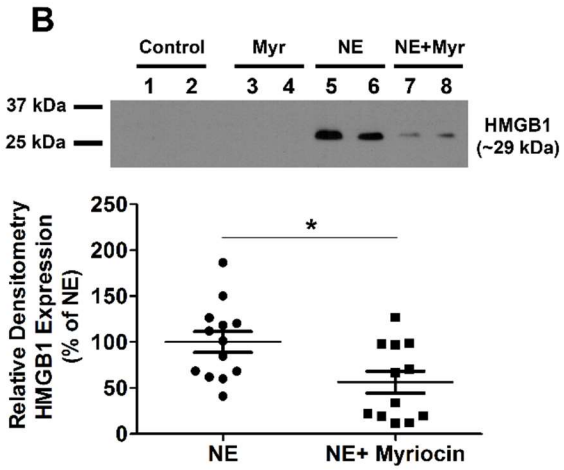
B
Control
Myr
NE
NE+Myr
1 2 3 4 5 6 7 8
37 kDa
25 kDa
HMGB1
(~29 kDa)
Relative Densitometry
HMGB1 Expression
(% of NE)
250
200
150
100
50
0
*
NE
NE+ Myriocin

Figure 12. The effect of myriocin on NE-induced KC and HMGB1 in BAL. Administration of myriocin (0.3 mg/kg) prior to oropharyngeal aspiration of NE decreased the level of BAL KC, compared to mice that received control vehicle prior to NE treatment, as determined by ELISA (n=13 per group in control, myriocin alone and NE+myriocin, n=14 in NE) (**A**). NE-induced expression of HMGB1 in BAL was decreased with myriocin administration (n=13 NE and n=12 NE+myriocin) (**B**) a representative blot, and relative densitometry, normalized to HMGB1 expression against average expression with NE (percentile). Data summarized mean ± SEM of 3 experiments, with groups compared by Mann-Whitney U (Wilcoxon Rank Sum) Test; ***, $p<0.001$; $^{+}$, $p=0.021$; *, $p=0.014$. These data have been published (59).

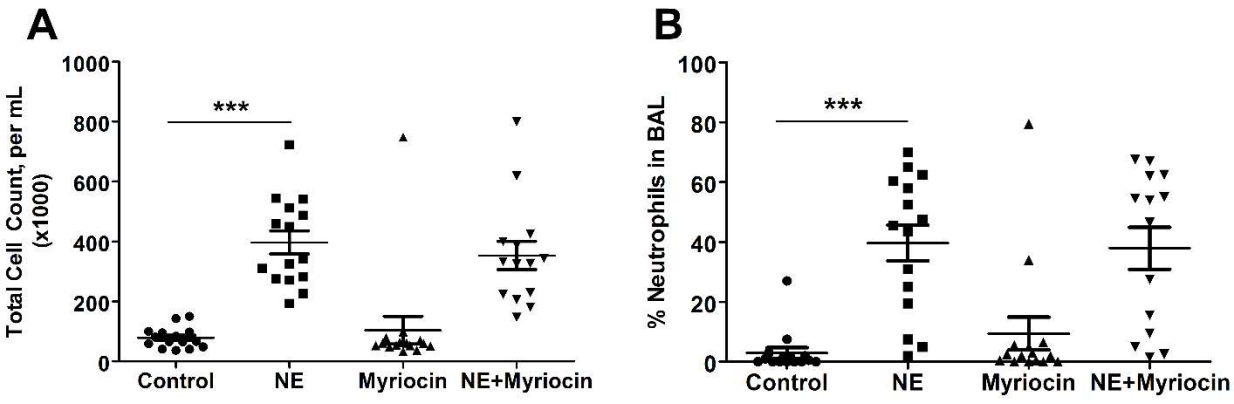
A
Total Cell Count, per mL (x1000)
1000
800
600
400
200
0
***
Control
NE
Myriocin
NE+Myriocin
B
% Neutrophils in BAL
100
80
60
40
20
0
***
Control
NE
Myriocin
NE+Myriocin

Figure 13. Total cell counts and percent neutrophils in BAL following pretreatment with myriocin or control vehicle and aspiration of NE or control vehicle. Aspiration of NE induced an increase in BAL total leukocytes (total cell count) (**A**), and in percent neutrophils (**B**). Administration of myriocin (0.3 mg/kg) by IP injection prior to NE administration did not change total cell count (total leukocytes) in murine BAL (**A**), or the percent neutrophils present in the BAL (**B**), compared to mice that received a vehicle control IP injection. Groups were compared by nonparametric ANOVA test (Kruskal-Wallis), with post-hoc comparisons among groups using Mann-Whitney U Tests (Wilcoxon Rank Sum Test); data are summarized from 3 experiments as mean ± SEM, with n= 15 per group (vehicle control, myriocin alone, NE alone), n=14 in NE+myriocin group; ***, $p<0.001$. These data have been published (59).

III. Associations between Sphingolipids, Neutrophil Elastase, and Clinical Status in Cystic Fibrosis Sputum.

Sputum Sphingolipids Increased During Hospitalization. We evaluated the sphingolipid profiles of sputum from CF patients by comparing intrasubject levels between hospitalization and outpatient visit to determine if there were any trends associated with more airway inflammation (hospitalization) versus less inflammation (outpatient visit). Three sphingolipid moieties demonstrated a statistically significant increase when the subjects were hospitalized for pulmonary exacerbation: $d_{18:1/14:0}$ ceramide by about 50% (p= 0.022), $d_{18:1/24:1}$ ceramide by about 37% (p= 0.041), and $d_{18:1/24:0}$ monohexosylceramide by about 38% (p=0.026) (**Figure 14C-E**). As expected, lung function, measured as FEV_1 % predicted, was significantly decreased during hospitalizations for pulmonary exacerbations compared to outpatient clinic visits (p=0.0182) (**Figure 14A**). There was a 5% difference between the average FEV_1 % predicted during outpatient visits and during hospitalization (**Figure 14A**). On the other hand, the sputum concentrations of active NE collected during hospitalizations for CF pulmonary exacerbations were not significantly different from samples collected during outpatient visits (p=0.468) (**Figure 14B**). However, this lack of difference in level of active NE was likely because our sputum donors had relatively high levels of chronic neutrophilic inflammation, as most had severe lung disease. Similar findings have been reported by others (105).

However, in contrast to the ceramide and monohexosylceramide species which increased for individuals during hospitalization (**Figure 14C-E**), there were no other intrasubject significant differences in sphingolipid levels between these two time points for other species: sphingomyelins (**Figure 15**), total ceramide and other ceramide species (**Figure 16**), monohexosylceramides (**Figure 17**), and sphingosine, sphinganine, S1P, and Sa1P (**Figure 18**). The lack of more

significant differences between hospitalization and outpatient visits may be due to the severity of lung disease in this patient population reflected by the high NE levels at both time points in many subjects.

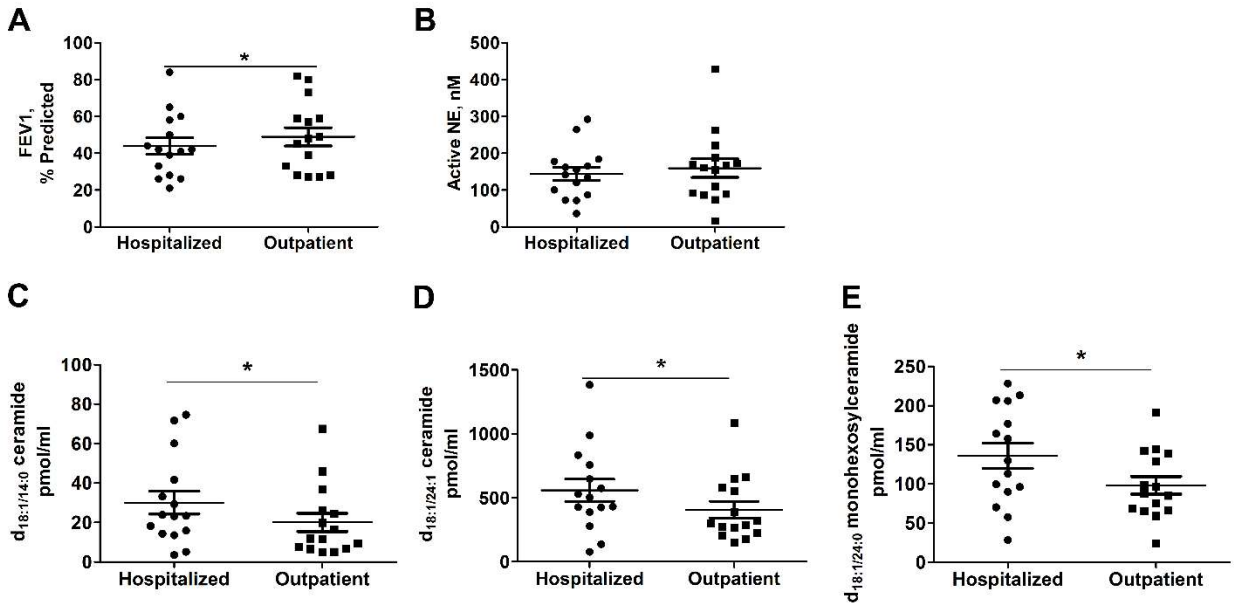
A
FEV1, % Predicted
100
80
60
40
20
0
*
Hospitalized
Outpatient
B
Active NE, nM
500
400
300
200
100
0
Hospitalized
Outpatient
C
d18:1/14:0 ceramide pmol/ml
100
80
60
40
20
0
*
Hospitalized
Outpatient
D
d18:1/24:1 ceramide pmol/ml
1500
1000
500
0
*
Hospitalized
Outpatient
E
d18:1/24:0 monohexosylceramide pmol/ml
250
200
150
100
50
0
*
Hospitalized
Outpatient

Figure 14. Differences in lung function and sputum concentrations of active NE and sphingolipids in patients with CF between hospitalization and outpatient visit. Sputum samples were collected during the course of hospitalization or during an outpatient visit (n=15 per group) and processed as described in the Methods. Lung function, expressed as FEV_1 % predicted, varied between the two groups; there was a statistically significant decrease in lung function during hospitalization for CF pulmonary exacerbation (**A**). Active NE was measured by a chromogenic microtiter plate assay; there was a wide range of NE activity among patients, but no statistically significant difference between the two sample groups (**B**). Sphingolipid content was measured by HPLC-ESI-MS/MS. Sputum concentrations of $d_{18:1/14:0}$ ceramide (**C**), $d_{18:1/24:1}$ ceramide (**D**) and $d_{18:1/24:0}$ monohexosylceramide (**E**) varied with clinical status, with increased concentrations of these sphingolipids found in samples collected during hospitalization. The differences between the two groups were statistically significant (*, $p<0.05$). Data (mean ± SEM) were compared by Wilcoxon Signed Rank Tests. These data have been submitted for publication.

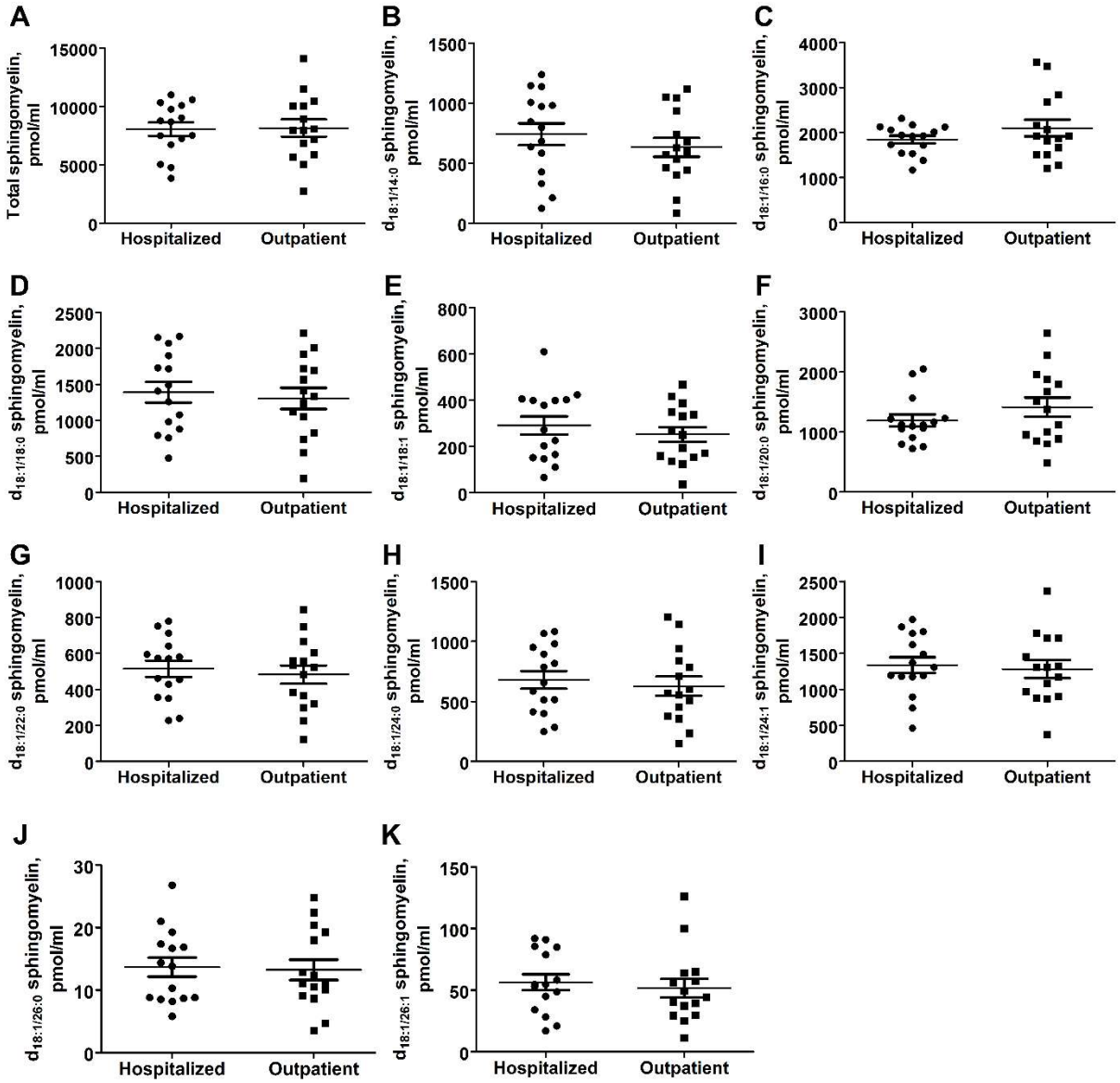
A
Total sphingomyelin, pmol/ml
15000
10000
5000
0
Hospitalized
Outpatient
B
d18:1/14:0 sphingomyelin, pmol/ml
1500
1000
500
0
Hospitalized
Outpatient
C
d18:1/16:0 sphingomyelin, pmol/ml
4000
3000
2000
1000
0
Hospitalized
Outpatient
D
d18:1/18:0 sphingomyelin, pmol/ml
2500
2000
1500
1000
500
0
Hospitalized
Outpatient
E
d18:1/18:1 sphingomyelin, pmol/ml
800
600
400
200
0
Hospitalized
Outpatient
F
d18:1/20:0 sphingomyelin, pmol/ml
3000
2000
1000
0
Hospitalized
Outpatient
G
d18:1/22:0 sphingomyelin, pmol/ml
1000
800
600
400
200
0
Hospitalized
Outpatient
H
d18:1/24:0 sphingomyelin, pmol/ml
1500
1000
500
0
Hospitalized
Outpatient
I
d18:1/24:1 sphingomyelin, pmol/ml
2500
2000
1500
1000
500
0
Hospitalized
Outpatient
J
d18:1/26:0 sphingomyelin, pmol/ml
30
20
10
0
Hospitalized
Outpatient
K
d18:1/26:1 sphingomyelin, pmol/ml
150
100
50
0
Hospitalized
Outpatient

Figure 15. Sputum concentrations of sphingomyelin in patients during hospitalization for a pulmonary exacerbation and during an outpatient visit. Sputum samples were collected during hospitalization or during an outpatient visit (n=15 per group) and processed as described in the Methods. Sphingolipid content was measured by HPLC-ESI-MS/MS. Sputum concentrations of total sphingomyelin (**A**) and $d_{18:1/14:0}$, $d_{18:1/16:0}$, $d_{18:1/18:0}$, $d_{18:1/18:1}$, $d_{18:1/20:0}$, $d_{18:1/22:0}$, $d_{18:1/24:0}$, $d_{18:1/24:1}$, $d_{18:1/26:0}$, $d_{18:1/26:1}$ sphingomyelin moieties (**B**-**K**). The differences between the two groups were not statistically significant. Data (mean ± SEM) were compared by Wilcoxon Signed Rank Tests. These data have been submitted for publication.

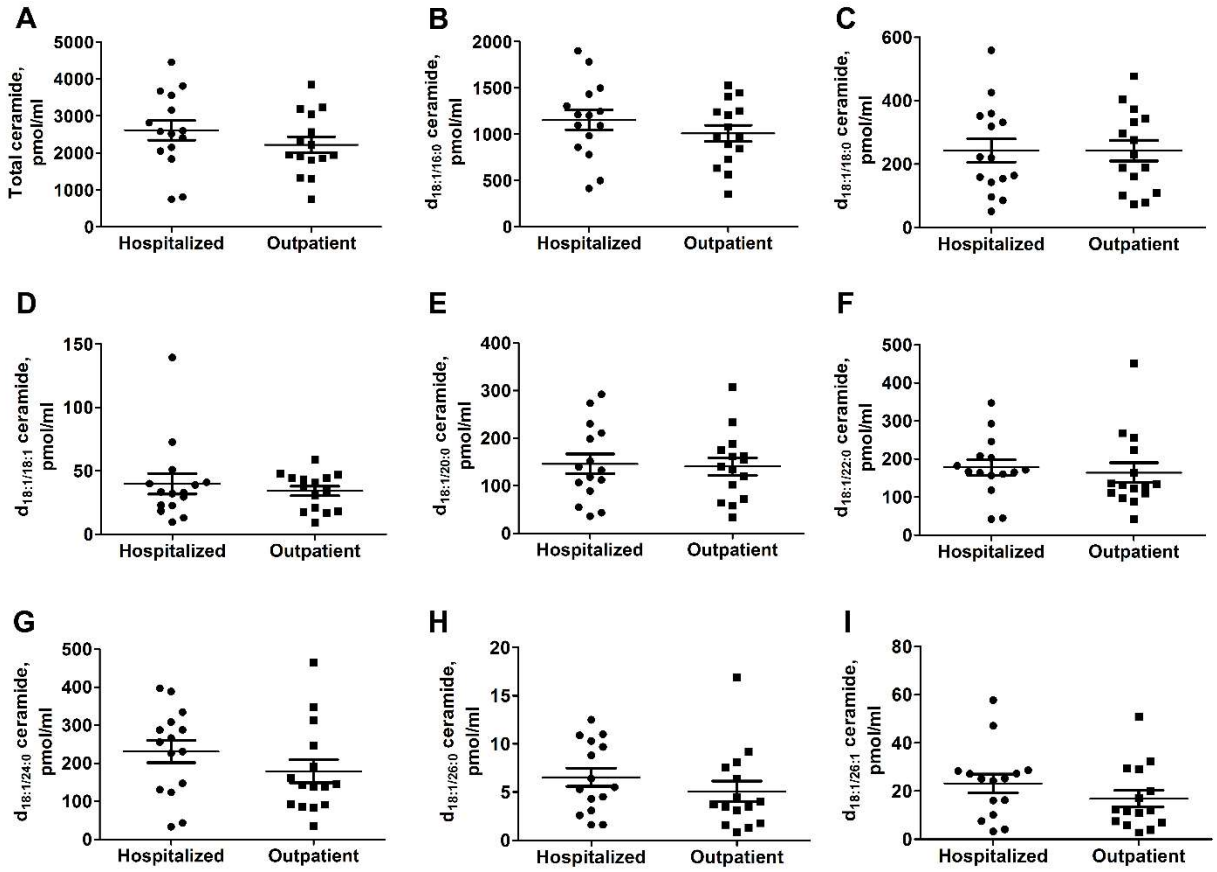
A
Total ceramide, pmol/ml
5000
4000
3000
2000
1000
0
Hospitalized
Outpatient
B
$d_{18:1/16:0}$ ceramide, pmol/ml
2000
1500
1000
500
0
Hospitalized
Outpatient
C
$d_{18:1/18:0}$ ceramide, pmol/ml
600
400
200
0
Hospitalized
Outpatient
D
$d_{18:1/18:1}$ ceramide, pmol/ml
150
100
50
0
Hospitalized
Outpatient
E
$d_{18:1/20:0}$ ceramide, pmol/ml
400
300
200
100
0
Hospitalized
Outpatient
F
$d_{18:1/22:0}$ ceramide, pmol/ml
500
400
300
200
100
0
Hospitalized
Outpatient
G
$d_{18:1/24:0}$ ceramide, pmol/ml
500
400
300
200
100
0
Hospitalized
Outpatient
H
$d_{18:1/26:0}$ ceramide, pmol/ml
20
15
10
5
0
Hospitalized
Outpatient
I
$d_{18:1/26:1}$ ceramide, pmol/ml
80
60
40
20
0
Hospitalized
Outpatient

Figure 16. Sputum concentrations of ceramide in patients during hospitalization for a pulmonary exacerbation and during an outpatient visit. Sputum samples were collected during hospitalization or during an outpatient visit (n=15 per group) and processed as described in the Methods. Sphingolipid content was measured by HPLC-ESI-MS/MS. Sputum concentrations of total ceramide (**A**) and $d_{18:1/16:0}$, $d_{18:1/18:0}$, $d_{18:1/18:1}$, $d_{18:1/20:0}$, $d_{18:1/22:0}$, $d_{18:1/24:0}$, $d_{18:1/26:0}$, $d_{18:1/26:1}$ ceramide moieties (**B**-**I**). The differences between the two groups were not statistically significant. Data (mean ± SEM) were compared by Wilcoxon Signed Rank Tests. These data have been submitted for publication.

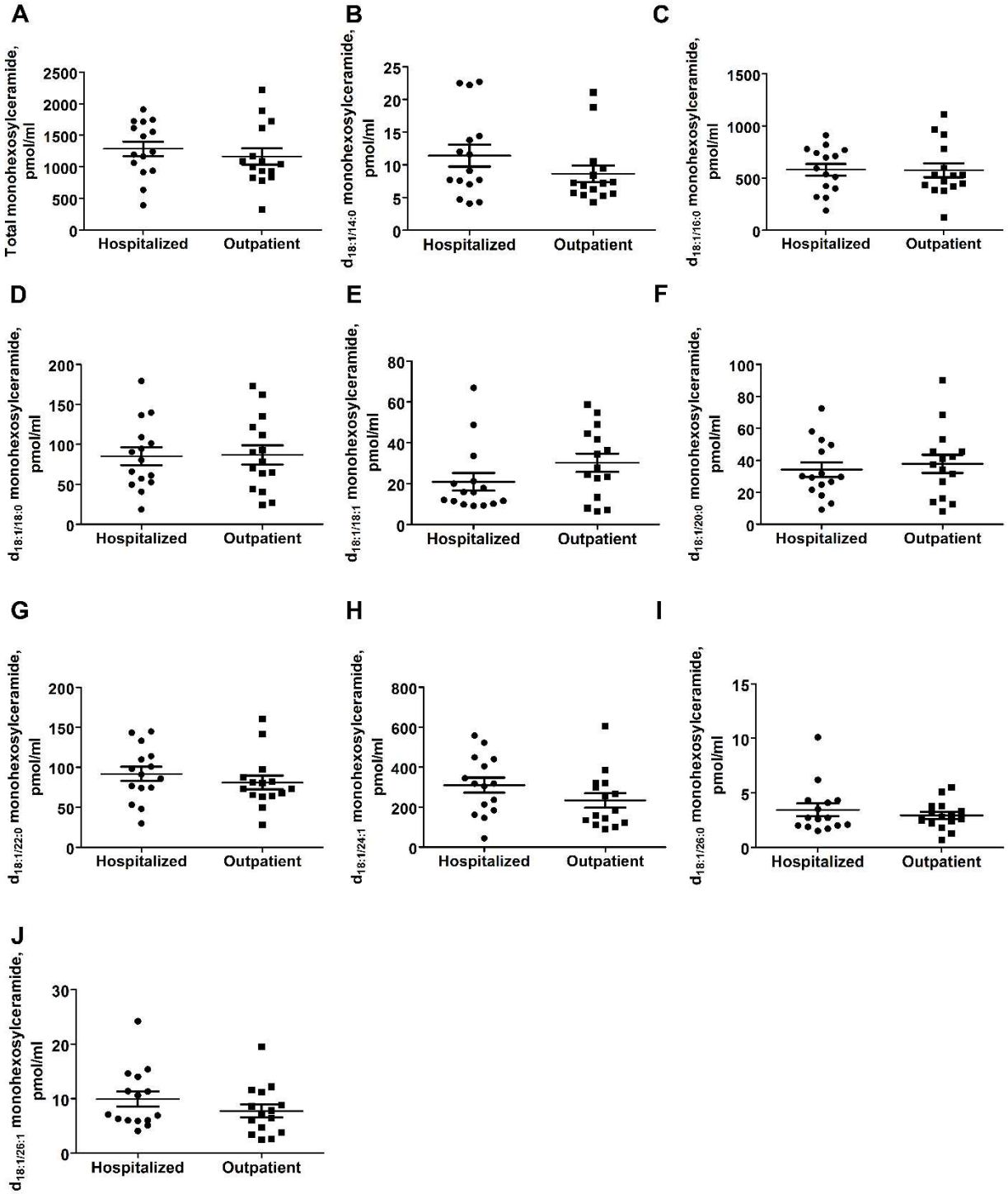
A
Total monohexosylceramide, pmol/ml
2500
2000
1500
1000
500
0
Hospitalized
Outpatient
B
d18:1/14:0 monohexosylceramide, pmol/ml
25
20
15
10
5
0
Hospitalized
Outpatient
C
d18:1/16:0 monohexosylceramide, pmol/ml
1500
1000
500
0
Hospitalized
Outpatient
D
d18:1/18:0 monohexosylceramide, pmol/ml
200
150
100
50
0
Hospitalized
Outpatient
E
d18:1/18:1 monohexosylceramide, pmol/ml
80
60
40
20
0
Hospitalized
Outpatient
F
d18:1/20:0 monohexosylceramide, pmol/ml
100
80
60
40
20
0
Hospitalized
Outpatient
G
d18:1/22:0 monohexosylceramide, pmol/ml
200
150
100
50
0
Hospitalized
Outpatient
H
d18:1/24:1 monohexosylceramide, pmol/ml
800
600
400
200
0
Hospitalized
Outpatient
I
d18:1/26:0 monohexosylceramide, pmol/ml
15
10
5
0
Hospitalized
Outpatient
J
d18:1/26:1 monohexosylceramide, pmol/ml
30
20
10
0
Hospitalized
Outpatient

Figure 17. Sputum concentrations of monohexosylceramide in patients during hospitalization for a pulmonary exacerbation and during an outpatient visit. Sputum samples were collected during the course of hospitalization or during an outpatient visit (n=15 per group) and processed as described in the Methods. Sphingolipid content was measured by HPLC-ESI-MS/MS. Sputum concentrations of total monohexosylceramide (**A**) and $d_{18:1/14:0}$, $d_{18:1/16:0}$, $d_{18:1/18:0}$, $d_{18:1/18:1}$, $d_{18:1/20:0}$, $d_{18:1/22:0}$, $d_{18:1/24:1}$, $d_{18:1/26:0}$, $d_{18:1/26:1}$ monohexosylceramide moieties (**B-J**). The differences between the two groups were not statistically significant. Data (mean ± SEM) were compared by Wilcoxon Signed Rank Tests. These data have been submitted for publication.

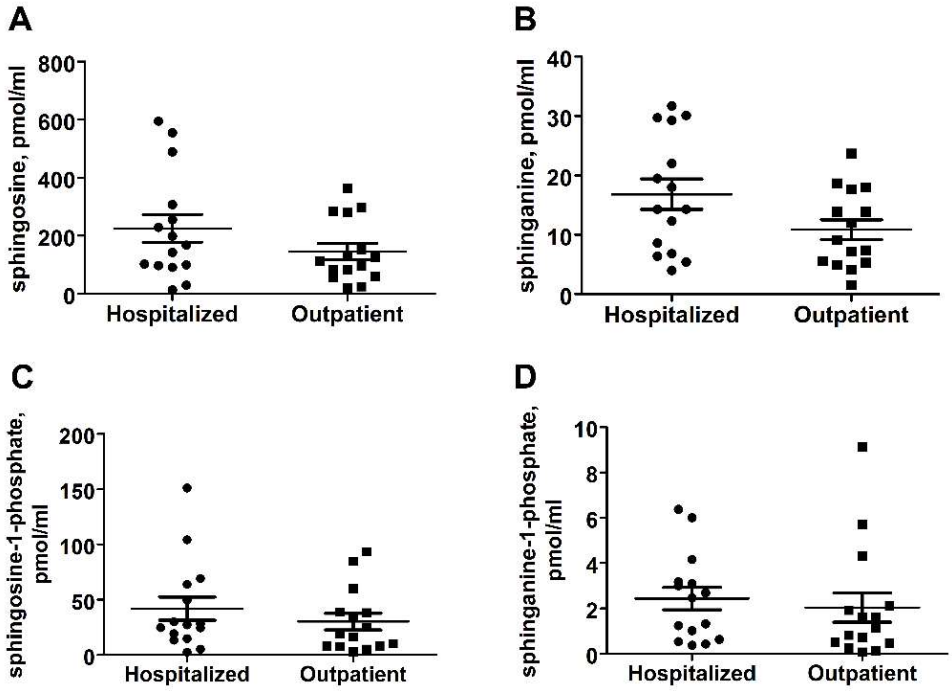
A
sphingosine, pmol/ml
800
600
400
200
0
Hospitalized
Outpatient
B
sphinganine, pmol/ml
40
30
20
10
0
Hospitalized
Outpatient
C
sphingosine-1-phosphate, pmol/ml
200
150
100
50
0
Hospitalized
Outpatient
D
sphinganine-1-phosphate, pmol/ml
10
8
6
4
2
0
Hospitalized
Outpatient

Figure 18. Sputum concentrations of sphingosine, sphinganine, S1P, and Sa1P in patients during hospitalization for a pulmonary exacerbation and during an outpatient visit. Sputum samples were collected during the course of hospitalization or during an outpatient visit (n=15 per group) and processed as described in the Methods. Sphingolipid content was measured by HPLC-ESI-MS/MS. Sputum concentrations of sphingosine (**A**), sphinganine (**B**), S1P (**C**), Sa1P (**D**). The differences between the two groups were not statistically significant. Data (mean ± SEM) were compared by Wilcoxon Signed Rank tests. These data have been submitted for publication.

A Rise in Sphingolipid Concentration Correlated with Increasing Proteolytically Active NE in Sputum from Cystic Fibrosis Patients. Based on our *in vivo* experiments with oropharyngeal aspiration of NE, which revealed that NE increased long chain ceramide levels, we tested whether levels of sputum sphingolipids correlate with NE activity. We found that as the concentration of active NE in sputum increased, so did the concentration of a wide variety of sphingolipids. There were linear correlations between the concentrations of active NE and total sphingomyelin (r^2=0.198; p=0.014), total ceramide (r^2=0.152; p=0.033), total monohexosylceramide (r^2=0.229; p=0.007), and S1P (r^2=0.257; p=0.004) (**Figure 19**) in subject sputa.

The concentrations of several different sphingomyelin moieties directly correlated with levels of active NE. There was a linear correlation between active NE and sphingomyelin $d_{18:1/14:0}$ (r^2=0.364; p<0.001), $d_{18:1/18:1}$ (r^2=0.156; p=0.031), $d_{18:1/22:0}$ (r^2=0.293; p=0.002), $d_{18:1/24:1}$ (r^2=0.295; p=0.002), and $d_{18:1/24:0}$ (r^2=0.141; p=0.041) (**Figure 20**). When assessing the association of active NE and ceramide of various chain lengths, we observed a statistically significant linear correlation between active NE and ceramide $d_{18:1/22:0}$ (r^2=0.148; p=0.036) and $d_{18:1/24:0}$ (r^2=0.262; p=0.004) (**Figure 21A-B**). Finally, two specific monohexosylceramide moieties increased with increasing NE activity— $d_{18:1/16:0}$ (r^2=0.273; p=0.003) and $d_{18:1/24:0}$ (r^2=0.164; p=0.026) (**Figure 21C-D**). Overall, we observed that sputum concentrations of various sphingomyelin, ceramide and monohexosylceramide moieties directly correlated with sputum NE activity.

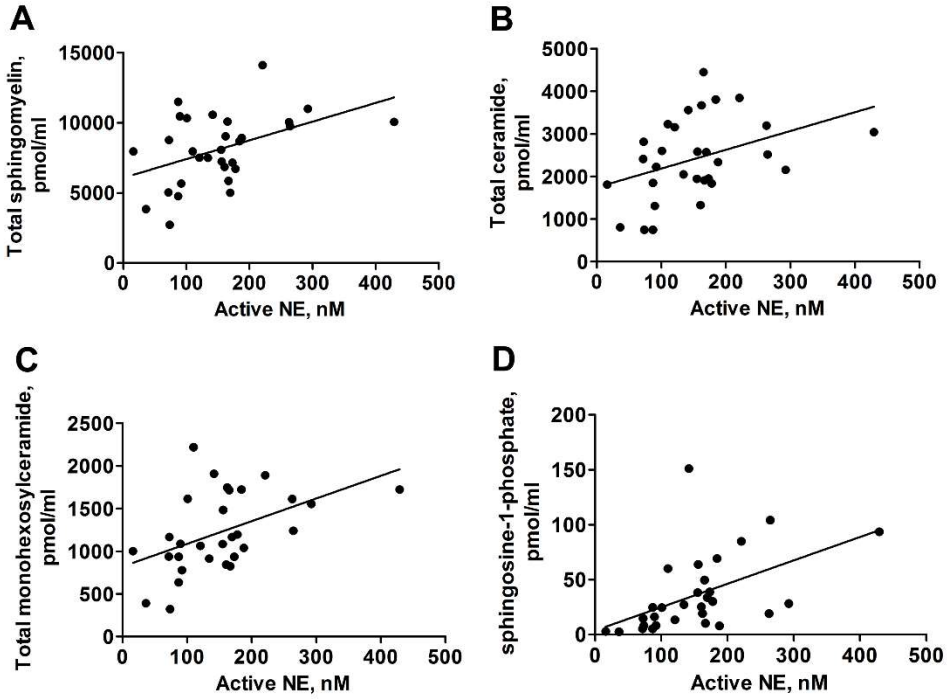
A
Total sphingomyelin, pmol/ml
15000
10000
5000
0
0
100
200
300
400
500
Active NE, nM
B
Total ceramide, pmol/ml
5000
4000
3000
2000
1000
0
0
100
200
300
400
500
Active NE, nM
C
Total monohexosylceramide, pmol/ml
2500
2000
1500
1000
500
0
0
100
200
300
400
500
Active NE, nM
D
sphingosine-1-phosphate, pmol/ml
200
150
100
50
0
0
100
200
300
400
500
Active NE, nM

Figure 19. A linear correlation between the concentration of active NE and total sphingomyelin (A), total ceramide (B), total monohexosylceramide (C) and S1P (D) in CF sputum. Sputum samples were collected (n=30 samples, from 15 donors), and processed as described in the Methods. Total sphingolipid content was measured by HPLC-ESI-MS/MS, and the concentration of active NE in sputum was assessed using an NE activity assay. There was a linear correlation between the concentration of active NE and total sphingomyelin (r^2=0.198; p=0.014), total ceramide (r^2=0.152; p=0.033), total monohexosylceramide (r^2=0.2293; p=0.007), and S1P (r^2=0.257; p=0.004) in CF sputum (**A** through **D**, respectively). These data have been submitted for publication.

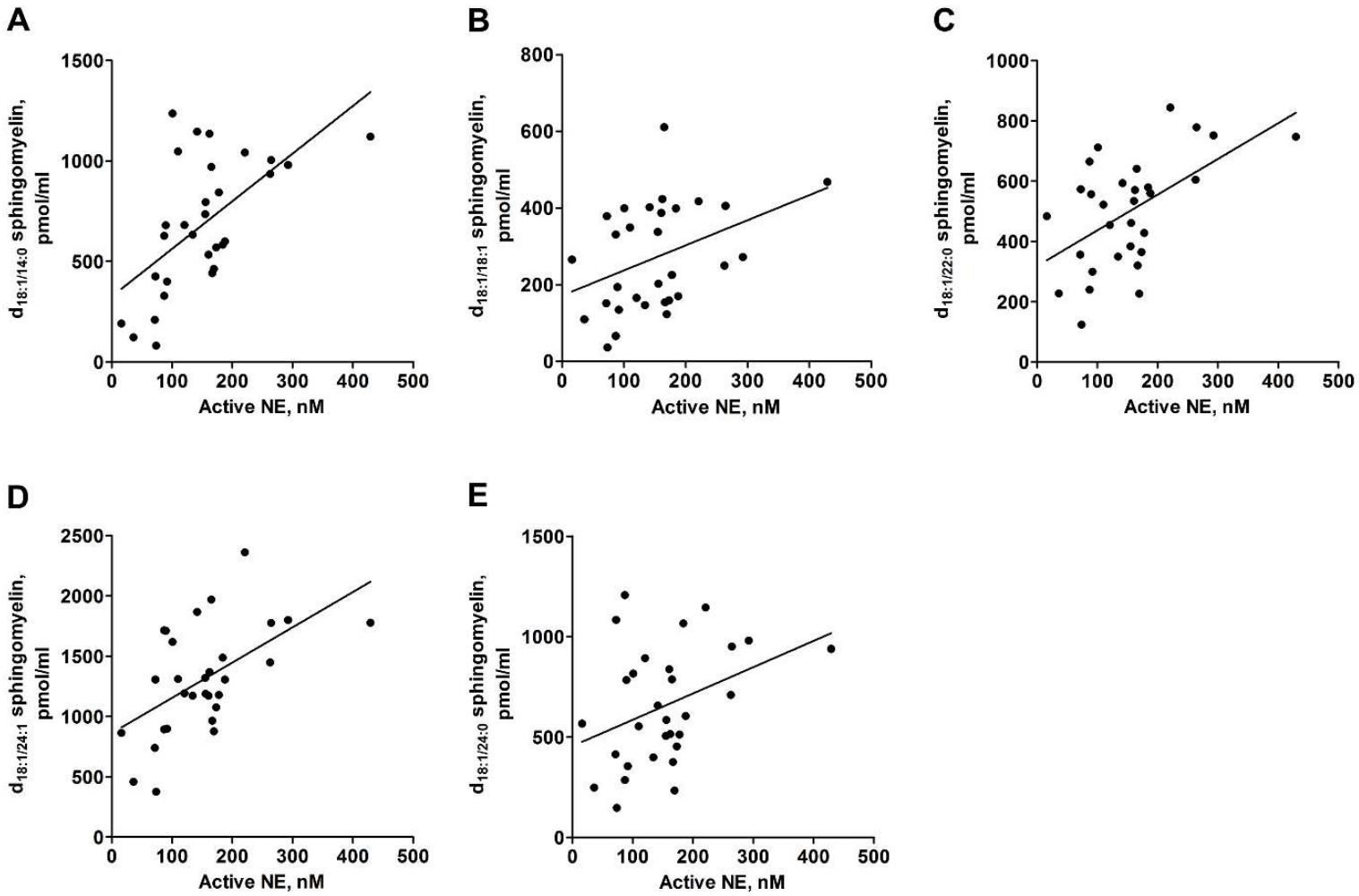
A
B
C
D
E
$d_{18:1/14:0}$ sphingomyelin, pmol/ml
$d_{18:1/18:1}$ sphingomyelin, pmol/ml
$d_{18:1/22:0}$ sphingomyelin, pmol/ml
$d_{18:1/24:1}$ sphingomyelin, pmol/ml
$d_{18:1/24:0}$ sphingomyelin, pmol/ml
Active NE, nM
0
100
200
300
400
500
500
1000
1500
2000
2500
200
400
600
800

Figure 20. Linear correlations between the concentration of active NE and five sphingomyelin moieties in CF sputum. Sputum samples were collected (n=30 samples, from 15 donors), and processed as described in the Methods. Sphingomyelin content was measured by HPLC-ESI-MS/MS, and the concentration of active NE in sputum was assessed using an NE activity assay. Most likely contributors to the observed increase in total sphingomyelin consisted of $d_{18:1/14:0}$ (r^2=0.364; p<0.001), $d_{18:1/18:1}$ (r^2=0.156; p=0.031), $d_{18:1/22:0}$ (r^2=0.293; p=0.002), $d_{18:1/24:1}$ (r^2=0.2945; p=0.002), and $d_{18:1/24:0}$ (r^2=0.141; p=0.041) sphingomyelin (**A** through **E**, respectively). These data have been submitted for publication.

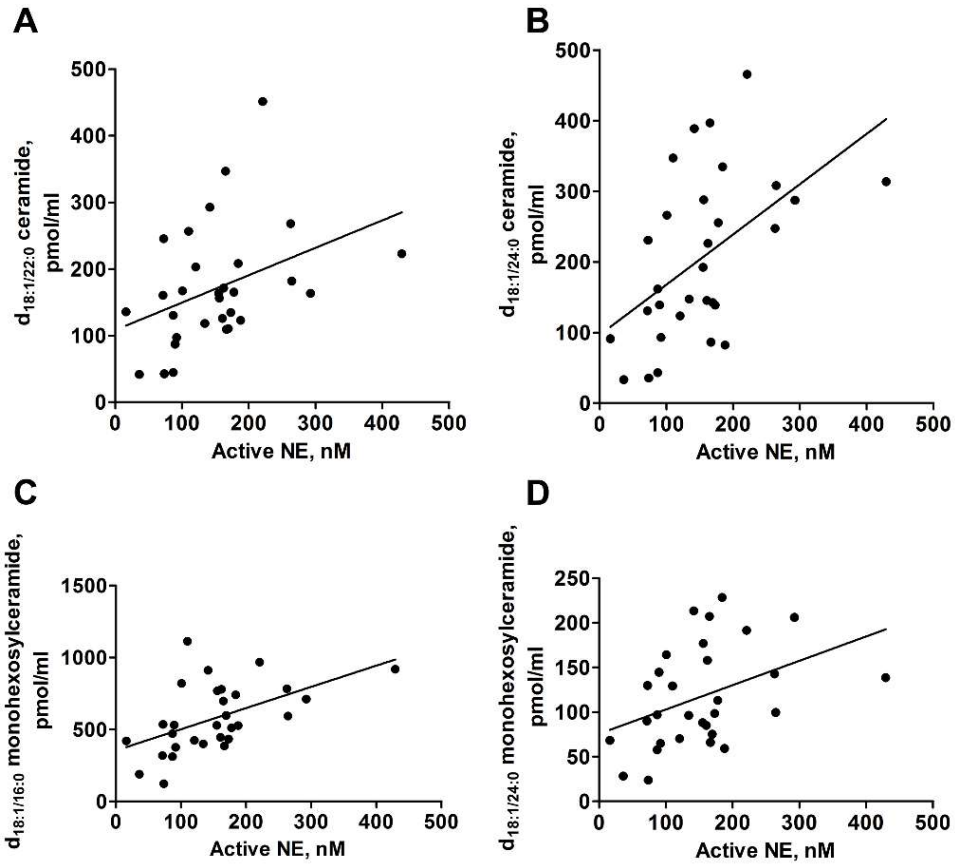
A
B
C
D
$d_{18:1/22:0}$ ceramide, pmol/ml
$d_{18:1/24:0}$ ceramide, pmol/ml
$d_{18:1/16:0}$ monohexosylceramide, pmol/ml
$d_{18:1/24:0}$ monohexosylceramide, pmol/ml
Active NE, nM
0
100
200
300
400
500
1000
1500
50
150
250

Figure 21. Linear correlations between the concentration of active NE and two ceramide and two monohexosylceramide moieties in CF sputum. Sputum samples were collected (n=30 samples, from 15 donors), and processed as described in the Methods. Ceramide and monohexosylceramide content was measured by HPLC-ESI-MS/MS. The concentration of active NE in sputum was assessed using an NE activity assay. The sphingolipid moieties that likely contributed to the increase in total ceramide were $d_{18:1/22:0}$ (r^2=0.148; p=0.036) (**A**) and $d_{18:1/24:0}$ (r^2=0.262; p=0.004) ceramide (**B**). The sphingolipid moieties that likely contributed to the increase in total monohexosylceramide were $d_{18:1/16:0}$ (r^2=0.273, p=0.003) (**C**) and $d_{18:1/24:0}$ (r^2=0.164, p=0.026) monohexosylceramide (**D**). These data have been submitted for publication.

IV. Modifying Factors That Alter Correlations between Sphingolipids and Neutrophil Elastase in Cystic Fibrosis Sputum.

The presence of bacteria in sputum, severity of lung disease, and patient gender modified the association between active NE and certain sphingolipid moieties in CF sputum. In sputum samples that were culture positive for MRSA, there was a statistically significant, stronger association between active NE and $d_{18:1/14:0}$ sphingomyelin (p=0.0034), $d_{18:1/24:0}$ ceramide (p=0. 0257), as well as total monohexosylceramide (p=0. 0064), due to changes in $d_{18:1/14:0}$ and $d_{18:1/16:0}$ monohexosylceramide (p=0.0007and p=0.003, respectively) (**Table 12**). Surprisingly, the presence of *P. aeruginosa* in sputum did not significantly affect the associations between sphingolipids and active NE. FEV_1 (% predicted) affected the association between $d_{18:1/14:0}$ sphingomyelin (p=0.0318) and active NE and $d_{18:1/14:0}$ monohexosylceramide (p=0. 0403); the higher the lung function, the weaker the association between active NE and these two $d_{18:1/14:0}$ sphingolipid moieties (**Table 12**); the change was statistically significant. Finally, the subject's gender significantly affected the association between $d_{18:1/14:0}$ sphingomyelin (p=0.0015) and $d_{18:1/14:0}$ monohexosylceramide (p=0.0472) and active NE. Females had a statistically significant, stronger association between those two sphingolipid moieties and active NE (**Table 12**).

Table 12. Modifying factors that influence the association between NE and sphingolipids in sputum from CF patients.

Modifying Factors	Sphingolipid	Change in Slope	Standard Error	p-value
MRSA Positive Culture	Sphingomyelin $d_{18:1/14:0}$	0.233	0.06406	0.0034
	Total Monohexosylceramide	0.183	0.05539	0.0064
	Monohexosylceramide $d_{18:1/14:0}$	13.816	3.0586	0.0007
	Monohexosylceramide $d_{18:1/16:0}$	0.367	0.09921	0.003
	Ceramide $d_{18:1/24:0}$	0.591	0.2324	0.0257
FEV_1 % predicted	Sphingomyelin $d_{18:1/14:0}$	-0.164	0.06836	0.0318
	Monohexosylceramide $d_{18:1/14:0}$	-8.823	3.8738	0.0403
Female Gender	Sphingomyelin $d_{18:1/14:0}$	0.282	0.07023	0.0015
	Monohexosylceramide $d_{18:1/14:0}$	8.105	3.6967	0.0472

These data have been submitted for publication.

Chapter 4. Discussion

I. Neutrophil Elastase Increased Airway Ceramide in a Mouse Model of Neutrophil Elastase-induced Inflammation.

Chronic infection and maladaptive, neutrophilic inflammation are characteristic of CF lung disease; consequently, eliminating pulmonary infections and decreasing inflammation are two of the primary therapeutic approaches to CF (33, 43, 144). Despite decades of research, safe and effective anti-inflammatory therapy remains an unmet need. NE, a neutrophil-derived protease, is a major contributor to lung injury and development of bronchiectasis in CF (113, 121) and emphysema in COPD (8). In this study, we make a novel observation: that exogenous NE increases the levels of ceramide in a mouse model of NE-induced, sterile inflammation. We demonstrate that NE specifically increases ceramide production via the *de novo* pathway, likely mediated via increased SPTLC2 protein levels. Sphingolipid metabolism is closely linked to inflammation in the lungs; increasing the concentration of ceramide favors the development of pathological inflammation (42), both in diseases with acute onset like pulmonary edema (45) as well as more chronic inflammatory diseases like CF and COPD (42, 94, 133). Our findings suggest that ceramide may mediate the induction of pro-inflammatory cytokines, whose release is stimulated by NE, which would be especially relevant in the context of inflammatory lung disease. Thus, the significance of our findings is a new paradigm of a potential self-perpetuating cycle of

inflammation in the CF airways: NE promotes ceramide production, which upregulates neutrophil chemokines, KC and HMGB1, thereby increasing neutrophilic inflammation and local NE load.

Ceramide moieties have a broad repertoire of pro-inflammatory activities (42), and the properties of ceramide are dependent on fatty acid chain length (48), though this phenomenon has yet to be fully explored. Thus, increased synthesis of ceramide moieties of different chain lengths is likely an important factor contributing to inflammation. In the context of neutrophilic inflammation, recent studies indicate that ceramide and other bioactive sphingolipids have a profound effect on neutrophil migration and function (34). First, in a mouse model of multiple sclerosis, different pools of ceramide regulate neutrophil migration—$d_{18:1/24:0}$ ceramide upregulates *Cxcr2* mRNA expression (5), while $d_{18:1/16:0}$ inhibits *Cxcr2* expression and neutrophil adhesion (31). Moreover, both exogenous and intracellular ceramide are important for neutrophil phagocytic function. For example, a rise in ceramide production correlates with the culmination of oxidative burst (34). Conversely, introducing exogenous short chain ceramides can inhibit IgG-induced phagocytosis (34). In our model of NE-induced inflammation, we observed increases in $d_{18:1/22:0}$, $d_{18:1/24:0}$ and $d_{18:1/24:1}$ ceramide moieties, which was reflected by a statistically significant, 2.5-fold increase in total ceramide (**Figure 4**). Likewise, in a mouse model of emphysema, where a bolus of porcine pancreatic elastase was delivered intratracheally to injure the airways, Tibboel et al. (2013) observed increases in $d_{18:1/22:0}$, $d_{18:1/24:0}$ and $d_{18:1/24:1}$ ceramide. However, they also described increases in other, shorter chain ceramides as well as two dihydroceramides (134). Since myriocin, a suicide inhibitor of SPT (147), alleviated elastase-induced changes in lung function and the increase in BAL ceramides, authors attributed the upregulation of ceramide to *de novo* sphingolipid synthesis (134). However, they also observed changes in the expression of

ceramidases and acid SMase after elastase injury, over a 21-day time course. In contrast, we chose to focus on the enzyme responsible for the rate-limiting step of *de novo* ceramide synthesis: SPT.

SPT is a critical enzyme in *de novo* ceramide synthesis, but its structure and subunit stoichiometry in mammals is still under debate (115). It is speculated that the active site(s) of SPT are likely formed by a heterodimer of SPTLC1 and either SPTLC2 or SPTLC3 (56). We detected a 2.5-fold increase in SPTLC2 protein levels at 24h after delivery of the final NE dose, compared to animals that aspirated vehicle control (**Figure 5**). We also observed a 30%, statistically significant decrease in SPTLC1. However, due to lack of a reliable antibody SPTLC3 was not assessed. The ratio of SPTLC2 to SPTLC3 within the multimeric protein may influence the enzymatic activity of SPT, and an increase in SPTLC2 may facilitate the production of $d_{18:1/18:0}$ and long chain ceramides, including $d_{18:1/22:0}$, $d_{18:1/24:0}$, and $d_{18:1/24:1}$ (56). Thus, the increase in long chain ceramide moieties we observed is consistent with increased SPTLC2 protein and activity, especially as the rise in ceramide levels was noted at the same time point as increased expression of SPTLC2.

Currently, the regulatory mechanisms that control SPT protein expression and activity are poorly defined (15, 16, 41, 89). Our data suggest that NE upregulates SPTLC2 by a post-transcriptional mechanism, as we did not detect a change in *SPTLC1* and *SPTLC2* mRNA at 24h, or at earlier time points (**Figure 6**). One mechanism that could increase SPT protein is downregulation of microRNA miR-137, 181c, -9 or 29a/b, which would permit increased transcription and/or translation of SPT (41), though the former would be reflected by increases in mRNA. We also assessed the expression of two known modulators of SPT activity— ORMDL3 and RTN4 (15, 16), in the lungs. Neither ORMDL3 nor RTN4 protein levels were significantly different when comparing animals that were administered a vehicle control versus NE (**Figure 7**).

Thus, administering NE does not appear to influence *de novo* sphingolipid production by modulating known negative regulators of SPT activity. This supports the idea that the observed increase in SPTLC2 affects the enzymatic activity of SPT in our mouse model of NE-induced inflammation.

Pre-treating mice with myriocin, an SPT inhibitor, prior to administering NE, reduced ceramide expression at 24h. There was a trend towards decreased total ceramide, due to statistically significant decreases in $d_{18:1/22:0}$ and $d_{18:1/24:1}$ ceramide moieties and downward trend in $d_{18:1/24:0}$ ceramide, in mice administered myriocin prior to NE aspiration. Interestingly, pre-treatment with myriocin did not significantly alter the expression profile of other sphingolipids present in BAL, with the exception of $d_{18:1/14:0}$ sphingomyelin, which was not induced by NE. Likewise, myriocin did not alter the expression of SPTLC2 protein in mouse lungs.

Notably, inhibiting SPT activity using myriocin, decreased ceramide levels as well as NE-induced expression of pro-inflammatory signaling molecules in murine BAL, including KC and HMGB1. Mice that were administered NE had approximately 40% neutrophils, compared to mice administered control vehicle which had approximately 5-10% neutrophils in BAL. However, neither the total number of leukocytes nor the proportion of neutrophils present in the BAL were significantly decreased when mice were administered an SPT inhibitor. These data corroborate the fact that NE can activate several signaling pathways that perpetuate neutrophil dominant airway inflammation (142), and while ceramide may provide yet another link between NE and cytokine expression, inhibiting *de novo* ceramide synthesis does not abrogate all of the pro-inflammatory effects stimulated by NE. This apparent disconnect between KC levels and neutrophil cell counts has been observed previously. In a model of myocardial infarction, suppression of KC using neutralizing antibodies did not decrease the influx of neutrophil that occurs shortly after an infarct

is induced (88). One possible pro-inflammatory signal that stimulates neutrophil chemotaxis in our model is IL33. Full length IL33 is intracellular, a non-histone DNA-binding protein that regulates gene expression. IL33 is released from damaged and necrotic cells and can be cleaved by neutrophil-derived proteases, including NE, into its mature form (69). Mature IL33, like HMGB1, is an alarmin and extracellular cytokine. IL33 has been detected in airway epithelium from patients with CF (110), and while IL33 is not directly chemotactic toward neutrophils, it potentiates neutrophil recruitment (4, 110). Other possible contributors that could stimulate neutrophil influx in our model includes bioactive lipids such as leukotriene B4 (LTB4). LTB4 is a secondary chemoattractant released by leukocytes, including neutrophils and macrophages, and contributes to both neutrophil activation and migration (2) (82). Finally, components of the complement system are major mediators of inflammation in a variety of diseases, and recent data indicate complement has a role in pulmonary inflammation in CF (50). Complement effectors C3a and C5a, could be involved with neutrophil influx in our model. A mouse model of pancreatic elastase-induced abdominal aortic aneurysm demonstrated that neutrophil recruitment was dependent on the alternative pathway of complement activation (90). This led to production of C3a and C5a, which subsequently stimulated neutrophil recruitment to the site of injury (90). It is likely that modifying ceramide levels alone is beneficial but not sufficient to block all NE-triggered pro-inflammatory pathways that facilitate neutrophilic inflammation in our mouse model of NE-induced inflammation.

There are limitations associated with this study, directing the focus of future research based on these data. First, we chose to focus on SPT and *de novo* sphingolipid biosynthesis. We have yet to evaluate whether NE changes expression or activity of SMases, CerS, or components of the salvage pathway *in vivo* to increase ceramide accumulation (**Figure 2**). SMases convert

sphingomyelin into ceramide. Generation of long chain ceramides, such as those we observed in our model, may also be due to increased expression of specific CerS. CerS are downstream of SPT in the *de novo* sphingolipid biosynthetic pathway, and are also involved in the salvage pathway (137). CerS2 and 5 are highly expressed in the lung (93), and CerS2 regulates the generation of $d_{18:1/22:0}$, $d_{18:1/24:1}$ and $d_{18:1/24:0}$ ceramides (67, 93). Additionally, one of the major limitations of studying the biological effects of long chain ceramide moieties, is that there is no reliable method of delivering exogenous long chain ceramides into cells, due to difficulties with cellular uptake. On the other hand, generation of novel inhibitors that would affect the activity of specific ceramide synthases, thereby limiting production of ceramides of different chain lengths, would propel our understanding of the mechanisms further. Overall, our data support the concept that more than one pathway of ceramide production are stimulated by NE, as $d_{18:1/24:0}$ ceramide, one of the moieties increased after administration of NE, trended downwards but was not significantly decreased when animals were pre-treated with myriocin.

Based on the novel mechanism we describe, *de novo* ceramide production may be induced by NE in airways of patients with chronic inflammatory lung diseases. This provides novel targets for anti-inflammatory therapeutics. We propose that this association between NE and ceramide may be present in patients that suffer from acute and chronic neutrophilic inflammation in the lungs, such as those with CF or COPD, who demonstrate high levels of NE in airway surface fluid (142). Thus, in the clinical portion of this project, we sought to determine whether there is an association between NE activity and sphingolipid profiles in the CF airway.

II. Associations Between Neutrophil Elastase and Sphingolipids in Cystic Fibrosis Sputum.

Our retrospective study of the sphingolipid content of CF sputum is the largest of its type in this cohort to date and is the first study investigating the association between NE and sphingolipids. Sputum sphingolipid levels varied among patients and with clinical status, demonstrating statistically significant increases in $d_{18:1/14:0}$ ceramide, $d_{18:1/24:1}$ ceramide, and $d_{18:1/24:0}$ monohexosylceramide during hospitalization for CF pulmonary exacerbation. Assessing the levels of active NE and sphingolipid content of sputum samples, we observed a linear correlation between concentrations of NE and sphingolipids present in the sputum of patients with CF. Increasing active NE was associated with higher levels of a variety of sphingolipids in sputum, with statistically significant linear correlations between the levels of active NE and the concentrations of total sphingomyelin, ceramide, monohexosylceramide, and S1P (**Figure 19**). The greatest variety in different chain-length sphingolipids that increased with elevated NE activity were sphingomyelin moieties. In contrast, with ceramide, there were statistically significant linear correlations between active NE and $d_{18:1/22:0}$ and $d_{18:1/24:0}$ ceramide, both of which we saw increase in the BAL of our *in vivo* model of NE-induced inflammation. Finally, there were two monohexosylceramide moieties that increased with a rise in NE activity. Our study confirmed the existence of an association between NE and sphingolipid content in CF sputum. Taken in concert with published data relevant to COPD (133) and CF (13, 100), our data suggest that neutrophilic inflammation contributes to the abnormal sphingolipid levels observed in the lungs of patients with CF, possibly exacerbating an imbalance caused by CFTR dysfunction.

The role of sphingolipids in the pathogenesis of CF lung disease in humans remains largely unexplored, though an association between increased ceramide and neutrophilic inflammation has been noted previously in CF lung tissue (13). To our knowledge, limited data are available

regarding the sphingolipid content in the BAL or sputum of patients with CF. Blood biomarkers are often preferable, due to ease of collection. Recent studies by Guilbault et al. demonstrated decreased ceramide in serum from CF patients, compared to healthy controls, particularly in $d_{18:1/14:0}$, $d_{18:1/20:1}$, $d_{18:1/22:1}$, $d_{18:1/24:0}$ ceramide moieties (49). In contrast, Brodlie et al. observed increased ceramide in explants of human lung tissue from CF subjects compared to non-CF controls (13). Also, they described an association between markers of neutrophilic inflammation and elevated $d_{18:1/16:0}$, $d_{18:1/18:0}$, and $d_{18:1/20:0}$ ceramide (13). Furthermore, in CF sputum, Quinn et al. also observed that sphingomyelin $d_{18:1/14:0}$, $d_{18:1/15:0}$, $d_{18:1/16:1}$, and $d_{18:1/16:0}$ as well as two $d_{18:1/16:0}$ glycosphingolipids, tetraglycosylceramide and lactosylceramide, were elevated when compared to non-CF sputum (100). In a single subject with CF followed for 4.2 years, ceramide was increased during treatment of pulmonary exacerbation (99). These studies support our conclusion, that sphingolipids are increased locally in the CF airways, emphasizing the importance of looking at both systemic and local changes in sphingolipid profile in lung diseases.

Methicillin-resistant *S. aureus* (MRSA) and *P. aeruginosa* are two of the most common bacterial pathogens that chronically infect CF airways. Thus, we examined whether the presence of MRSA and *P. aeruginosa* in sputum modified the association between active NE and the concentrations of various sphingolipids. While ceramide metabolites are critical components in host responses to various bacterial, viral and fungal infections (92, 117), in a recent study that focused on sputum metabolomics and bacteriology, Quinn et al. determined that the sputum levels of sphingolipids, including sphingomyelin, ceramide, and lactosylceramide, did not correlate with the multitude of bacterial genera they observed in the CF sputum (100). Our data revealed that the presence of MRSA modified the association of active NE and $d_{18:1/14:0}$ sphingomyelin, $d_{18:1/24:0}$ ceramide and total monohexosylceramide— likely due to $d_{18:1/14:0}$ and $d_{18:1/16:0}$

monohexosylceramide (**Table 12**). The presence of MRSA in patient sputum strengthened the association between active NE and the concentrations of these sphingolipids. This is notable, as others have reported that *CFTR*-deficient mice are more susceptible to *S. aureus* infection, and that an imbalance between sphingosine and ceramide appears to be the culprit (131). In contrast, we observed no modifying effects when sputum cultures were positive for *P. aeruginosa*. This corroborates the data reported by Yu et al., in which the presence of *P. aeruginosa* stimulated acid SMase activity and ceramide synthesis in normal airway epithelial cells and wild-type mice, but not in *CFTR*-deficient cells or Cftr knockout mice (156). Cftr knockout mice are more susceptible to *P. aeruginosa* infection, possibly due to a decrease in sphingosine and increase in ceramide in their airways caused by lower enzymatic activity of acid ceramidase (96).

MRSA or *P. aeruginosa* infection of the lungs can lead to decreased lung function, detected as a drop in FEV_1 % predicted, indicating a flare or exacerbation of CF lung disease— a CF pulmonary exacerbation. FEV_1 is known to be inversely associated with NE in CF (76), but, we wanted to determine whether patient lung function modified the association between NE and sphingolipids. Most of our subjects were adults with severe (FEV_1<50% predicted) obstructive lung disease. Thus, the differences in lung function between outpatient visits and hospitalization, while statistically significant, were relatively small: a 5% drop in FEV_1 % predicted during hospitalization. When the data collected from all 30 samples were analyzed using a linear mixed model, we observed that higher FEV_1 % predicted weakened the association between NE and sputum sphingolipid content, i.e., the better the lung function, the weaker the association between active NE and $d_{18:1/14:0}$ sphingomyelin and $d_{18:1/14:0}$ monohexosylceramide (**Table 12**).

Lastly, there are data that indicate that gender affects the progression of CF, with female patients having increased morbidity and shorter life expectancies (53, 129). Thus, we assessed the

effect of patient gender on the correlation between active NE and sphingolipids. There was an increased association between two sputum sphingolipids— $d_{18:1/14:0}$ sphingomyelin and $d_{18:1/14:0}$ monohexosylceramide, and NE in female subjects (**Table 12**); the same two sphingolipid moieties that had stronger associations with active NE with poorer lung function. However, five out of seven of the female subjects participating in our study had severe lung disease, with the other two having moderate lung disease as defined by FEV_1 % predicted criteria. Of the eight male subjects that provided sputum samples, three had mild, four had moderate, and only one had severe lung disease. Thus, it is possible the change in correlation between NE and $d_{18:1/14:0}$ sphingomyelin and $d_{18:1/14:0}$ monohexosylceramide with gender reflected the poorer lung function in female than in male subjects in our study. On the other hand, sphingolipids in serum and plasma are known to vary between genders (52). For example, healthy female subjects have increased $d_{18:1/18:0}$, $d_{18:1/22:0}$ and $d_{18:1/24:0}$ dihydroceramide moieties in the blood, and overall demonstrate a trend towards higher levels of dihydroceramides (52). The significance of these sex-related influences on sphingolipid and NE associations remains to be determined. As we and others (13, 99, 100) have demonstrated, local changes in pulmonary sphingolipid levels do not necessarily reflect those seen systemically (49). Thus, it is critical to determine whether there is gender-based variability in airway sphingolipid profiles.

While our analysis of CF sputum demonstrates a possible relationship between active NE and *de novo* sphingolipid biosynthesis, our study has several limitations. First, the number of samples assessed in this study was low, with a total of fifteen subjects participating in the study. As all of the sputum samples in the VCU Biospecimen Repository are spontaneously expectorated, this limits sample availability; only a fraction of patients with CF— those with severe mutations— spontaneously expectorate sputum, especially when not hospitalized for CF pulmonary

exacerbation. Additionally, most of the subjects had severe (FEV_1<50% predicted) obstructive lung disease, as was reflected by the low, but still statistically significant, difference in FEV_1 % predicted when patients were hospitalized for CF pulmonary exacerbation versus outpatient visits. Concentrations of active NE in sputum did not differ significantly between samples collected during hospitalization versus outpatient visits, likely because our sputum donors had relatively high levels of chronic neutrophilic inflammation, as most had severe lung disease. Similar observations have been reported by others (105).

III. Future Studies: *In Vitro*, *In Vivo*, *Ex Vivo*.

Future studies will focus on mapping the signaling pathways that connect NE, inflammation, and sphingolipid synthesis, describing the metabolic pathways that contribute to NE-induced ceramide, and evaluating whether CFTR dysfunction and bacterial infection modulate these pathways. The presence of a strong Lipidomics Core at VCU gives our lab a unique opportunity; using quantitative lipidomic analyses, we can investigate sphingolipid homeostasis in the airways by using cellular and animal models as well as biological samples.

Establishing an *in vitro* cell culture model would provide a more tractable system to investigate the mechanisms behind NE-induced changes in sphingolipid generation. However, which cell type or types are responsible for the NE-induced increases in ceramide detected in murine BAL, as well as those responsible for the associations between active NE and various sphingolipids in CF sputum, are currently unknown. Brodlie et al. potentially localized the increase in ceramide in the lower airways to epithelial and inflammatory cells using immunohistochemistry (13). The first step of establishing an *in vitro* model would involve determining whether the

sphingolipid profile observed in NE-treated cells recapitulates that of our mouse model of NE-induced inflammation or the association observed in CF sputum. If so, we could use these cells to approximate NE-induced changes in sphingolipid production in the lungs.

If we determine that NE treatment alters sphingolipid homeostasis and increases ceramide accumulation in differentiated cultures of primary human tracheal epithelial cells, we could examine whether reactive oxygen species (ROS) are required for this mechanism by inhibition of oxidative stress prior to and during NE treatment. NE is known to increase free iron and oxidative stress in airway epithelial cells (36). ROS can affect sphingolipid homeostasis by affecting both enzymatic activity and cellular levels of enzymes involved in sphingolipid production (72). On the other hand, ceramide, sphingosine, and S1P have been reported to modulate cellular redox via a variety of methods. For example, ceramide can stimulate NADPH oxidase activity, xanthine oxidase and enzymes in the mitochondrial respiratory chain to generate ROS (72). We could also test whether inhibiting key enzymatic steps involved in the different pathways of ceramide production, using genetic silencing or pharmacologic inhibition, modulates the production of ROS, as well as the biosynthesis and release of pro-inflammatory chemokines and cytokines.

More than one cell type could contribute to NE-induced changes in sphingolipid metabolism, and an *in vitro* model may prove difficult to establish. If so, we would undertake a more in-depth study of the pathways that contribute to the increase in ceramide induced by NE using our translational model. We could assess the effect of inhibiting the SMase pathway on ceramide production and neutrophilic inflammation in our model using desipramine. Inhibition of both *de novo* and SMase-derived ceramides could act in an additive or synergistic fashion to mitigate neutrophilic inflammation. Localized gene silencing using RNA interference (RNAi), by delivering siRNA to the lungs, could be used to verify our results with pharmacological inhibitors.

Appropriate methods for evaluating siRNA distribution and quantifying expression levels in tissue have been described previously (54). Thus, RNAi could be used to further dissect the metabolic pathways that contribute to the NE-induced increase in ceramide. Additionally, intranasal delivery of siRNA has been demonstrated in other animal models, including a rhesus macaque model used to study severe acute respiratory syndrome (71), and may allow for not only knockdown of SPTLC and SMase, but also of specific CerS.

Finally, we have yet to investigate whether CFTR deficiency could influence NE-induced inflammation and airway sphingolipid levels. Administering NE to *Cftr*-knockout mice may provide a model that more closely approximates inflammation in CF lung disease. It is possible we would observe upregulation and downregulation of different sphingolipid species due to alteration in enzyme expression in *Cftr*-knockout mice. We could also investigate how bacterial infection interacts with our model of NE-induced inflammation and alters pulmonary sphingolipid profiles. While most bacteria do not produce sphingolipids, many are able to repurpose host-derived sphingolipids to promote virulence (55). For example, some intracellular pathogens can use ceramide-enriched lipid microdomains or rafts to enter cells, while other bacteria scavenge sphingolipids for incorporation into their cell membranes (55, 74). Thus, we are well-positioned to decipher the contribution of NE, CFTR, and bacterial infection on sphingolipid homeostasis.

Future clinical trials should include a study group of patients with CF that have a greater range of lung function; including healthier patients with milder mutations which would allow us to determine whether the severity of CFTR dysfunction affects sphingolipid expression in individuals. The study protocol should include sputum induction, to elicit the collection of airway secretions from those that do not spontaneously produce sputum. Likewise, collecting induced

sputum would allow for a much larger, more varied study group. Consequently, a larger future trial could be used to determine whether gender could affect airway sphingolipid homeostasis.

In summary, this dissertation describes a novel mechanism that modulates inflammation and *de novo* ceramide biosynthesis in mouse lungs, induced by oropharyngeal aspiration of human NE. Analysis of sphingolipids in CF sputum detected a link between NE and long chain ceramide generation. Therefore, a similar mechanism may exist in humans: endogenous NE in CF could contribute to persistent inflammation in the human airway. Our results prompt a paradigm shift in our understanding of sphingolipid homeostasis in CF, as a novel pathway likely contributes to persistent airway inflammation: a potential feed-forward mechanism of neutrophilic inflammation and ceramide accumulation. While there is compelling published evidence that sphingolipid homeostasis plays an important role in innate immune function and regulation of inflammation in inflammatory lung diseases, the cellular sources of these effects are poorly understood. Our lab is positioned to further evaluate the molecular and cellular mechanisms that govern the contribution of NE-induced ceramide to inflammation. In aggregate, our results merit further exploration to elucidate biological pathways in human tissues and identify new therapeutic targets to control the excessive and injurious inflammation in CF lung disease.

List of References

1. **Adams C, Icheva V, Deppisch C, Lauer J, Herrmann G, Graepler-Mainka U, Heyder S, Gulbins E, and Riethmueller J**. Long-Term Pulmonal Therapy of Cystic Fibrosis-Patients with Amitriptyline. *Cell Physiol Biochem* 39: 565-572, 2016.

2. **Afonso PV, Janka-Junttila M, Lee YJ, McCann CP, Oliver CM, Aamer KA, Losert W, Cicerone MT, and Parent CA**. LTB4 is a signal-relay molecule during neutrophil chemotaxis. *Dev Cell* 22: 1079-1091, 2012.

3. **Alton E, Armstrong DK, Ashby D, Bayfield KJ, Bilton D, Bloomfield EV, Boyd AC, Brand J, Buchan R, Calcedo R, Carvelli P, Chan M, Cheng SH, Collie DDS, Cunningham S, Davidson HE, Davies G, Davies JC, Davies LA, Dewar MH, Doherty A, Donovan J, Dwyer NS, Elgmati HI, Featherstone RF, Gavino J, Gea-Sorli S, Geddes DM, Gibson JSR, Gill DR, Greening AP, Griesenbach U, Hansell DM, Harman K, Higgins TE, Hodges SL, Hyde SC, Hyndman L, Innes JA, Jacob J, Jones N, Keogh BF, Limberis MP, Lloyd-Evans P, Maclean AW, Manvell MC, McCormick D, McGovern M, McLachlan G, Meng C, Montero MA, Milligan H, Moyce LJ, Murray GD, Nicholson AG, Osadolor T, Parra-Leiton J, Porteous DJ, Pringle IA, Punch EK, Pytel KM, Quittner AL, Rivellini G, Saunders CJ, Scheule RK, Sheard S, Simmonds NJ, Smith K, Smith SN, Soussi N, Soussi S, Spearing EJ, Stevenson BJ, Sumner-Jones SG, Turkkila M, Ureta RP, Waller MD, Wasowicz MY, Wilson JM, Wolstenholme-Hogg P, and Consortium UKCFGT**. Repeated nebulisation of non-viral CFTR

gene therapy in patients with cystic fibrosis: a randomised, double-blind, placebo-controlled, phase 2b trial. *Lancet Respir Med* 3: 684-691, 2015.

4. **Alves-Filho JC, Sonego F, Souto FO, Freitas A, Verri WA, Jr., Auxiliadora-Martins M, Basile-Filho A, McKenzie AN, Xu D, Cunha FQ, and Liew FY**. Interleukin-33 attenuates sepsis by enhancing neutrophil influx to the site of infection. *Nat Med* 16: 708-712, 2010.

5. **Barthelmes J, de Bazo AM, Pewzner-Jung Y, Schmitz K, Mayer CA, Foerch C, Eberle M, Tafferner N, Ferreiros N, Henke M, Geisslinger G, Futerman AH, Grosch S, and Schiffmann S**. Lack of ceramide synthase 2 suppresses the development of experimental autoimmune encephalomyelitis by impairing the migratory capacity of neutrophils. *Brain Behav Immun* 46: 280-292, 2015.

6. **Beckmann N, Sharma D, Gulbins E, Becker KA, and Edelmann B**. Inhibition of acid sphingomyelinase by tricyclic antidepressants and analogons. *Front Physiol* 5: 331, 2014.

7. **Bell SC, De Boeck K, and Amaral MD**. New pharmacological approaches for cystic fibrosis: promises, progress, pitfalls. *Pharmacol Ther* 145: 19-34, 2015.

8. **Bihlet AR, Karsdal MA, Sand JM, Leeming DJ, Roberts M, White W, and Bowler R**. Biomarkers of extracellular matrix turnover are associated with emphysema and eosinophilic-bronchitis in COPD. *Respir Res* 18: 22, 2017.

9. **Bobadilla JL, Macek, Jr., M., Fine, J.P., Farrell, P.M.** Cystic Fibrosis: a worldwide analysis of CFTR mutations-correlation with incidence data and application to screening. *Hum Mutat* 19: 575-606, 2002.

10. **Bodas M, Min T, Mazur S, and Vij N**. Critical modifier role of membrane-cystic fibrosis transmembrane conductance regulator-dependent ceramide signaling in lung injury and emphysema. *J Immunol* 186: 602-613, 2011.

11. **Boucher R**. New concepts of the pathogenesis of cystic fibrosis lung disease. *Eur Respir J* 23: 146-158, 2004.

12. **Boyle MP, Bell SC, Konstan MW, McColley SA, Rowe SM, Rietschel E, Huang X, Waltz D, Patel NR, Rodman D, and group VXs**. A CFTR corrector (lumacaftor) and a CFTR potentiator (ivacaftor) for treatment of patients with cystic fibrosis who have a phe508del CFTR mutation: a phase 2 randomised controlled trial. *Lancet Respir Med* 2: 527-538, 2014.

13. **Brodlie M, McKean MC, Johnson GE, Gray J, Fisher AJ, Corris PA, Lordan JL, and Ward C**. Ceramide is increased in the lower airway epithelium of people with advanced cystic fibrosis lung disease. *Am J Respir Crit Care Med* 182: 369-375, 2010.

14. **Bruscia EM, and Bonfield TL**. Cystic Fibrosis Lung Immunity: The Role of the Macrophage. *J Innate Immun* 8: 550-563, 2016.

15. **Cai L, Oyeniran C, Biswas DD, Allegood J, Milstien S, Kordula T, Maceyka M, and Spiegel S**. ORMDL proteins regulate ceramide levels during sterile inflammation. *J Lipid Res* 57: 1412-1422, 2016.

16. **Cantalupo A, Zhang Y, Kothiya M, Galvani S, Obinata H, Bucci M, Giordano FJ, Jiang XC, Hla T, and Di Lorenzo A**. Nogo-B regulates endothelial sphingolipid homeostasis to control vascular function and blood pressure. *Nat Med* 21: 1028-1037, 2015.

17. **Cantin AM, Hartl D, Konstan MW, and Chmiel JF**. Inflammation in cystic fibrosis lung disease: Pathogenesis and therapy. *Journal of cystic fibrosis : official journal of the European Cystic Fibrosis Society* 14: 419-430, 2015.

18. **Castellani C, Cuppens H, Macek M, Jr., Cassiman JJ, Kerem E, Durie P, Tullis E, Assael BM, Bombieri C, Brown A, Casals T, Claustres M, Cutting GR, Dequeker E, Dodge J, Doull I, Farrell P, Ferec C, Girodon E, Johannesson M, Kerem B, Knowles M, Munck A, Pignatti PF, Radojkovic D, Rizzotti P, Schwarz M, Stuhrmann M, Tzetis M, Zielenski J, and Elborn JS**. Consensus on the use and interpretation of cystic fibrosis mutation analysis in clinical practice. *Journal of cystic fibrosis : official journal of the European Cystic Fibrosis Society* 7: 179-196, 2008.

19. **Chalmers JD, Moffitt KL, Suarez-Cuartin G, Sibila O, Finch S, Furrie E, Dicker A, Wrobel K, Elborn JS, Walker B, Martin SL, Marshall SE, Huang JT, and Fardon TC**. Neutrophil Elastase Activity Is Associated with Exacerbations and Lung Function Decline in Bronchiectasis. *Am J Respir Crit Care Med* 195: 1384-1393, 2017.

20. **Chirico V, Lacquaniti A, Leonardi S, Grasso L, Rotolo N, Romano C, Di Dio G, Lionetti E, David A, Arrigo T, Salpietro C, and La Rosa M**. Acute pulmonary exacerbation and lung function decline in patients with cystic fibrosis: high-mobility group box 1 (HMGB1) between inflammation and infection. *Clinical microbiology and infection : the official publication of the European Society of Clinical Microbiology and Infectious Diseases* 21: 368 e361-369, 2015.

21. **Cholon DM, Quinney NL, Fulcher ML, Esther CR, Jr., Das J, Dokholyan NV, Randell SH, Boucher RC, and Gentzsch M**. Potentiator ivacaftor abrogates pharmacological correction of DeltaF508 CFTR in cystic fibrosis. *Science translational medicine* 6: 246ra296, 2014.

22. **Chung S, Vu S, Filosto S, and Goldkorn T**. Src regulates cigarette smoke-induced ceramide generation via neutral sphingomyelinase 2 in the airway epithelium. *Am J Respir Cell Mol Biol* 52: 738-748, 2015.

23. **Cohen-Cymberknoh M, Kerem E, Ferkol T, and Elizur A**. Airway inflammation in cystic fibrosis: molecular mechanisms and clinical implications. *Thorax* 68: 1157-1162, 2013.

24. **Cohen TS, and Prince A**. Cystic fibrosis: a mucosal immunodeficiency syndrome. *Nat Med* 18: 509-519, 2012.

25. **Davies J, Sheridan H, Bell N, Cunningham S, Davis SD, Elborn JS, Milla CE, Starner TD, Weiner DJ, Lee PS, and Ratjen F**. Assessment of clinical response to ivacaftor with lung clearance index in cystic fibrosis patients with a G551D-CFTR mutation and preserved spirometry: a randomised controlled trial. *Lancet Respir Med* 1: 630-638, 2013.

26. **Davies JC, Wainwright CE, Canny GJ, Chilvers MA, Howenstine MS, Munck A, Mainz JG, Rodriguez S, Li H, Yen K, Ordonez CL, Ahrens R, and Group VXS**. Efficacy and safety of ivacaftor in patients aged 6 to 11 years with cystic fibrosis with a G551D mutation. *Am J Respir Crit Care Med* 187: 1219-1225, 2013.

27. **De Boeck K, Munck A, Walker S, Faro A, Hiatt P, Gilmartin G, and Higgins M**. Efficacy and safety of ivacaftor in patients with cystic fibrosis and a non-G551D gating mutation. *Journal of cystic fibrosis : official journal of the European Cystic Fibrosis Society* 13: 674-680, 2014.

28. **de Boer K, Vandemheen KL, Tullis E, Doucette S, Fergusson D, Freitag A, Paterson N, Jackson M, Lougheed MD, Kumar V, and Aaron SD**. Exacerbation frequency and clinical outcomes in adult patients with cystic fibrosis. *Thorax* 66: 680-685, 2011.

29. **Ding J, Cui X, and Liu Q**. Emerging role of HMGB1 in lung diseases: friend or foe. *J Cell Mol Med* 21: 1046-1057, 2017.

30. **Doring G, Flume P, Heijerman H, Elborn JS, and Consensus Study G**. Treatment of lung infection in patients with cystic fibrosis: current and future strategies. *Journal of cystic fibrosis : official journal of the European Cystic Fibrosis Society* 11: 461-479, 2012.

31. **Eberle M, Ebel P, Mayer CA, Barthelmes J, Tafferner N, Ferreiros N, Ulshofer T, Henke M, Foerch C, de Bazo AM, Grosch S, Geisslinger G, Willecke K, and Schiffmann S**. Exacerbation of experimental autoimmune encephalomyelitis in ceramide synthase 6 knockout mice is associated with enhanced activation/migration of neutrophils. *Immunol Cell Biol* 93: 825-836, 2015.

32. **Eigen H, Rosenstein BJ, FitzSimmons S, and Schidlow DV**. A multicenter study of alternate-day prednisone therapy in patients with cystic fibrosis. Cystic Fibrosis Foundation Prednisone Trial Group. *J Pediatr* 126: 515-523, 1995.

33. **Elborn JS**. Cystic fibrosis. *Lancet* 388: 2519-2531, 2016.

34. **Espaillat MP, Snider AJ, Qiu Z, Channer B, Coant N, Schuchman EH, Kew RR, Sheridan BS, Hannun YA, and Obeid LM**. Loss of acid ceramidase in myeloid cells suppresses intestinal neutrophil recruitment. *FASEB J* 2017.

35. **Evans CM, Raclawska DS, Ttofali F, Liptzin DR, Fletcher AA, Harper DN, McGing MA, McElwee MM, Williams OW, Sanchez E, Roy MG, Kindrachuk KN, Wynn TA, Eltzschig HK, Blackburn MR, Tuvim MJ, Janssen WJ, Schwartz DA, and Dickey BF**. The polymeric mucin Muc5ac is required for allergic airway hyperreactivity. *Nature communications* 6: 6281, 2015.

36. **Fischer BM, Domowicz DA, Zheng S, Carter JL, McElvaney NG, Taggart C, Lehmann JR, Voynow JA, and Ghio AJ**. Neutrophil elastase increases airway epithelial nonheme iron levels. *Clin Transl Sci* 2: 333-339, 2009.

37. **Fischer BM, and Voynow JA**. Neutrophil elastase induces MUC5AC gene expression in airway epithelium via a pathway involving reactive oxygen species. *Am J Respir Cell Mol Biol* 26: 447-452, 2002.

38. **Fisher JT, Zhang Y, and Engelhardt JF**. Comparative biology of cystic fibrosis animal models. *Methods Mol Biol* 742: 311-334, 2011.

39. **Fryer A, Huang YC, Rao G, Jacoby D, Mancilla E, Whorton R, Piantadosi CA, Kennedy T, and Hoidal J**. Selective O-desulfation produces nonanticoagulant heparin that retains pharmacological activity in the lung. *J Pharmacol Exp Ther* 282: 208-219, 1997.

40. **Garic D, De Sanctis JB, Wojewodka G, Houle D, Cupri S, Abu-Arish A, Hanrahan JW, Hajduch M, Matouk E, and Radzioch D**. Fenretinide differentially modulates the levels of long- and very long-chain ceramides by downregulating Cers5 enzyme: evidence from bench to bedside. *J Mol Med (Berl)* 95: 1053-1064, 2017.

41. **Geekiyanage H, and Chan C**. MicroRNA-137/181c regulates serine palmitoyltransferase and in turn amyloid beta, novel targets in sporadic Alzheimer's disease. *J Neurosci* 31: 14820-14830, 2011.

42. **Ghidoni R, Caretti A, and Signorelli P**. Role of Sphingolipids in the Pathobiology of Lung Inflammation. *Mediators of inflammation* 2015: 487508, 2015.

43. **Giddings O, and Esther CR, Jr.** Mapping targetable inflammation and outcomes with cystic fibrosis biomarkers. *Pediatr Pulmonol* 52: S21-S28, 2017.

44. **Gilligan PH**. Infections in patients with cystic fibrosis: diagnostic microbiology update. *Clin Lab Med* 34: 197-217, 2014.

45. **Goggel R, Winoto-Morbach S, Vielhaber G, Imai Y, Lindner K, Brade L, Brade H, Ehlers S, Slutsky AS, Schutze S, Gulbins E, and Uhlig S**. PAF-mediated pulmonary edema: a new role for acid sphingomyelinase and ceramide. *Nat Med* 10: 155-160, 2004.

46. **Grassme H, Riethmuller J, and Gulbins E**. Ceramide in cystic fibrosis. *Handb Exp Pharmacol* 265-274, 2013.

47. **Griffin KL, Fischer BM, Kummarapurugu AB, Zheng S, Kennedy TP, Rao NV, Foster WM, and Voynow JA**. 2-O, 3-O-Desulfated Heparin Inhibits Neutrophil Elastase-Induced HMGB-1 Secretion and Airway Inflammation. *Am J Respir Cell Mol Biol* 50: 684-689, 2014.

48. **Grosch S, Schiffmann S, and Geisslinger G**. Chain length-specific properties of ceramides. *Progress in lipid research* 51: 50-62, 2012.

49. **Guilbault C, De Sanctis JB, Wojewodka G, Saeed Z, Lachance C, Skinner TA, Vilela RM, Kubow S, Lands LC, Hajduch M, Matouk E, and Radzioch D**. Fenretinide corrects newly found ceramide deficiency in cystic fibrosis. *Am J Respir Cell Mol Biol* 38: 47-56, 2008.

50. **Hair PS, Sass LA, Vazifedan T, Shah TA, Krishna NK, and Cunnion KM**. Complement effectors, C5a and C3a, in cystic fibrosis lung fluid correlate with disease severity. *PLoS ONE* 12: e0173257, 2017.

51. **Hamai H, Keyserman F, Quittell LM, and Worgall TS**. Defective CFTR increases synthesis and mass of sphingolipids that modulate membrane composition and lipid signaling. *J Lipid Res* 50: 1101-1108, 2009.

52. **Hammad SM, Pierce JS, Soodavar F, Smith KJ, Al Gadban MM, Rembiesa B, Klein RL, Hannun YA, Bielawski J, and Bielawska A**. Blood sphingolipidomics in healthy humans: impact of sample collection methodology. *J Lipid Res* 51: 3074-3087, 2010.

53. **Harness-Brumley CL, Elliott AC, Rosenbluth DB, Raghavan D, and Jain R**. Gender differences in outcomes of patients with cystic fibrosis. *J Womens Health (Larchmt)* 23: 1012-1020, 2014.

54. **Hatakeyama H, Wu SY, Mangala LS, Lopez-Berestein G, and Sood AK**. Assessment of In Vivo siRNA Delivery in Cancer Mouse Models. *Methods Mol Biol* 1402: 189-197, 2016.

55. **Heung LJ, Luberto C, and Del Poeta M**. Role of sphingolipids in microbial pathogenesis. *Infect Immun* 74: 28-39, 2006.

56. **Hornemann T, Penno A, Rutti MF, Ernst D, Kivrak-Pfiffner F, Rohrer L, and von Eckardstein A**. The SPTLC3 subunit of serine palmitoyltransferase generates short chain sphingoid bases. *J Biol Chem* 284: 26322-26330, 2009.

57. **Hornemann T, Wei Y, and von Eckardstein A**. Is the mammalian serine palmitoyltransferase a high-molecular-mass complex? *Biochem J* 405: 157-164, 2007.

58. **Jackson PL, Xu X, Wilson L, Weathington NM, Clancy JP, Blalock JE, and Gaggar A**. Human neutrophil elastase-mediated cleavage sites of MMP-9 and TIMP-1: implications to cystic fibrosis proteolytic dysfunction. *Molecular medicine* 16: 159-166, 2010.

59. **Karandashova S, Kummarapurugu AB, Zheng S, Chalfant C, and Voynow JA**. Neutrophil elastase increases airway ceramide levels via upregulation of serine palmitoyltransferase. *Am J Physiol Lung Cell Mol Physiol* ajplung 00322 02017, 2017.

60. **Keiser NW, Birket SE, Evans IA, Tyler SR, Crooke AK, Sun X, Zhou W, Nellis JR, Stroebele EK, Chu KK, Tearney GJ, Stevens MJ, Harris JK, Rowe SM, and Engelhardt JF**. Defective innate immunity and hyperinflammation in newborn cystic fibrosis transmembrane conductance regulator-knockout ferret lungs. *Am J Respir Cell Mol Biol* 52: 683-694, 2015.

61. **Kelly E, Greene CM, and McElvaney NG**. Targeting neutrophil elastase in cystic fibrosis. *Expert Opin Ther Targets* 12: 145-157, 2008.

62. **Kirkham S, Sheehan, JK, Knight, D, Richardson, PS, Thornton, DJ**. Heterogeneity of airways mucus: variations in the amounts and glycoforms of the major oligomeric mucins MUC5AC and MUC5B. *Biochem J* 361: 537-546, 2002.

63. **Konstan MW, Byard PJ, Hoppel CL, and Davis PB**. Effect of high-dose ibuprofen in patients with cystic fibrosis. *N Engl J Med* 332: 848-854, 1995.

64. **Konstan MW, Krenicky JE, Finney MR, Kirchner HL, Hilliard KA, Hilliard JB, Davis PB, and Hoppel CL**. Effect of ibuprofen on neutrophil migration in vivo in cystic fibrosis and healthy subjects. *J Pharmacol Exp Ther* 306: 1086-1091, 2003.

65. **Lands LC, Milner R, Cantin AM, Manson D, and Corey M**. High-dose ibuprofen in cystic fibrosis: Canadian safety and effectiveness trial. *J Pediatr* 151: 249-254, 2007.

66. **Lavelle GM, White MM, Browne N, McElvaney NG, and Reeves EP**. Animal Models of Cystic Fibrosis Pathology: Phenotypic Parallels and Divergences. *Biomed Res Int* 2016: 5258727, 2016.

67. **Laviad EL, Kelly S, Merrill AH, Jr., and Futerman AH**. Modulation of ceramide synthase activity via dimerization. *J Biol Chem* 287: 21025-21033, 2012.

68. **Lee SY, Kim JR, Hu Y, Khan R, Kim SJ, Bharadwaj KG, Davidson MM, Choi CS, Shin KO, Lee YM, Park WJ, Park IS, Jiang XC, Goldberg IJ, and Park TS**. Cardiomyocyte specific deficiency of serine palmitoyltransferase subunit 2 reduces ceramide but leads to cardiac dysfunction. *J Biol Chem* 287: 18429-18439, 2012.

69. **Lefrancais E, Roga S, Gautier V, Gonzalez-de-Peredo A, Monsarrat B, Girard JP, and Cayrol C**. IL-33 is processed into mature bioactive forms by neutrophil elastase and cathepsin G. *Proc Natl Acad Sci U S A* 109: 1673-1678, 2012.

70. **Levy H, and Farrell PM**. New challenges in the diagnosis and management of cystic fibrosis. *J Pediatr* 166: 1337-1341, 2015.

71. **Li BJ, Tang Q, Cheng D, Qin C, Xie FY, Wei Q, Xu J, Liu Y, Zheng BJ, Woodle MC, Zhong N, and Lu PY**. Using siRNA in prophylactic and therapeutic regimens against SARS coronavirus in Rhesus macaque. *Nat Med* 11: 944-951, 2005.

72. **Li PL, and Gulbins E**. Bioactive Lipids and Redox Signaling: Molecular Mechanism and Disease Pathogenesis. *Antioxid Redox Signal* 2018.

73. **Liou TG, Adler FR, Keogh RH, Li Y, Jensen JL, Walsh W, Packer K, Clark T, Carveth H, Chen J, Rogers SL, Lane C, Moore J, Sturrock A, Paine R, 3rd, Cox DR, and Hoidal JR**. Sputum biomarkers and the prediction of clinical outcomes in patients with cystic fibrosis. *PLoS ONE* 7: e42748, 2012.

74. **Maceyka M, and Spiegel S**. Sphingolipid metabolites in inflammatory disease. *Nature* 510: 58-67, 2014.

75. **Mall MA, and Schultz C**. A new player in the game: epithelial cathepsin S in early cystic fibrosis lung disease. *Am J Respir Crit Care Med* 190: 126-127, 2014.

76. **Mayer-Hamblett N, Aitken ML, Accurso FJ, Kronmal RA, Konstan MW, Burns JL, Sagel SD, and Ramsey BW**. Association between pulmonary function and sputum biomarkers in cystic fibrosis. *Am J Respir Crit Care Med* 175: 822-828, 2007.

77. **McKone EF, Borowitz D, Drevinek P, Griese M, Konstan MW, Wainwright C, Ratjen F, Sermet-Gaudelus I, Plant B, Munck A, Jiang Y, Gilmartin G, Davies JC, and Group VXS**.

Long-term safety and efficacy of ivacaftor in patients with cystic fibrosis who have the Gly551Asp-CFTR mutation: a phase 3, open-label extension study (PERSIST). *Lancet Respir Med* 2: 902-910, 2014.

78. **Meyer ML, Potts-Kant EN, Ghio AJ, Fischer BM, Foster WM, and Voynow JA**. NAD(P)H quinone oxidoreductase 1 regulates neutrophil elastase-induced mucous cell metaplasia. *Am J Physiol Lung Cell Mol Physiol* 303: L181-188, 2012.

79. **Meyerholz DK**. Lessons learned from the cystic fibrosis pig. *Theriogenology* 86: 427-432, 2016.

80. **Moffatt MF, Kabesch M, Liang L, Dixon AL, Strachan D, Heath S, Depner M, von Berg A, Bufe A, Rietschel E, Heinzmann A, Simma B, Frischer T, Willis-Owen SA, Wong KC, Illig T, Vogelberg C, Weiland SK, von Mutius E, Abecasis GR, Farrall M, Gut IG, Lathrop GM, and Cookson WO**. Genetic variants regulating ORMDL3 expression contribute to the risk of childhood asthma. *Nature* 448: 470-473, 2007.

81. **Mogayzel PJ, Jr., Naureckas ET, Robinson KA, Mueller G, Hadjiliadis D, Hoag JB, Lubsch L, Hazle L, Sabadosa K, and Marshall B**. Cystic fibrosis pulmonary guidelines. *Am J Respir Crit Care Med* 187: 680-689, 2013.

82. **Monteiro AP, Pinheiro CS, Luna-Gomes T, Alves LR, Maya-Monteiro CM, Porto BN, Barja-Fidalgo C, Benjamim CF, Peters-Golden M, Bandeira-Melo C, Bozza MT, and Canetti C**. Leukotriene B4 mediates neutrophil migration induced by heme. *J Immunol* 186: 6562-6567, 2011.

83. **Nahrlich L, Mainz JG, Adams C, Engel C, Herrmann G, Icheva V, Lauer J, Deppisch C, Wirth A, Unger K, Graepler-Mainka U, Hector A, Heyder S, Stern M, Doring G, Gulbins E, and Riethmuller J**. Therapy of CF-patients with amitriptyline and placebo--a randomised, double-blind, placebo-controlled phase IIb multicenter, cohort-study. *Cell Physiol Biochem* 31: 505-512, 2013.

84. **Nakamura H, Yoshimura K, McElvaney NG, and Crystal RG**. Neutrophil elastase in respiratory epithelial lining fluid of individuals with cystic fibrosis induces interleukin-8 gene expression in a human bronchial epithelial cell line. *J Clin Invest* 89: 1478-1484, 1992.

85. **Nishiuma T, Nishimura Y, Okada T, Kuramoto E, Kotani Y, Jahangeer S, and Nakamura S**. Inhalation of sphingosine kinase inhibitor attenuates airway inflammation in asthmatic mouse model. *Am J Physiol Lung Cell Mol Physiol* 294: L1085-1093, 2008.

86. **Olivera A, Kitamura Y, Wright LD, Allende ML, Chen W, Kaneko-Goto T, Yoshihara Y, Proia RL, and Rivera J**. Sphingosine-1-phosphate can promote mast cell hyper-reactivity through regulation of contactin-4 expression. *J Leukoc Biol* 94: 1013-1024, 2013.

87. **Ono JG, Worgall TS, and Worgall S**. Airway reactivity and sphingolipids-implications for childhood asthma. *Mol Cell Pediatr* 2: 13, 2015.

88. **Oral H, Kanzler I, Tuchscheerer N, Curaj A, Simsekyilmaz S, Sonmez TT, Radu E, Postea O, Weber C, Schuh A, and Liehn EA**. CXC chemokine KC fails to induce neutrophil infiltration and neoangiogenesis in a mouse model of myocardial infarction. *J Mol Cell Cardiol* 60: 1-7, 2013.

89. **Oyeniran C, Sturgill JL, Hait NC, Huang WC, Avni D, Maceyka M, Newton J, Allegood JC, Montpetit A, Conrad DH, Milstien S, and Spiegel S**. Aberrant ORM (yeast)-like protein isoform 3 (ORMDL3) expression dysregulates ceramide homeostasis in cells and ceramide exacerbates allergic asthma in mice. *J Allergy Clin Immunol* 136: 1035-1046 e1036, 2015.

90. **Pagano MB, Zhou HF, Ennis TL, Wu X, Lambris JD, Atkinson JP, Thompson RW, Hourcade DE, and Pham CT**. Complement-dependent neutrophil recruitment is critical for the development of elastase-induced abdominal aortic aneurysm. *Circulation* 119: 1805-1813, 2009.

91. **Parkins MD, and Floto RA**. Emerging bacterial pathogens and changing concepts of bacterial pathogenesis in cystic fibrosis. *Journal of cystic fibrosis : official journal of the European Cystic Fibrosis Society* 14: 293-304, 2015.

92. **Petrache I, and Berdyshev EV**. Ceramide Signaling and Metabolism in Pathophysiological States of the Lung. *Annu Rev Physiol* 78: 463-480, 2016.

93. **Petrache I, Kamocki K, Poirier C, Pewzner-Jung Y, Laviad EL, Schweitzer KS, Van Demark M, Justice MJ, Hubbard WC, and Futerman AH**. Ceramide synthases expression and role of ceramide synthase-2 in the lung: insight from human lung cells and mouse models. *PLoS ONE* 8: e62968, 2013.

94. **Petrache I, Medler TR, Richter AT, Kamocki K, Chukwueke U, Zhen L, Gu Y, Adamowicz J, Schweitzer KS, Hubbard WC, Berdyshev EV, Lungarella G, and Tuder RM**. Superoxide dismutase protects against apoptosis and alveolar enlargement induced by ceramide. *Am J Physiol Lung Cell Mol Physiol* 295: L44-53, 2008.

95. **Petrache I, Natarajan V, Zhen L, Medler TR, Richter AT, Cho C, Hubbard WC, Berdyshev EV, and Tuder RM**. Ceramide upregulation causes pulmonary cell apoptosis and emphysema-like disease in mice. *Nat Med* 11: 491-498, 2005.

96. **Pewzner-Jung Y, Tavakoli Tabazavareh S, Grassme H, Becker KA, Japtok L, Steinmann J, Joseph T, Lang S, Tuemmler B, Schuchman EH, Lentsch AB, Kleuser B, Edwards MJ, Futerman AH, and Gulbins E**. Sphingoid long chain bases prevent lung infection by Pseudomonas aeruginosa. *EMBO Mol Med* 6: 1205-1214, 2014.

97. **Price MM, Oskeritzian CA, Falanga YT, Harikumar KB, Allegood JC, Alvarez SE, Conrad D, Ryan JJ, Milstien S, and Spiegel S**. A specific sphingosine kinase 1 inhibitor attenuates airway hyperresponsiveness and inflammation in a mast cell-dependent murine model of allergic asthma. *J Allergy Clin Immunol* 131: 501-511 e501, 2013.

98. **Proesmans M, Vermeulen F, Boulanger L, Verhaegen J, and De Boeck K**. Comparison of two treatment regimens for eradication of Pseudomonas aeruginosa infection in children with cystic fibrosis. *Journal of cystic fibrosis : official journal of the European Cystic Fibrosis Society* 12: 29-34, 2013.

99. **Quinn RA, Lim YW, Mak TD, Whiteson K, Furlan M, Conrad D, Rohwer F, and Dorrestein P**. Metabolomics of pulmonary exacerbations reveals the personalized nature of cystic fibrosis disease. *PeerJ* 4: e2174, 2016.

100. **Quinn RA, Phelan VV, Whiteson KL, Garg N, Bailey BA, Lim YW, Conrad DJ, Dorrestein PC, and Rohwer FL**. Microbial, host and xenobiotic diversity in the cystic fibrosis sputum metabolome. *ISME J* 10: 1483-1498, 2016.

101. **Rab A, Rowe SM, Raju SV, Bebok Z, Matalon S, and Collawn JF**. Cigarette smoke and CFTR: implications in the pathogenesis of COPD. *Am J Physiol Lung Cell Mol Physiol* 305: L530-541, 2013.

102. **Ramsey BW, Davies J, McElvaney NG, Tullis E, Bell SC, Drevinek P, Griese M, McKone EF, Wainwright CE, Konstan MW, Moss R, Ratjen F, Sermet-Gaudelus I, Rowe SM, Dong Q, Rodriguez S, Yen K, Ordonez C, and Elborn JS**. A CFTR potentiator in patients with cystic fibrosis and the G551D mutation. *N Engl J Med* 365: 1663-1672, 2011.

103. **Ramsey KA, Ranganathan S, Park J, Skoric B, Adams AM, Simpson SJ, Robins-Browne RM, Franklin PJ, de Klerk NH, Sly PD, Stick SM, Hall GL, and Arest CF**. Early respiratory infection is associated with reduced spirometry in children with cystic fibrosis. *Am J Respir Crit Care Med* 190: 1111-1116, 2014.

104. **Ratjen F, Munck A, Kho P, and Angyalosi G**. Treatment of early Pseudomonas aeruginosa infection in patients with cystic fibrosis: the ELITE trial. *Thorax* 65: 286-291, 2010.

105. **Ratjen F, Waters V, Klingel M, McDonald N, Dell S, Leahy TR, Yau Y, and Grasemann H**. Changes in airway inflammation during pulmonary exacerbations in patients with cystic fibrosis and primary ciliary dyskinesia. *Eur Respir J* 47: 829-836, 2016.

106. **Rauvala H, and Hallman M**. Glycolipid accumulation in bronchoalveolar space in adult respiratory distress syndrome. *J Lipid Res* 25: 1257-1262, 1984.

107. **Riethmuller J, Anthonysamy J, Serra E, Schwab M, Doring G, and Gulbins E**. Therapeutic efficacy and safety of amitriptyline in patients with cystic fibrosis. *Cell Physiol Biochem* 24: 65-72, 2009.

108. **Rogers CS, Hao Y, Rokhlina T, Samuel M, Stoltz DA, Li Y, Petroff E, Vermeer DW, Kabel AC, Yan Z, Spate L, Wax D, Murphy CN, Rieke A, Whitworth K, Linville ML, Korte SW, Engelhardt JF, Welsh MJ, and Prather RS**. Production of CFTR-null and CFTR-DeltaF508 heterozygous pigs by adeno-associated virus-mediated gene targeting and somatic cell nuclear transfer. *J Clin Invest* 118: 1571-1577, 2008.

109. **Rosenow T, Oudraad MC, Murray CP, Turkovic L, Kuo W, de Bruijne M, Ranganathan SC, Tiddens HA, Stick SM, and Australian Respiratory Early Surveillance Team for Cystic F**. PRAGMA-CF. A Quantitative Structural Lung Disease Computed Tomography Outcome in Young Children with Cystic Fibrosis. *Am J Respir Crit Care Med* 191: 1158-1165, 2015.

110. **Roussel L, Farias R, and Rousseau S**. IL-33 is expressed in epithelia from patients with cystic fibrosis and potentiates neutrophil recruitment. *J Allergy Clin Immunol* 131: 913-916, 2013.

111. **Rowe SM, Heltshe SL, Gonska T, Donaldson SH, Borowitz D, Gelfond D, Sagel SD, Khan U, Mayer-Hamblett N, Van Dalfsen JM, Joseloff E, Ramsey BW, and Network GIotCFFTD**. Clinical mechanism of the cystic fibrosis transmembrane conductance regulator potentiator ivacaftor in G551D-mediated cystic fibrosis. *Am J Respir Crit Care Med* 190: 175-184, 2014.

112. **Sagel SD, Chmiel JF, and Konstan MW**. Sputum biomarkers of inflammation in cystic fibrosis lung disease. *Proc Am Thorac Soc* 4: 406-417, 2007.

113. **Sagel SD, Wagner BD, Anthony MM, Emmett P, and Zemanick ET**. Sputum biomarkers of inflammation and lung function decline in children with cystic fibrosis. *Am J Respir Crit Care Med* 186: 857-865, 2012.

114. **Saiman L, and Siegel J**. Infection control recommendations for patients with cystic fibrosis: Microbiology, important pathogens, and infection control practices to prevent patient-to-patient transmission. *American journal of infection control* 31: S1-62, 2003.

115. **Sasset L, Zhang Y, Dunn TM, and Di Lorenzo A**. Sphingolipid De Novo Biosynthesis: A Rheostat of Cardiovascular Homeostasis. *Trends Endocrinol Metab* 27: 807-819, 2016.

116. **Schneider CA, Rasband WS, and Eliceiri KW**. NIH Image to ImageJ: 25 years of image analysis. *Nat Methods* 9: 671-675, 2012.

117. **Seitz AP, Grassme H, Edwards MJ, Pewzner-Jung Y, and Gulbins E**. Ceramide and sphingosine in pulmonary infections. *Biol Chem* 396: 611-620, 2015.

118. **Shah VS, Meyerholz DK, Tang XX, Reznikov L, Abou Alaiwa M, Ernst SE, Karp PH, Wohlford-Lenane CL, Heilmann KP, Leidinger MR, Allen PD, Zabner J, McCray PB, Jr., Ostedgaard LS, Stoltz DA, Randak CO, and Welsh MJ**. Airway acidification initiates host defense abnormalities in cystic fibrosis mice. *Science* 351: 503-507, 2016.

119. **Simanshu DK, Kamlekar RK, Wijesinghe DS, Zou X, Zhai X, Mishra SK, Molotkovsky JG, Malinina L, Hinchcliffe EH, Chalfant CE, Brown RE, and Patel DJ**. Non-vesicular trafficking by a ceramide-1-phosphate transfer protein regulates eicosanoids. *Nature* 500: 463-467, 2013.

120. **Sly PD, Brennan S, Gangell C, de Klerk N, Murray C, Mott L, Stick SM, Robinson PJ, Robertson CF, and Ranganathan SC**. Lung disease at diagnosis in infants with cystic fibrosis detected by newborn screening. *Am J Respir Crit Care Med* 180: 146-152, 2009.

121. **Sly PD, Gangell CL, Chen L, Ware RS, Ranganathan S, Mott LS, Murray CP, and Stick SM**. Risk factors for bronchiectasis in children with cystic fibrosis. *N Engl J Med* 368: 1963-1970, 2013.

122. **Spagnolo P, Fabbri LM, and Bush A**. Long-term macrolide treatment for chronic respiratory disease. *Eur Respir J* 42: 239-251, 2013.

123. **Stenbit AE, and Flume PA**. Pulmonary exacerbations in cystic fibrosis. *Curr Opin Pulm Med* 17: 442-447, 2011.

124. **Stockley RA, and Burnett D**. Alpha$_1$-antitrypsin and leukocyte elastase in infected and noninfected sputum. *Am Rev Respir Dis* 120: 1081-1086, 1979.

125. **Stoltz DA, Meyerholz DK, Pezzulo AA, Ramachandran S, Rogan MP, Davis GJ, Hanfland RA, Wohlford-Lenane C, Dohrn CL, Bartlett JA, Nelson GAt, Chang EH, Taft PJ, Ludwig PS, Estin M, Hornick EE, Launspach JL, Samuel M, Rokhlina T, Karp PH, Ostedgaard LS, Uc A, Starner TD, Horswill AR, Brogden KA, Prather RS, Richter SS, Shilyansky J, McCray PB, Jr., Zabner J, and Welsh MJ**. Cystic fibrosis pigs develop lung disease and exhibit defective bacterial eradication at birth. *Science translational medicine* 2: 29ra31, 2010.

126. **Stoltz DA, Meyerholz DK, and Welsh MJ**. Origins of cystic fibrosis lung disease. *N Engl J Med* 372: 351-362, 2015.

127. **Sun X, Olivier AK, Liang B, Yi Y, Sui H, Evans TI, Zhang Y, Zhou W, Tyler SR, Fisher JT, Keiser NW, Liu X, Yan Z, Song Y, Goeken JA, Kinyon JM, Fligg D, Wang X, Xie W, Lynch TJ, Kaminsky PM, Stewart ZA, Pope RM, Frana T, Meyerholz DK, Parekh K, and Engelhardt JF**. Lung Phenotype of Juvenile and Adult CFTR-Knockout Ferrets. *Am J Respir Cell Mol Biol* 50: 502-512, 2014.

128. **Sun X, Sui H, Fisher JT, Yan Z, Liu X, Cho HJ, Joo NS, Zhang Y, Zhou W, Yi Y, Kinyon JM, Lei-Butters DC, Griffin MA, Naumann P, Luo M, Ascher J, Wang K, Frana T, Wine JJ, Meyerholz DK, and Engelhardt JF**. Disease phenotype of a ferret CFTR-knockout model of cystic fibrosis. *J Clin Invest* 120: 3149-3160, 2010.

129. **Sweezey NB, and Ratjen F**. The cystic fibrosis gender gap: potential roles of estrogen. *Pediatr Pulmonol* 49: 309-317, 2014.

130. **Taccetti G, Bianchini E, Cariani L, Buzzetti R, Costantini D, Trevisan F, Zavataro L, and Campana S**. Early antibiotic treatment for Pseudomonas aeruginosa eradication in patients with cystic fibrosis: a randomised multicentre study comparing two different protocols. *Thorax* 67: 853-859, 2012.

131. **Tavakoli Tabazavareh S, Seitz A, Jernigan P, Sehl C, Keitsch S, Lang S, Kahl BC, Edwards M, Grassme H, Gulbins E, and Becker KA**. Lack of Sphingosine Causes Susceptibility to Pulmonary Staphylococcus Aureus Infections in Cystic Fibrosis. *Cell Physiol Biochem* 38: 2094-2102, 2016.

132. **Teichgraber V, Ulrich M, Endlich N, Riethmuller J, Wilker B, De Oliveira-Munding CC, van Heeckeren AM, Barr ML, von Kurthy G, Schmid KW, Weller M, Tummler B, Lang**

F, Grassme H, Doring G, and Gulbins E. Ceramide accumulation mediates inflammation, cell death and infection susceptibility in cystic fibrosis. *Nat Med* 14: 382-391, 2008.

133. **Telenga ED, Hoffmann RF, Ruben tK, Hoonhorst SJ, Willemse BW, van Oosterhout AJ, Heijink IH, van den Berge M, Jorge L, Sandra P, Postma DS, Sandra K, and ten Hacken NH**. Untargeted lipidomic analysis in chronic obstructive pulmonary disease. Uncovering sphingolipids. *Am J Respir Crit Care Med* 190: 155-164, 2014.

134. **Tibboel J, Reiss I, de Jongste JC, and Post M**. Ceramides: a potential therapeutic target in pulmonary emphysema. *Respir Res* 14: 96, 2013.

135. **Trifilieff A, and Fozard JR**. Sphingosine-1-phosphate-induced airway hyper-reactivity in rodents is mediated by the sphingosine-1-phosphate type 3 receptor. *J Pharmacol Exp Ther* 342: 399-406, 2012.

136. **Tuggle KL, Birket SE, Cui X, Hong J, Warren J, Reid L, Chambers A, Ji D, Gamber K, Chu KK, Tearney G, Tang LP, Fortenberry JA, Du M, Cadillac JM, Bedwell DM, Rowe SM, Sorscher EJ, and Fanucchi MV**. Characterization of defects in ion transport and tissue development in cystic fibrosis transmembrane conductance regulator (CFTR)-knockout rats. *PLoS ONE* 9: e91253, 2014.

137. **Uchida Y**. Ceramide signaling in mammalian epidermis. *Biochim Biophys Acta* 1841: 453-462, 2014.

138. **Van Goor F, Hadida S, Grootenhuis PD, Burton B, Stack JH, Straley KS, Decker CJ, Miller M, McCartney J, Olson ER, Wine JJ, Frizzell RA, Ashlock M, and Negulescu PA**.

Correction of the F508del-CFTR protein processing defect in vitro by the investigational drug VX-809. *Proc Natl Acad Sci U S A* 108: 18843-18848, 2011.

139. **Van Goor F, Yu H, Burton B, and Hoffman BJ**. Effect of ivacaftor on CFTR forms with missense mutations associated with defects in protein processing or function. *Journal of cystic fibrosis : official journal of the European Cystic Fibrosis Society* 13: 29-36, 2014.

140. **Veit G, Avramescu RG, Perdomo D, Phuan PW, Bagdany M, Apaja PM, Borot F, Szollosi D, Wu YS, Finkbeiner WE, Hegedus T, Verkman AS, and Lukacs GL**. Some gating potentiators, including VX-770, diminish DeltaF508-CFTR functional expression. *Science translational medicine* 6: 246ra297, 2014.

141. **von Bismarck P, Wistadt CF, Klemm K, Winoto-Morbach S, Uhlig U, Schutze S, Adam D, Lachmann B, Uhlig S, and Krause MF**. Improved pulmonary function by acid sphingomyelinase inhibition in a newborn piglet lavage model. *Am J Respir Crit Care Med* 177: 1233-1241, 2008.

142. **Voynow JA, Fischer BM, and Zheng S**. Proteases and cystic fibrosis. *Int J Biochem Cell Biol* 40: 1238-1245, 2008.

143. **Voynow JA, Fischer, B.M., Malarkey, D.E., Burch, L.H., Wong, T., Longphre, M., Ho, S.B., Foster, W.M.** Neutrophil elastase induces mucus cell metaplasia in mouse lung. *Am J Physiol Lung Cell Mol Physiol* 287: L1293-1302, 2004.

144. **Voynow JA, Mascarenhas M, Kelly A, and Scanlin TF**. Cystic Fibrosis. In: *Fishman's Pulmonary Disesases and Disorders*

edited by Grippi MA, Elias JA, Fishman JA, Kotloff RM, Pack AI, Senior RM, and Siegel MD. New York: McGraw-Hill Education, 2015, p. 757-778.

145. **Voynow JA, and Rubin BK**. Mucins, mucus, and sputum. *Chest* 135: 505-512, 2009.

146. **Voynow JA, Young, L.R., Wang, Y., Horger, T., Rose, M.C., Fischer, B.M.** Neutrophil elastase increases *MUC5AC* mRNA and protein expression in respiratory epithelial cells. *Am J Physiol* 276: L835-L843, 1999.

147. **Wadsworth JM, Clarke DJ, McMahon SA, Lowther JP, Beattie AE, Langridge-Smith PR, Broughton HB, Dunn TM, Naismith JH, and Campopiano DJ**. The chemical basis of serine palmitoyltransferase inhibition by myriocin. *J Am Chem Soc* 135: 14276-14285, 2013.

148. **Wan W, Deng X, Archer KJ, and Sun SS**. Pubertal pathways and the relationship to anthropometric changes in childhood: The Fels longitudinal study. *Open J Pediatr* 2: 2012.

149. **Waters V, Stanojevic S, Atenafu EG, Lu A, Yau Y, Tullis E, and Ratjen F**. Effect of pulmonary exacerbations on long-term lung function decline in cystic fibrosis. *Eur Respir J* 40: 61-66, 2012.

150. **Weathington NM, van Houwelingen AH, Noerager BD, Jackson PL, Kraneveld AD, Galin FS, Folkerts G, Nijkamp FP, and Blalock JE**. A novel peptide CXCR ligand derived from extracellular matrix degradation during airway inflammation. *Nat Med* 12: 317-323, 2006.

151. **Wijesinghe DS, Allegood JC, Gentile LB, Fox TE, Kester M, and Chalfant CE**. Use of high performance liquid chromatography-electrospray ionization-tandem mass spectrometry for the analysis of ceramide-1-phosphate levels. *J Lipid Res* 51: 641-651, 2010.

152. **Yang C, Chilvers M, Montgomery M, and Nolan SJ**. Dornase alfa for cystic fibrosis. *Cochrane database of systematic reviews* 4: CD001127, 2016.

153. **Yang J, Eiserich JP, Cross CE, Morrissey BM, and Hammock BD**. Metabolomic profiling of regulatory lipid mediators in sputum from adult cystic fibrosis patients. *Free Radic Biol Med* 53: 160-171, 2012.

154. **Yu H, Burton B, Huang CJ, Worley J, Cao D, Johnson JP, Jr., Urrutia A, Joubran J, Seepersaud S, Sussky K, Hoffman BJ, and Van Goor F**. Ivacaftor potentiation of multiple CFTR channels with gating mutations. *Journal of cystic fibrosis : official journal of the European Cystic Fibrosis Society* 11: 237-245, 2012.

155. **Yu H, Valerio M, and Bielawski J**. Fenretinide inhibited de novo ceramide synthesis and proinflammatory cytokines induced by Aggregatibacter actinomycetemcomitans. *J Lipid Res* 54: 189-201, 2013.

156. **Yu H, Zeidan YH, Wu BX, Jenkins RW, Flotte TR, Hannun YA, and Virella-Lowell I**. Defective acid sphingomyelinase pathway with Pseudomonas aeruginosa infection in cystic fibrosis. *Am J Respir Cell Mol Biol* 41: 367-375, 2009.

157. **Zhou Z, Duerr J, Johannesson B, Schubert SC, Treis D, Harm M, Graeber SY, Dalpke A, Schultz C, and Mall MA**. The ENaC-overexpressing mouse as a model of cystic fibrosis lung disease. *Journal of cystic fibrosis : official journal of the European Cystic Fibrosis Society* 10 Suppl 2: S172-182, 2011.

158. **Ziobro RM, Henry BD, Lentsch AB, Edwards MJ, Riethmüller J, and Gulbins E**. Ceramide in cystic fibrosis. *Clinical Lipidology* 8: 681-692, 2013.

Vita

Sophia Karandashova was born December 9, 1986 in Moscow, Russia; she is a naturalized American citizen. She graduated from Mills. E. Godwin High School, Henrico, Virginia in 2005. She received her Honors Bachelor of Science in Microbiology with a Minor in Chemistry from Oregon State University, Corvallis, Oregon in 2008. Her honors thesis, "The introduction of myxozoan parasites through the release of feeder goldfish (*Carassius auratus*)" was conducted under the supervision of Jerri Bartholomew, PhD. She received her Master of Science in Biotechnology from Stephen F. Austin State University, Nacogdoches, Texas in 2010; the research portion of her Master's was conducted at the University of Texas Health Science Center at Tyler under the supervision of Steven Idell, M.D., Ph.D. Her Masters' research was published in the *American Journal of Respiratory Cell and Molecular Biology* under the title "Intrapleural adenoviral delivery of human plasminogen activator inhibitor-1 exacerbates tetracycline-induced pleural injury in rabbits" in 2013— a first-author paper. After graduation, she worked as a Research Assistant and later Research Associate at the University of Texas Health Science Center in Tyler, Texas until 2012, contributing to several publications, including "Remarkable stabilization of plasminogen activator inhibitor 1 in a "molecular sandwich" complex", "Active α-macroglobulin is a reservoir for urokinase after fibrinolytic therapy in rabbits with tetracycline-induced pleural injury and in human pleural fluids", "Targeting of plasminogen activator inhibitor

1 improves fibrinolytic therapy for tetracycline-induced pleural injury in rabbits", "Plasminogen activator inhibitor-1 suppresses profibrotic responses in fibroblasts from fibrotic lungs", "Dose dependency of outcomes of intrapleural fibrinolytic therapy in new rabbit empyema models", and "Targeting Plasminogen Activator Inhibitor 1 in Tetracycline-Induced Pleural Injury in Rabbits". Ms. Karandashova entered the MD/PhD program at Virginia Commonwealth University in 2012, beginning her graduate work in Clinical and Translational Sciences, with a concentration in Cancer and Molecular Medicine, in 2014, under the supervision of Judith A Voynow, MD. Her current research explores the effects of neutrophil elastase on sphingolipid homeostasis in the airways. During her graduate work so far, Ms. Karandashova has published one first-author peer-reviewed paper and has given talks or poster presentations at several national conferences. In support of her work, she has received an internal grant from the Children's Hospital Fund (2016-2017) subsidizing part of her research, which was used to generate preliminary data for a Cystic Fibrosis Foundation Research Grant (2018-2020). She has also received two travel grants, one from VCU's Center for Clinical and Translational Research (Spring 2017), as well as the VCU Graduate Student Travel Grant (Fall 2017). She has also received a Graduate School Dissertation Assistantship (2017-2018) from VCU. Following completion of medical school, Ms. Karandashova hopes to pursue further research into the inflammatory processes that contribute to CF and other chronic inflammatory diseases of the lungs.